ELSEVIER

Coordination Chemistry Reviews
160 (1997) 237–294

COORDINATION CHEMISTRY REVIEWS

# Annual survey of organometallic metal cluster chemistry for the year 1995

Michael G. Richmond *

*Center for Organometallic Research and Education, Department of Chemistry, University of North Texas, Denton, TX 76203, USA*

Received 23 August 1996

**Contents**

## Abstract

The synthetic, mechanistic, and structural chemistry of organometallic metal cluster compounds is reviewed for the year 1995. © 1997 Elsevier Science S.A.

*Keywords:* Organometallic metal cluster compounds

---

* *Corresponding author.*

*PII* S0010-8545(96)01324-0

## 1. Dissertations

The reaction between $PhPCl_2$ and $[Ni_6(CO)_{12}]^{2-}$ affords the anionic clusters $[Ni_{10}(PPh)_2(CO)_{18}]^{2-}$, $[Ni_9(PPh)_3(CO)_{15}]^{2-}$, $[Ni_8(PPh)_4(CO)_{12}]^{2-}$, and $[Ni_8(PPh)_2(CO)_{14}]^{2-}$. The latter three clusters are shown to possess noncentered $Ni_{12-x}P_x$ icosahedral cages (where $x = 2, 3, 4$). Each of these clusters was examined by IR and $^{31}P$-NMR spectroscopy and cyclic voltammetry, with trends discussed relative to the number of phenylphosphinidene groups. Treatment of $[Ni_6(CO)_{12}]^{2-}$ with $Pd(OAc)_2$ gives the unexpected Pd–Ni carbonyl cluster $[Pd_{16}Ni_{16}(CO)_x]^{4-}$. A complete X-ray diffraction study was limited due to severe crystal decay [1]. Thermolysis of $Os_3(CO)_9(\mu\text{-}H)_3(\mu_3\text{-}BCO)$ yields the dihedral, "butterfly", boride cluster $HOs_4(CO)_{12}(BH_2)$. The pentagonal bipyramidal cluster $HOs_5(CO)_{16}B$ has been isolated from $HOs_4(CO)_{12}(BH_2)$ at elevated temperature. The identity of these new clusters was established by solution spectroscopic and X-ray diffraction methods. $Os_3(CO)_9(\mu\text{-}H)_3(\mu_3\text{-}CCO)$ reacts with diborane to give the corresponding methylidyne-capped cluster $Os_3(CO)_9(\mu\text{-}H)_3(\mu_3\text{-}CCH_3)$ [2]. The new clusters $Ru_4Pt(CO)_{13}(COD)(\mu\text{-}H)_2$, $Ru_3Pt(CO)_9(\mu\text{-}CO)(COD)(\mu\text{-}H)_2$, $Ru_4Pt_2(CO)_{11}(COD)_2(\mu_3\text{-}H)_2$, and $Ru_5Pt_2(CO)_{18}(COD)_2(\mu_3\text{-}H)_2$ have been isolated from the reaction between $Pt(COD)_2$ and $Ru_4(CO)_{13}(\mu\text{-}H)_2$ at room temperature. The solid-state structure of each cluster is presented. The clusters $Ru_8Pt_2(CO)_{23}(\mu_3\text{-}H)_2$ and $Ru_7Pt_3(CO)_{21}(\mu\text{-}CO)(\mu_3\text{-}H)_2$, prepared from $Ru_4Pt(CO)_{18}$ with added $Ru_4(CO)_{13}(\mu\text{-}H)_2$ and $Ru_3Pt(CO)_{10}(COD)(\mu\text{-}H)_2$, respectively, have been structurally characterized and examined for their ligand substitution reactivity. $Ru_4Pt_2(CO)_{18}$ reacts with $H_2$ to afford the new cluster $Ru_6Pt_3(CO)_{21}(\mu\text{-}H)_3(\mu_3\text{-}H)$. The reactivity of this $Ru_6Pt_3$ cluster with diphenylacetylene has been explored, and the resulting alkyne-substituted cluster studied in hydrogenation catalysis [3]. The conversion of $[Re_7C(CO)_{21}]^{3-}$ into $[Re_6C(CO)_{19}]^{2-}$ is reported to occur in the presence of $PPh_3$ and the oxidant $[Cp_2Fe]^+$ (two equiv.). The X-ray structure of the hexarhenium cluster reveals an extremely congested ligand environment. When the same starting heptarhenium cluster is treated with $[Cp_2Fe]^+$ (two equiv.) in the presence of diazomethane, the carbene cluster $[Re_7C(CO)_{21}(CH_2)]^-$ is obtained as the major product. Treatment of $[Re_6C(CO)_{19}]^{2-}$ with $Mo(CO)_6$ and $Ru_3(CO)_{12}$ under photochemical conditions gives the mixed-metal clusters $[Re_6C(CO)_{18}Mo(CO)_4]^{2-}$ and $[Re_6C(CO)_{18}Ru(CO)_3]^{2-}$, respectively. One-electron oxidation of $[Re_7C(CO)_{21}]^{3-}$ using $[Cp_2Fe]^+$ affords the paramagnetic cluster $[Re_7C(CO)_{21}]^{2-}$, which has been shown to react with added $Bu_3SnH$ or silane to give the hydride cluster $[HRe_7C(CO)_{21}]^{2-}$. $[Re_7C(CO)_{21}]^{2-}$ also reacts with acetone and THF to furnish the same hydride cluster. The role played by the gegencation and the ferrocenium oxidant in these reactions is discussed [4]. The preparation and characterization of $Os_3(CO)_{10}(MeCN)\{Si(OR)_3\}(\mu\text{-}H)$ from $Os_3(CO)_{10}(MeCN)_2$ and $(RO)_3SiH$ (where R = Me, Et) have been discussed. The interconversion and ligand substitution properties of these trialkoxysilyl-containing clusters were also explored. The hydrosilylation of *trans*-cinnamaldehyde by $Et_3SiH$ was examined by using the cluster catalysts $Pt_3Ru_6(CO)_{20}(\mu\text{-}C_2Ph_2)(\mu\text{-}H)_2$ and $Pt_3Ru_6(CO)_{21}(\mu_3\text{-}H)_3$. $Pt_2Os_4(CO)_{18}$ reacts with $H_2$ to give $Pt_5Os_6(CO)_{25}$, with no evidence obtained for the presence of hydride ligands in the product [5]. The synthesis, characterization, and catalytic behavior of the zeolite-encapsulated clusters $[Pt_6(CO)_{21}]^{2-}$ and $[Pt_9(CO)_{18}]^{2-}$ are reported. NaY zeolites were used in these studies. Treatment of $Na_2PtCl_6$ and $RhCl_3$ in the presence of CO and MgO gives the mixed-metal cluster $[PtRh_5(CO)_{15}]^-$ in 84% yield [6].

The use of bimetallic bridging sulfur compounds in the synthesis of metalla-sulfur cubane clusters has been reported. The compounds $Cp^*M(PR_3)S_2IrCp^*$ (where R = Me, M = Rh, Ir; R = *p*-tolyl, M = Ir) give $(Cp^*MS)_2(Cp^*IrS)_2$ upon thermolysis. Mechanistic information on the cubane-assembly reaction is included [7]. The reactivity of $(MeCp)_2Mo_2Co_3S_3(CO)_4$ with organic sulfur compounds has been investigated, with thiol desulfurization schemes discussed. Thiolate anions initially coordinate to a cobalt center at low temperature, as shown by $^1H$-NMR spectroscopy. Conversion of this adduct to a $\mu_2$-sulfido and a $\mu_2$-thiolate ligand occurs above −20°C. The anion $[(MeCp)_2Mo_2Co_2S_4(CO)_4]^-$ and the corresponding hydrocarbon-based radical result when the $Mo_2Co_3$ cluster and organic thiol are heated above 50°C. The molecular structure of this latter $Mo_2Co_2$ cluster was established by X-ray crystallography, and the presence of the organic radical was demonstrated by the observed rearrangement of the intermediate cyclopropylmethyl radical to 1-butene-$d_1$ in $CD_3CN$ solvent [8]. The reactivity of $HRu_3(\mu_3\text{-}\eta^3\text{-}XCCRCR')(CO)_{9-n}(PPh_3)_n$ (where $X = R = R' = Me$, $n = 1$; $X = MeO$, $R = H$, $R' = EtO$, $n = 2,3$; $X = Et_2N$, $R = H$, $R' = Me$, $n = 1$) with electrophiles has been examined and found to proceed by one-electron transfer or by Lewis acid-base formation. The electrochemical behavior of these clusters reveals the presence of an accessible one-electron oxidation, whose reversibility depends on the nature of the $\pi$ donor capability of the allyl substituents and the number of $PPh_3$ ligands present. The radical cations, generated by chemical oxidation, are stable at low temperature, and have been characterized by IR and EPR spectroscopy. The clusters $H_3Ru_3(\mu_3\text{-}CR)(CO)_6(PPh_3)_3$ (where R = Me, Ph) have been studied for their reactivity with $[Ag]^+$ reagents, and a silver–triruthenium complex that contains an agostic hydrogen has been identified by spectroscopic methods [9]. The synthesis, reactivity, and bonding in carbide and sulfur oxide clusters are described. $SO_2$ reacts with $[HFe_3(CO)_{11}]^-$ to give $HFe_3(CO)_9(SO_2)$, which possesses a $\mu_3,\eta^2\text{-}SO_2$ ligand. Methylation and acetylation of the oxygen atom of $SO_2$ that is not bonded to iron yields $HFe_3(CO)_9(SO_2Me)$ and $HFe_3(CO)_9\{SO_2C(O)Me\}$, respectively. The clusters $[Ru_3(CO)_{11}]^{2-}$ and $[HRu_3(CO)_{11}]^-$ have been allowed to react with $SO_2$ to produce $[Ru_3(CO)_9(\mu_3,\eta^2\text{-}SO_2)]^{2-}$, $[Ru_3(CO)_7(\mu_3,\eta^2\text{-}SO_2)(\mu_2\text{-}SO_2)_2]^{2-}$, and $[HRu_3(CO)_9(\mu_2\text{-}SO_2)_2]^-$. Extended Hückel calculations on the bonding of a variety of organic and inorganic capping fragments to $Fe_3(CO)_9$ have been carried out in order to examine the origins of the tilt angle associated with the $\mu_3$-ligand. $C_\alpha$–$C_\beta$ bond scission in the ketenylidene cluster $[Os_3(CO)_9(CCO)]^-$ occurs upon treatment with $Ni(CO)_4$ and gives the clusters $[Os_3Ni_3C(CO)_{13}]^{2-}$ and $[Os_3Ni_4C(CO)_{15}]^{2-}$.

These carbide clusters have been fully characterized [10]. UV irradiation of $Ru_3(CO)_{12}$ that has been physisorbed on porous Vycor glass leads to the oxidative addition of a surface silanol group and formation of $Ru_3(CO)_{10}(\mu\text{-}H)(\mu\text{-}OSi\equiv)$. The reactivity of this surface grafted cluster in alkene isomerization and hydrogenation reactions was probed [11].

Treatment of $Co_2(CO)_8$ with $BH_3 \cdot SMe_2$ gives $B_2H_4Co_2(CO)_6$ and $Co_5(CO)_{13}(\mu\text{-}CO)(B_2H)$. The X-ray structure of the $Co_5$ cluster reveals that it does not conform to the theoretically predicted trigonal biprismatic geometry expected for an 80-electron cluster. The synthesis and spectroscopic characterization of $FeCo_2(CO)_9(\mu\text{-}CO)(BH)$ and $FeCo_2(CO)_9(BH)_2$ are described. $Co_2(CO)_8$ reacts with $HFe_4(CO)_{12}(BH_2)$ to give $HFe_3Co(CO)_{12}(BH)$. The cobalt atom is shown to occupy a wing-tip position in this cluster. Heating this same cluster leads to $Fe_3Co(CO)_{12}(BH_2)$ [12]. The cluster $(CpTi)_6(\mu_3\text{-}Te)_6(\mu_3\text{-}O)_2$ has been isolated in low yield from the reaction of $Cp_2Ti(TeSiPh_3)_2$ with Lewis bases [13]. The synthesis and reactivity of $[HAs\{Fe(CO)_4\}_3]^{2-}$, $[Te\{Fe(CO)_4\}_3]^{2-}$, and $[Se\{Fe(CO)_4\}_3]^{2-}$ are described. Whereas the latter two clusters readily lose CO to give the corresponding *closo* clusters $[XFe_3(CO)_9]^{2-}$, the former cluster yields the higher nuclearity compound $[As_2Fe_5(CO)_{17}]^{2-}$ under comparable conditions. The reactivity of related bismuth derivatives has also been investigated [14].

CO substitution in $PhCCo_3(CO)_9$ by the diphosphine ligand bma gives $PhCCo_3(CO)_7(bma)$, which is unstable and decomposes via a first-order process involving CO loss to furnish $Co_3(CO)_6\{\mu_2\text{-}\eta^2,\eta^1\text{-}C(Ph)\,\overline{C{=}C(PPh_2)C(O)OC}\,(O)\}(\mu_2\text{-}PPh_2)$. The model cluster complex $PhCCo_3(CO)_7\{(Z)\text{-}Ph_2PCH{=}CHPPh_2\}$ is inert with respect to the diphosphine/benzylidyne ligand activation experienced by the bma ligand. $Co_3(CO)_6\{\mu_2\text{-}\eta^2,\eta^1\text{-}C(Ph)\,\overline{C{=}C(PPh_2)C(O)OC}\,(O)\}(\mu_2\text{-}PPh_2)$ reacts with $PMe_3$ to give an adduct with an expanded molecular polyhedron. The decomposition of this intermediate and the kinetics for the addition of a second $PMe_3$ ligand to $Co_3(CO)_5(PMe_3)\{\mu_2\text{-}\eta^2,\eta^1\text{-}C(Ph)\,\overline{C{=}C(PPh_2)C(O)OC}\,(O)\}(\mu_2\text{-}PPh_2)$ are reported. Mechanisms for the bma/benzylidyne ligand activation and the site-selective $PMe_3$ addition reactions are presented. Each new cluster compound has been fully characterized [15]. $CS_2$ reacts with the paramagnetic 46-electron cluster $Cp^*_3Co_3(\mu_2\text{-}H)_3(\mu_3\text{-}H)$ to afford the sulfide thiocarbonyl cluster $Cp^*_3Co_3(\mu_3\text{-}S)(\mu_3\text{-}CS)$. Nitric oxide and phenyl isocyanate react with the tetrahydride cluster to yield $Cp^*_3Co_3(\mu_3\text{-}NO)_2$ and $Cp^*_2Co_2(\mu_2,\mu_2\text{-}\eta^2\text{-}PhNCONPh)$, respectively. The mono(ethylidyne) clusters $Cp^*_3Co_3(\mu_3\text{-}CMe)(\mu_3\text{-}H)$ and $Cp^*_3Co_3(\mu_3\text{-}CMe)(\mu_2\text{-}H)_3$ are obtained from $Cp^*_3Co_3(\mu_2\text{-}H)_3(\mu_3\text{-}H)$ and acetylene at elevated temperature. Spectroscopic data related to pertinent intermediates and deuterium labeling studies are presented. The reactivity of *tert*-butyl isonitriles and trimethylsilyl(diazomethane) with $Cp^*_3Co_3(\mu_3\text{-}CMe)(\mu_3\text{-}H)$ has also been examined [16]. The synthesis of $Cp^*_3M_3(\mu_3\text{-}CH)(\mu_3\text{-}H)$ (where M = Co, Ni) from either $[Cp^*MCl]_2$ or $Cp^*M(acac)$ with MeLi is reported. The reactivity of these clusters with oxidants and hydrogen is discussed. 2D EXSY NMR measurements on $Cp^*_3Co_3(\mu_3\text{-}CH)(\mu_3\text{-}H)_3$ reveal that the carbyne and bridging hydride protons exchange via an intramolecular mechanism, whose rate is estimated at $1\ s^{-1}$ [17].

## 2. Homometallic clusters

### 2.1. Group 4 clusters

The compound $\{Cp^*Ti(\mu\text{-}O)\}_3(\mu_3\text{-}CH)$ has been used as a Lewis acid in the reaction with $CpM(CO)_3H$ (where M = Mo, W). Spectroscopic data indicate that the titanium centers coordinate the oxygen atom of a $[CpM(CO)_3]^-$ fragment, with the hydrogen atom of $CpM(CO)_3H$ being transferred to the $\mu_3$-carbyne ligand to afford a coordinated methyl group [18].

### 2.2. Group 6 clusters

The reaction of $W_2(O_2CBu^t)_6$ and CpNa gives $Na_2W_4O_4Cp_4(O_2CBu^t)_6$, which has been crystallographically characterized [19]. $\{CpCr(CO)_3\}_2$ reacts with $P_4S_3$ to give as the major product $Cp_4Cr_4(CO)_9(P_4S_3)$, whose X-ray structure has been solved. Thermolysis of this cluster affords a variety of $CpCr(CO)_2$-substituted P- and S-containing compounds [20]. Optical excitation of $(RCp)_2Mo_2(CO)_6$ (where R = H, Me) in the presence of $HSiMe_2Ph$ gives the tetrahedral clusters $MeCMo_3(RCp)_3(CO)_6$. Both of these clusters have been isolated and crystallographically characterized. The fluxional properties of each cluster were investigated by variable-temperature NMR measurements, and mechanisms accounting for the observed dynamic Cp ligand behavior discussed. The relevance of this work towards deoxygenative reduction of CO is discussed [21]. Treatment of $[CpM(CO)_3]^-$ (where M = Mo, W) with $PCl_3$ yields $\{CpM(CO)_2\}_3PM(CO)_5$ and $\{CpM(CO)_2\}_3P$. All four of these products were characterized by spectroscopic and crystallographic methods [22]. The clusters $[(OC)_5MoAsMo_3(CO)_9(\mu_3\text{-}OR)_3Mo(CO)_3]^{2-}$ (where R = Me, Et) have been prepared from $Mo(CO)_6$ and $NaAsO_2$ in refluxing ROH. The X-ray structure of the methyl derivative (Fig. 1) reveals the existence of a tetrahedral $AsMo_3$ core. The remaining $Mo(CO)_3$ and $Mo(CO)_5$ moieties are bound to bridging methoxy groups and the capping $\mu_3$-As center, respectively. The bonding in these clusters was explored by extended Hückel calculations. The failure of these clusters to obey the usual electron-counting rules is discussed relative to the MO calculations [23].

### 2.3. Group 7 clusters

A series of cationic manganese(II) aryl compounds have been prepared. The X-ray structure of $Mn_3(2,4,6\text{-}Me_3C_6H_2)_6$ is included, and the use of this complex as a starting material for other complexes is presented [24]. The reaction of $Mn_2(CO)_{10}$ and $Me_3Al$ in a hexane/THF solvent mixture leads to $[Mn][Mn_7(THF)_6(CO)_{12}]_2$, $Mn_3(THF)_2(CO)_{10}$, and $[Mn(THF)_6][Mn(CO)_5]_2$; the latter two compounds are thermally unstable. All three of these compounds have been characterized in solution and by X-ray crystallography. Fig. 2 shows the X-ray structure of the $Mn_{15}$ cluster [25].

The X-ray structure of the cubane cluster $\{Mn(CO)_3(\mu_3\text{-}OH)\}_4$ has been solved [26]. Network hydrogen bonding and crystal engineering are discussed in a

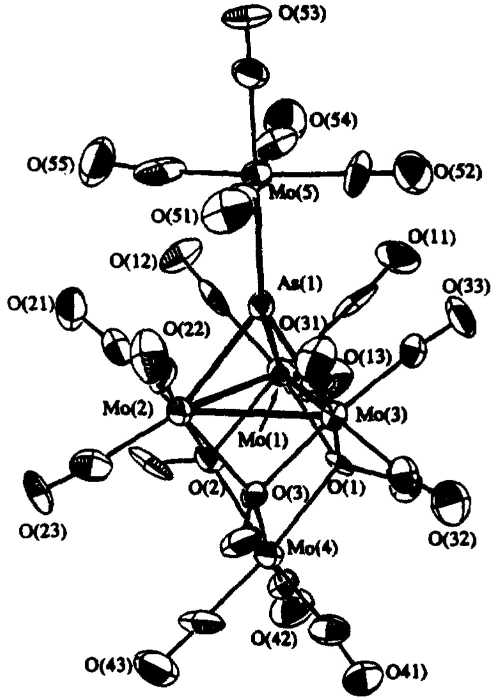

Fig. 1. X-ray structure of $[(OC)_5MoAsMo_3(CO)_9(\mu_3\text{-}OMe)_3Mo(CO)_3]^{2-}$. Reprinted with permission from Inorganic Chemistry. Copyright 1995 American Chemical Society.

paper dealing with the X-ray structures of $\{Mn(CO)_3(\mu_3\text{-}OH)\}_4 \cdot 2(2,3,5,6\text{-}Me_4pyrazine) \cdot 2H_2O \cdot 2MeCN$ and $\{Mn(CO)_3(\mu_3\text{-}OH)\}_4 \cdot 4,4'\text{-}bpy \cdot 2MeCN$. The ability of MeCN to act as a hydrogen bond acceptor in the construction of the observed 2-D grid (former complex) and 1-D strands (latter complex) is discussed [27]. Another publication describing the supramolecular chemistry of $\{M(CO)_3(\mu_3\text{-}OH)\}_4$ (where M = Mn. Re) has appeared. Fourteen new X-ray structures that contain three-dimensional superdiamondoid lattice networks are included [28]. Treatment of $[\{MeCpMn(CO)_2\}_2H]^-$ with $SnCl_2$ gives the inidene complex $[\{MeCpMn(CO)_2Sn\}_2\{\mu_2\text{-}Mn(CO)_2MeCp\}_2(\mu_2\text{-}Cl)]^-$. The spectroscopic properties and the X-ray structure are presented, and the relationship of this complex to the [1.1.1]propellane system is discussed [29].

H/D exchange via reversible pyridine ortho-metalation in $[Re_3(CO)_{10}(\mu\text{-}H)_3(\mu\text{-}NC_5H_4)]^-$ has been examined by NMR spectroscopy. Rate constants are reported, and the observed equilibrium isotope effect is discussed with respect to the proposed mechanism. When the exchange reaction is conducted under CO the cluster $[Re_3(CO)_{12}(\mu\text{-}H)_2]^-$ is obtained. Using $[Re_3(CO)_{10}(\mu\text{-}H)_4]^-$ in the presence of CO and pyridine has allowed for the calculation of the competition ratio between CO coordination and pyridine ortho-metalation. The X-ray structure of $[Re_3(CO)_{11}(py)(\mu\text{-}H)_2]^-$ accompanies this report [30]. The unsaturated

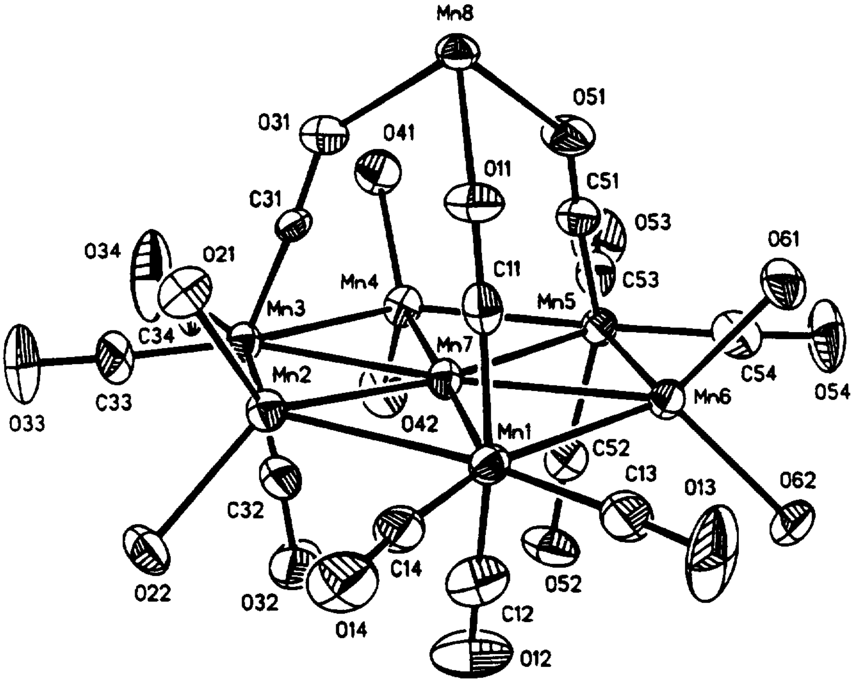

Fig. 2. X-ray structure of half of $[Mn][Mn_7(THF)_6(CO)_{12}]_2$, with the THF carbon atoms omitted. Reprinted with permission from Journal of American Chemical Society. Copyright 1995 American Chemical Society.

cluster $Re_4(CO)_{12}(\mu_3\text{-}H)_4$ readily adds four acetonitrile molecules to give $Re_4(CO)_{12}(MeCN)_4(\mu_3\text{-}H)_4$. The product exists as a mixture of two isomers that display a spiked-triangle metallic skeleton. These isomers fragment at room temperature to give $[Re_3(CO)_9(MeCN)(\mu\text{-}H)_4]^-$ and $[Re(CO)_3(MeCN)_3]^+$. The effects of additives on the fragmentation reaction and a reaction mechanism that illustrates how the acetonitrile-substituted cluster decomposes in solution are presented [31].

### 2.4. Group 8 clusters

A review dealing with the development of osmium and ruthenium carbonyl compounds has appeared. The physical techniques used to establish cluster structure (solution and solid state), synthetic methods leading to the directed synthesis of polynuclear clusters, redox chemistry, and cluster framework rearrangements are several of the topics discussed [32]. Mechanistic information on the photofragmentation and photosubstitution processes in $M_3(CO)_{12}$ (where $M = Ru$, Os) has been reviewed. The synthetic potential of photochemically generated Ru and Os intermediates and the role of cluster photochemistry in catalysis are discussed [33]. Picosecond pump-probe photochemistry studies have been carried out on $Fe_3(CO)_{12}$. Excited $Fe_3(CO)_{12}$ transforms into a coordinatively unsaturated cluster as a result of Fe-Fe bond scission. This $Fe_3(CO)_{12}$ (unsaturated) isomer is detected within 15 ps. The rate constants for the return to the ground state and fragmentation are reported, and a discussion of these data relative to the earlier work of Cotton and Hunter on the CO mobility in $Fe_3(CO)_{12}$ is presented [34]. $Ru_3(CO)_{12}$ physisorbed onto porous Vycor glass affords $Ru_3(CO)_{10}(\mu\text{-}H)(\mu\text{-}OSi{\equiv})$ upon UV photolysis. This cluster is shown to react with 1-pentene to give the stable adduct $HRu_3(CO)_{10}(\mu\text{-}OSi{\equiv})$(1-pentene), which releases 2-pentene upon photolysis. The photoassisted catalytic cycle is discussed [35]. Several dimeric compounds and $[Fe_3(CO)_{11}]^{2-}$ have been examined by molecular mechanics computations using Cotton's charge equalization principle. The steric versus electronic effects in determining ligand stereochemistry are fully outlined [36]. Extended Hückel molecular orbital calculations have been performed on $Fe_3(CO)_{12}$ and $Ru_3(CO)_{12}$. The origin of the bridged structure observed in the solid state of $Fe_3(CO)_{12}$ is attributed to electronic effects involving a weaker Fe-Fe repulsion in the lighter congener [37]. Treatment of $Fe_3(CO)_{12}$ with halides in aprotic solvents leads to a disproportionation reaction and the radical anion $[Fe_3(CO)_{11}]^{\cdot-}$. This cluster has been isolated and characterized by X-ray diffraction analysis (Fig. 3), which has revealed the presence of one semibridging CO group. This same cluster also forms when $[Fe_3(CO)_{11}]^{2-}$ is treated with $PhNO_2$. The reaction of halide anions with other clusters is described, and the role of radical intermediates in the reduction of aromatic nitro compounds is presented. Also included in this report are the X-ray structures of $[Fe_3(CO)_9(\mu_3\text{-}NPh)]^{2-}$ and $[HFe_3(CO)_9(\mu_3\text{-}NPh)]^-$ [38].

$Ru_3(CO)_{12}$ was examined by NMR methods in order to evaluate the activation energy for intramolecular CO exchange. Reported data include $^{13}C$-spin-lattice ($T_1$) and spin-spin ($T_2$) relaxation times of the CO groups. The use of MAS $^{13}C$-NMR data and the variable-temperature relaxation data has allowed for accu-

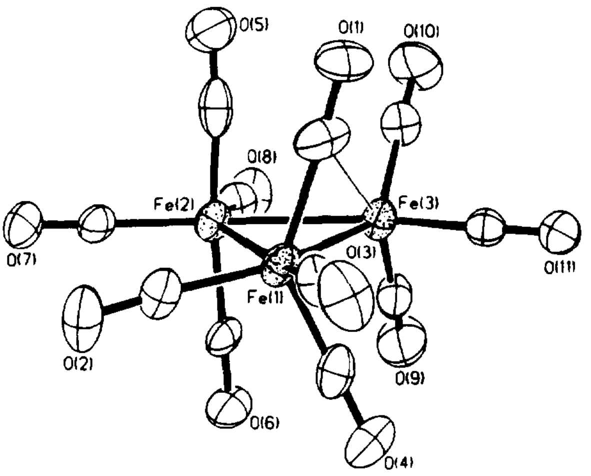

Fig. 3. X-ray structure of $[Fe_3(CO)_{11}]^{\cdot-}$. Reprinted with permission from Organometallics. Copyright 1995 American Chemical Society.

rate calculation of the barrier associated with intramolecular CO exchange [39]. A paper describing the effect of chloride ions on the ruthenium-catalyzed hydroesterification of ethylene has appeared. $[Ru_4(CO)_{11}(\mu\text{-}Cl)_2][PPN]_2$ has been isolated from the reaction between $Ru_3(CO)_{12}$ and [PPN][Cl] and crystallographically characterized. The solid-state structure consists of a $Ru_3(CO)_9$ triangular frame with one face supported by a spiked "$Ru(CO)_2Cl_2$" moiety. Extended Hückel calculations reveal the presence of a large HOMO-LUMO gap (1.45 eV) in the cluster. The reaction of $O_2$ with the $Ru_4$ cluster affords $[Ru_4(CO)_{10}(\mu\text{-}Cl)_4(\mu_4\text{-}O)][PPN]_2$, whose structure has been established by X-ray crystallography. Analyses of the recovered catalysis reaction solutions from the various ruthenium reagents reveal the presence of $[Ru_6(C)(CO)_{16}]^{2-}$ as the principal metal-containing cluster. Catalytic studies using this carbido cluster are presented, as are the results of other mononuclear ruthenium precursors [40]. The kinetics and mechanism of azide addition to $Ru_3(CO)_{12}$ have been investigated. A rate law dependent on the concentrations of both $Ru_3(CO)_{12}$ and azide and the activation parameters support a rate-limiting sequence involving azide attack on a coordinated CO ligand. The intermediate cluster $[Ru_3(CO)_{11}(CON_3)]^-$ decomposes via a Curtius-type rearrangement to give $[Ru_3(CO)_{11}(NCO)]^-$ and $N_2$. This latter cluster decomposes in the absence of CO to afford the bridged isocyanato cluster $[Ru_3(CO)_{10}(\mu\text{-}NCO)]^-$ [41].

The addition of phosphine/phosphite ligands to the 46-electron cluster $Os_3(CO)_{10}(\mu_2\text{-}H)_2$ has been the subject of a detailed kinetics study. The experimentally found second-order rate constants were fit to a multiparameter equation involving the $pK_a$, $\sigma$-donicity, Tolman cone angle, and steric threshold of each individual ligand. The concept of a transition-state isomer is presented [42]. The kinetics for ligand substitution in $Os_3(CO)_{10}(\mu_2\text{-}H)_2$ were examined as a function of pressure and temperature, and the volumes of activation ($\Delta V^{\neq}$) reported. On the basis of the $\Delta V^{\neq}$ data, it is suggested that all of the $Os\cdots P$ bond lengths in the transition state are the same for all nucleophiles possessing a Tolman cone angle less than 160°. Mechanistic considerations are thoroughly discussed [43]. $^1H$-MAS-NMR spectral data for $H_2Os_3(CO)_{10}$, $H_2FeRu_3(CO)_{13}$, $HRu_3(CO)_9(\mu_3,\eta^2\text{-}C{\equiv}CBu^t)$, $H_2Os_3(CO)_{11}$, and $H_2Os_3(CO)_{10}(NH_3)$ are reported. The use of this NMR method in the elucidation of the structure of hydrido clusters is discussed [44]. The diyne ligand $HOCH_2C_4CH_2OH$ reacts with $H_2Os_3(CO)_{10}$ to yield $O_3(CO)_{10}(\mu\text{-}H)(\mu_2,\eta^3\text{-}\overline{OCH{=}CH{-}C{=}C}\text{-}C\text{-}Me)$. The metallocycle ring forms a pseudo-furan ring bearing an $\alpha$ C-methyl group. Reactions of $H_2Os_3(CO)_{10}$ with the diyne compounds $\{Co_2(CO)_6\}(\mu_2,\eta^2\text{-}HOCH_2C_4CH_2OH)$ and $\{Co_2(CO)_6\}_2(\mu_2,\eta^2{:}\mu_2,\eta^2\text{-}HOCH_2C_4CH_2OH)$ are also described [45]. The clusters $Os_3(CO)_{10}(\mu\text{-}H)(\mu\text{-}OH)$ and $Os_3(CO)_8(PPh_3)_2(\mu\text{-}H)(\mu\text{-}OH)$ (two isomers) have been isolated from the reaction between $[Os_3(CO)_{11}(\mu\text{-}H)]^-$ and $Cu(PPh_3)_2(BH_4)$. All three clusters were characterized in solution and by X-ray crystallography [46]. The X-ray structure of $Os_3(CO)_{10}(\mu\text{-}H)(\mu\text{-}OH)$ reveals the existence of an osmium triangle, bridged on one side by the hydrido and hydroxy groups [47].

The reactivity of the "lightly stabilized" clusters $Os_3(CO)_{11}L$ (where L = ethylene, MeCN) with the gaseous reactants CO, $NH_3$, and $H_2$ has been explored in the context of solid–gas reactions. The site selectivity of these ligand substitution reactions has been assessed by NMR methods. These "lightly stabilized" clusters are shown to react via L loss and formation of the reactive unsaturated cluster $Os_3(CO)_{11}$ [48]. Variable-temperature $^{13}C$- and $^{31}P$-NMR studies have been conducted on $Fe_3(CO)_{11}(CNBu^t)$ and $Fe_3(CO)_{10}(CNBu^t)\{P(OMe)_3\}$ in order to study the fluxional pathways associated with CO and $P(OMe)_3$ exchange. Two isomers were observed in solution for the $P(OMe)_3$-substituted cluster; one of these isomers was isolated and crystallographically characterized [49]. $Os_3(CO)_{11}(MeCN)$ reacts with $Bu^t_2PF$ to give the phosphine-substituted cluster $Os_3(CO)_{11}(Bu^t_2PF)$. Reaction of the bis-acetonitrile cluster $Os_3(CO)_{10}(MeCN)_2$ with the same ligand yields $Os_3(CO)_{10}(Bu^t_2PF)_2$ and $Os_3(CO)_{10}(Bu^t_2PF)(Bu^tPF_2)$. Each of these products was characterized in solution by IR and NMR spectroscopy and mass spectrometry. The X-ray structures of the former two clusters were determined by X-ray crystallography [50]. The substitution chemistry of $Ru_3(CO)_{12}$ with the polyfunctional phosphines tris(2-thienyl)phosphine and tris(diethylamino)phosphine is described. The compounds $Ru_3(CO)_{10}\{P(C_4H_3S)_3\}_2$ and $Ru(CO)_3\{P(C_4H_3S)_3\}_2$ have been characterized by X-ray crystallography. Use of the latter phosphine ligand affords $Ru_3(CO)_{10}\{P(NEt_2)_3\}_2$, whose IR spectrum reveals the presence of bridging CO ligands. This latter aspect is discussed relative to other clusters of this genre which do not exhibit bridging CO ligands [51]. The substitution kinetics of $Ru_3(CO)_{11}L$ and $Ru_3(CO)_{10}L_2$ (where L = various phosphines and phosphites) using $AsPh_3$ and various P-donor ligands are reported. Reaction rates (first-order and second-order) are analyzed relative to electronic and steric parameters [52]. Dppp has been allowed to react with $Os_3(CO)_{10}(MeCN)_2$ and $Os_3(CO)_{10}(\eta^4$-*cis*-butadiene) to give only $Os_3(CO)_{10}(\mu$-dppp). Protonation using TFA occurs at the dppp-bridged Os–Os bond to yield $[HOs_3(CO)_{10}(\mu\text{-dppp})]^+$. Both $Os_3(CO)_{10}(\mu$-dppm) and $Os_3(CO)_{10}(\mu$-dppp) react with additional diphosphine ligand to give $Os_3(CO)_8(\mu\text{-dppm})_2$ and $Os_3(CO)_9(\mu\text{-dppp})(\eta^1\text{-dppp})$. Protonation of $Os_3(CO)_8(\mu\text{-dppm})_2$ with TFA leads to $[HOs_3(CO)_8(\mu\text{-dppm})_2]^+$, where the hydride ligand resides across the non-dppm-bridged Os–Os bond. The X-ray structures of three triosmium clusters are reported, and the effect of the phosphine ligand's methylene chain length on the coordination chemistry is discussed [53]. The reaction of impure cycloheptatriene with $Ru_3(CO)_{10}(\mu$-dppm) leads to $Ru_3(CO)_7(\mu_3\text{-}C_7H_8)(\mu\text{-dppm})$ and $Ru_3(CO)_7(\mu_3\text{-}C_7H_{10})(\mu\text{-dppm})$. The exact molecular structures of these clusters were established by X-ray crystallography [54].

The reaction between the redox-active diphosphine ligand bpcd and $Ru_3(CO)_{12}$ has been examined. While the cluster $Ru_3(CO)_{10}$(bpcd) may be isolated under controlled conditions, it is shown to decompose readily at ambient temperature to afford $Ru_3(CO)_{12}$, $Ru_2(CO)_6$(bpcd), and $Ru_2(CO)_6\{\mu\text{-}\overline{C{=}C(PPh_2)C(O)CH_2C}(O)\}(\mu_2\text{-}PPh_2)$. The redox properties of the bpcd-substituted complexes were explored by cyclic voltammetry, and the nature of the HOMO and LUMO in these complexes was established by extended Hückel MO calculations [55]. The disubstituted triosmium clusters $Os_3(CO)_{10}L$ (where L = 2,2′-bpy, 2,2′-bpm, dpp, dpb) have been prepared and their photochemistry explored. Irradiation into the MLCT transitions does not lead to productive photochemistry in toluene solvent. However, use of coordinating solvents affords a transient species, whose structure is formulated as $Os^-(CO)_4\text{-}Os(CO)_4\text{-}Os^+(CO)_2$(solvent)L, on the basis of spectroscopic analyses. When 2-MeTHF is used as a solvent, a stable, zwitterionic photoproduct may be obtained at 133 K. The photochemistry and the nature of the ancillary L group in promoting the heterolytic Os–Os bond cleavage are fully discussed [56]. Pentaphenylcyclopentaphosphine reacts with $Os_3(CO)_{10}(MeCN)_2$ to yield a pair of inversion isomers having the molecular formula $Os_3(CO)_{10}(PC_6H_5)_5$. When the same phosphine is allowed to react with $Os_3(CO)_{11}(MeCN)$, the clusters $Os_3(CO)_{11}(PC_5H_5)_5$ and $\{Os_3(CO)_{11}\}_2(PC_5H_5)_5$ are isolated as the sole products. The X-ray structures of all four of these clusters reveal the presence of an intact cyclopolyphosphine ring [57]. The solution structures and the dynamic ligand behavior of the clusters $M_3(CO)_{12-x}(MeCN)_x$ (where $M = Os$, $x = 1, 2$; $M = Ru$, $x = 1, 2, 3$) were investigated by $^{13}C$-NMR spectroscopy. The lowest energy CO exchange process in these clusters involves a delocalized type merry-go-round mechanism, with a localized exchange occurring at higher energy. The ability of the acetonitrile ligand(s) to stabilize bridging CO ligands and the role of the MeCN ligand(s) in facilitating CO exchange are discussed [58]. The 48-electron cluster $Ru_3(CO)_8(\mu_3,\eta^4$-PhPCPhCPhPPhCPhCPh) has been obtained from the reaction between $Ru_3(CO)_{12}$ and 1,2,3-triphenylphosphirene in refluxing THF. The X-ray structure (Fig. 4.) confirms the coupling of the two opened phosphirene rings present in the product. A working mechanism involving ring opening and P–C bond cleavage is presented [59].

The alkynyl-bridged cluster $Ru_3(CO)_9(\mu_2\text{-}H)(\mu_3,\eta^2\text{-}C{\equiv}CBu^t)$ reacts with the

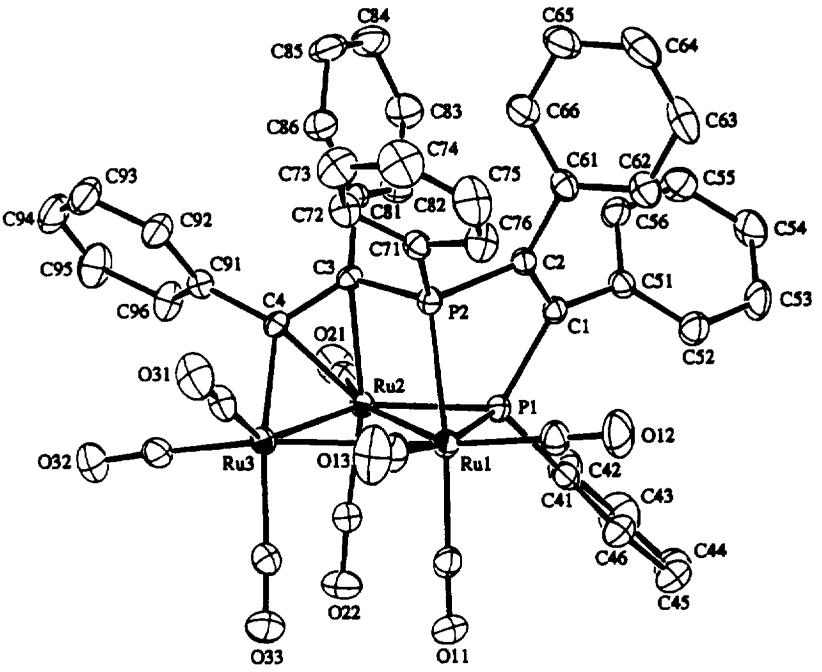

Fig. 4. X-ray structure of $Ru_3(CO)_8(\mu_3,\eta^4$–PhPCPhCPhPPhCPhCPh). Reprinted with permission from Organometallics. Copyright 1995 American Chemical Society.

diphosphine ligand bpcd in the presence of $Me_3NO$ to give $Ru_3(CO)_7(\mu_2\text{-}H)(\mu_3,\eta^2\text{-}C{\equiv}CBu^t)(bpcd)$. X-ray diffraction analysis shows that the bpcd ligand coordinates to the unique ruthenium atom in a chelating fashion. Cyclic voltammetric data and the results of extended Hückel MO calculations are reported [60].

Treatment of $Fe_3(CO)_{12}$ with asymmetric alkynes ($RC_2R'$) gives a variety of tri- and dinuclear complexes. Each of the products exists in two or three isomeric forms [61]. Diphenylacetylene reacts with $Ru_3(CO)_{10}(MeCN)_2$ to give $Ru_3(CO)_8(PhC{\equiv}CPh)_2$ and $Ru_3(CO)_8(C_4Ph_4)$. This latter cluster arises from the coupling of two alkyne ligands, giving a cluster that possesses a pentagonal bipyramidal $Ru_3C_4$ core, as confirmed by X-ray crystallography [62]. The osmacyclopentadiene ring present in the cluster $Os_3(CO)_9\{\mu_3,\eta^1{:}\eta^1{:}\eta^2{:}\eta^2\text{-}C(SiMe_3)C(Me)C(H)C(Ph)\}$, which is the product from the reaction between phenylacetylene and $Os_3(CO)_9(\mu\text{-}CO)(\mu_3\text{-}Me_3SiC_2Me)$, has been verified by X-ray crystallography (Fig. 5). Thermolysis of this same cluster in refluxing benzene yields $Os_3(CO)_8(\mu\text{-}H)\{\mu_3\text{-}C(SiMe_3)C(Me)C(H)C(C_6H_4)\}$ and $Os_2(CO)_6\{\mu,\eta^1{:}\eta^1{:}\eta^4\text{-}C(SiMe_3)C(Me)C(H)C(Ph)\}$. The rearranged osmacyclopentadiene moiety in the former cluster is coordinated to one edge of the cluster. Solution characterization and $PPh_3$ substitution reactivity are presented [63].

The alkynes $RC{\equiv}CH$ (where $R = Ph$, $SiMe_3$) and $RC{\equiv}CR'$ (where $R = R' = Me$,

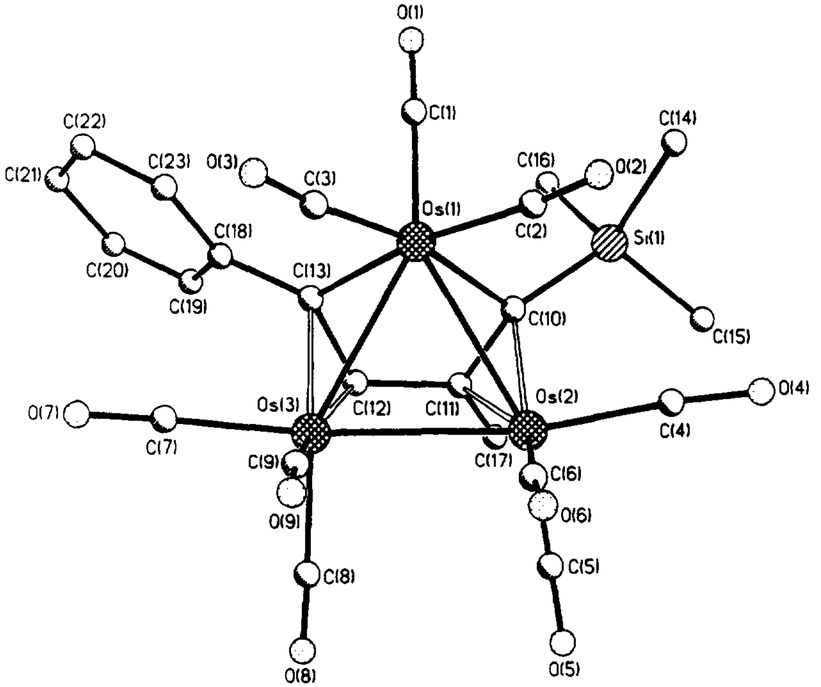

Fig. 5. X-ray structure of $Os_3(CO)_9\{\mu_3,\eta^1{:}\eta^1{:}\eta^2{:}\eta^2\text{-}C(SiMe_3)C(Me)C(H)C(Ph)\}$. Reprinted with permission from Organometallics. Copyright 1995 American Chemical Society.

Ph; R = Me, R′ = Et) have been allowed to react with $Ru_3(CO)_9(MeCN)_3$. The terminal alkynes yield the acetylide-bridged clusters $HRu_3(CO)_9(\mu_3,\eta^2\text{-}C{\equiv}CR)$ in high yield, while the disubstituted alkynes give the aryl-bridged cluster $Ru_3(CO)_9(\mu_3\text{-}\eta^2{:}\eta^2{:}\eta^2\text{-}C_6R_3R'_3)$, via a [2+2+2] cyclotrimerization sequence. All of the product clusters were characterized in solution by the normal methods and by comparison to known compounds [64]. Binuclear and tetranuclear ruthenium compounds containing an $\eta^3$-coordinated dihydropyranyl ring have been isolated from the reaction between $Ru_3(CO)_{12}$ and the enones PhCH=CHC(O)R (where R = Me, $C_6H_4Me$-4). The identity of the dihydropyranyl ring in each compound was ascertained by X-ray crystallography [65]. Treatment of $Ru_3(CO)_{12}$ with potassium-benzophenone affords the acyl-substituted cluster $Ru_3(CO)_9(\mu_2\text{-}H)\{\mu_3\text{-}\sigma{:}\sigma{:}\eta^2\text{-}C(O)Ph\}$. The solid-state structure confirms the presence of the bridging acyl ligand, whose origin is presumed to be from benzophenone [66].

The clusters $Ru_3(CO)_{12}$, $Ru_3(CO)_9(\mu_3\text{-}\eta^2{:}\eta^2{:}\eta^2\text{-}C_6H_6)$, and the 1,3,5-trithiacyclohexane derivative $Ru_3(CO)_9(\mu_3\text{-}\eta^2{:}\eta^2{:}\eta^2\text{-}S_3C_3H_6)$ have been explored by extended Hückel MO calculations, empirical atom–atom pairwise packing potential energy calculations, and computer graphics in order to study the relationship between the molecular and crystal structures. The nature of the facial ligand in promoting bridging CO groups is discussed relative to the extended Hückel data. The presence of hydrogen-bonding networks involving the facial C–H bonds and the carbonyl oxygens is also discussed [67]. Thermolysis of the [2.2]paracyclophane-substituted cluster $Ru_3(CO)_9(\mu_3\text{-}\eta^2{:}\eta^2{:}\eta^2\text{-}C_{16}H_{16})$ in octane furnishes the carbido cluster $Ru_6C(CO)_{14}(\mu_3\text{-}\eta^2{:}\eta^2{:}\eta^2\text{-}C_{16}H_{16})$, which upon treatment with $Me_3NO$ in $CH_2Cl_2$ gives the original triruthenium cluster. The cyclophane ligand in $Ru_3(CO)_9(\mu_3\text{-}\eta^2{:}\eta^2{:}\eta^2\text{-}C_{16}H_{16})$ is converted to a terminally bonded ligand when treated with diphenylacetylene, as demonstrated by the cluster products $Ru_3(CO)_7(\mu_3\text{-}\eta^2{:}\eta^2{:}\eta^2\text{-}C_2Ph_2)(\eta^6\text{-}C_{16}H_{16})$ and $Ru_3(CO)_7\{\mu_3\text{-}\eta^2\text{-}PhC_2C(O)Ph\}(\eta^6\text{-}C_{16}H_{16})$. Four X-ray structures and the solution NMR data are presented in this paper [68]. $Ru_3(CO)_{12}$ reacts with (−)-bromomenthyltetraphenylcyclopentadiene to give the mononuclear complex $[(C_5Ph_4R)Ru(CO)_3][Br]$ (where R = menthyl), which upon heating loses CO to furnish the corresponding neutral compound $(C_5Ph_4R)Ru(CO)_2Br$. The X-ray structure of the latter compound accompanies this report [69]. Two different coordination modes for benzene in $Os_3(CO)_6(\mu_3\text{-}\eta^2{:}\eta^2{:}\eta^2\text{-}C_6H_6)(\eta^6\text{-}C_6H_6)$ have been confirmed by X-ray analysis. This particular bis(benzene) cluster was isolated from the diene cluster $Os_3(CO)_8(\mu_3\text{-}\eta^2{:}\eta^2{:}\eta^2\text{-}C_6H_6)(\eta^4\text{-}C_6H_8)$ through a multistep sequence [70]. Several new [60]fullerene-substituted clusters have been prepared and characterized by IR and $^{13}C$-NMR spectroscopy. The clusters include $Os_3(CO)_{11}(\eta^2\text{-}C_{60})$, $Os_3(CO)_{10}(PPh_3)(\eta^2\text{-}C_{60})$, and $Os_3(CO)_9(PPh_3)_2(\eta^2\text{-}C_{60})$ [71]. The Wittig reagent $H_2C{=}PPh_3$ reacts with $Os_3(CO)_9(\mu_3\text{-}\eta^2{:}\eta^2{:}\eta^2\text{-}C_6H_5Ph)$ at the arene ring to afford the carbene complex $Os_3(CO)_9(\mu_3\text{-}\eta^2{:}\eta^2{:}\eta^2\text{-}H_2C{=}C_6H_5Ph)$. The product was characterized in solution by IR and $^1H$-NMR spectroscopy, and the molecular structure was determined by X-ray diffraction analysis [72]. The synthesis and X-ray structures of $Ru_3(CO)_7\{\mu_3\text{-}\eta^2{:}\eta^2{:}\eta^2\text{-}C_6H_4\text{-}(\eta^2\text{-}CCH_3CH_2)_2\text{-}1,3\}$, $Ru_4(CO)_9\{\mu_3\text{-}\eta^2{:}\eta^2{:}\eta^2\text{-}C_6H_4\text{-}(\eta^2\text{-}CCH_3CH_2)_2\text{-}1,3\}$, $Ru_3(CO)_8\{\mu_3\text{-}\eta^2{:}\eta^2{:}\eta^2\text{-}C_6H_5\text{-}(\eta^2\text{-}CCH_3CH_2)\}$, and $Ru_4(CO)_{10}\{\mu_3\text{-}\eta^2{:}\eta^2{:}\eta^2\text{-}C_6H_5\text{-}(\eta^2\text{-}CCH_3CH_2)\}$ (Fig. 6)

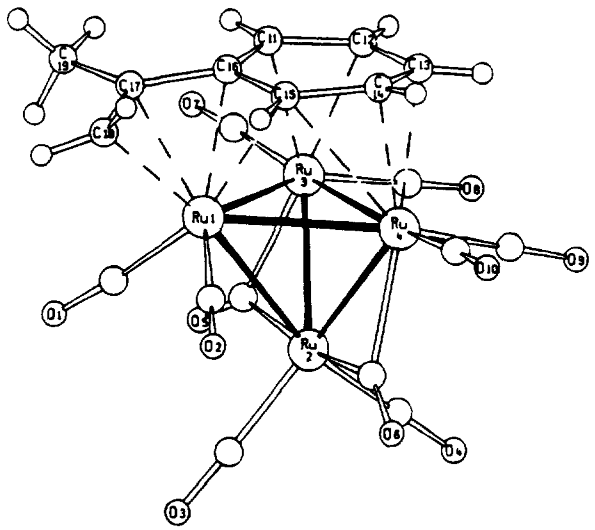

Fig. 6. X-ray structure of $Ru_4(CO)_{10}\{\mu_3\text{-}\eta^2\text{:}\eta^2\text{:}\eta^2\text{-}C_6H_5\text{-}(\eta^2\text{-}CCH_3CH_2)\}$. Reprinted with permission from Organometallics. Copyright 1995 American Chemical Society.

have been published. The observed facial coordination exhibited by the aromatic rings is discussed relative to the propenyl substituent(s) [73].

The imido-capped cluster $Ru_3(CO)_9(\mu_3\text{-}CO)(\mu_3\text{-}NPh)$ has been examined by $^{13}C$-NMR spectroscopy and $^{13}C$-spin-lattice ($T_1$) relaxation times for the phenyl group and the equatorial carbonyl groups. These groups were studied as a function of temperature and resonance frequency. A small barrier to the internal rotation of the phenyl group has been found, the nature of which is attributed to intramolecular steric interactions between the carbonyl groups and the *ortho* protons of the phenyl group. While both Fenske-Hall and extended Hückel calculations confirm the presence of this rotation barrier, the former method substantially overestimates the barrier [74]. Variable-temperature $^{13}C$-NMR studies on $Ru_3(CO)_9(\mu_3\text{-}CO)(\mu_3\text{-}NPh)$ were conducted and two distinct CO exchange processes observed. The lowest energy exchange pathway involves the 3-fold scrambling of equatorial/axial CO groups at each ruthenium center. At higher temperatures the $\mu_3$-bridging CO group is shown to exchange with only the equatorial CO groups. The direct exchange of the $\mu_3$-CO group with an axial CO group was ruled out on the basis of 2D EXSY measurements. Fig. 7 shows the likely exchange pathway associated with the higher energy process [75].

$Fe_3(CO)_{12}$ reacts with aromatic nitriles under hydrogen to yield the nitrile-capped clusters $Fe_3(CO)_9(\mu_3\text{-}\eta^2\text{-}RC{\equiv}N)$. The stability of the resulting products is related to the electronic properties of the aromatic moiety. Electron-donating groups on the aromatic ring decrease the stability of the nitrile-capped clusters, as does phosphine-ligand substitution in these clusters. The X-ray structure of $Fe_3(CO)_8\{P(OMe)_3\}(\mu_3\text{-}\eta^2\text{-}PhC{\equiv}N)$ is included in this report [76]. Thermolysis of $Ru_3(CO)_{12}$ in octane with 7-isopropyl-1,4-dimethylazulene yields the crystallographi-

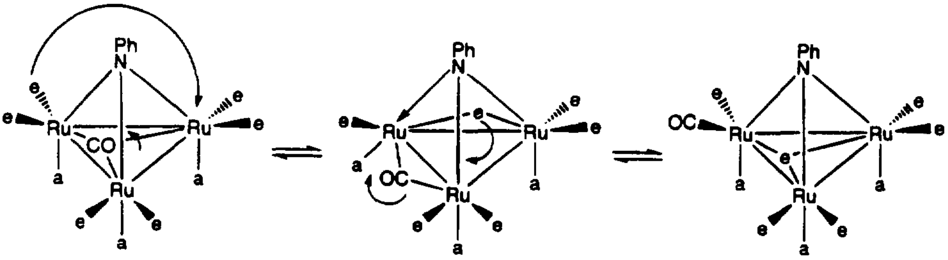

Fig. 7. Pathway for $\mu_3$-CO/equatorial CO exchange in $Ru_3(CO)_9(\mu_3\text{-}CO)(\mu_3\text{-}NPh)$. Reprinted with permission from Organometallics. Copyright 1995 American Chemical Society.

cally characterized clusters $Ru_3(CO)_7(\mu_3\text{-}\eta^5{:}\eta^3{:}\eta^3\text{-}C_{15}H_{18})$ and $Ru_4(CO)_9(\mu_3\text{-}\eta^5{:}\eta^3{:}\eta^3\text{-}C_{15}H_{18})$ [77]. The Schiff base 4-hydroxyphenyl-*N*,*N*′-dimethylimide reacts with $Ru_3(CO)_{12}$ in refluxing cyclohexane to give $Ru_3(CO)_9(\mu\text{-}H)_2\{\mu_3\text{-}\eta^2\text{-}(N,C)\text{-}4\text{-}HOC_6H_4N{=}CMeCH\}$. X-ray crystallography confirms the double C–H bond activation of the methyl ligand. Data are presented that show that this reaction is specific for the imine-bound methyl group [78]. The reaction of various diazaheterocycles with $Os_3(CO)_{11}(MeCN)$ is reported. The products from these reactions, $Os_3(CO)_{11}(L\text{-}H)$ (where L-H = 1-vinylimidazole, imidazole, pyrazole), undergo further reaction at elevated temperature to yield $Os_3(CO)_{10}(\mu\text{-}H)(\mu\text{-}L)$. Reaction of the imidazole ligands with $Ru_3(CO)_{12}$ in the presence of sodium-benzophenone gives the cyclometalated clusters $Ru_3(CO)_{10}(\mu\text{-}H)(\mu\text{-}2,3\text{-}\eta^2\text{-}\,\overline{C{=}NCH{=}HN}\,R)$. Two of the many products were crystallographically characterized [79]. New asymmetrically bridged 2,7-disubstituted naphthyridine compounds have been synthesized from $Ru_3(CO)_{12}$ and the corresponding heterocycle. X-ray structures and $^1H$-NMR data are presented [80]. The coordination of diphenylacetylene to $Ru_3(CO)_9(\mu\text{-}H)(\mu_3\text{-ampy})$ has been investigated with respect to cluster-promoted alkyne hydrogenation reactivity. This report includes the synthesis and characterization of a cationic 48-electron triruthenium carbonyl cluster that does not contain ancillary hydride ligands [81]. The interaction of $Ru_3(CO)_9(\mu\text{-}H)(\mu_3\text{-ampy})$ with silica and $\gamma$-alumina has been studied by IR spectroscopy, and the resulting surface-supported clusters examined for their catalytic activity in phenylacetylene hydrogenation reactions. Data are presented showing that (1) the silica-derived catalysts are more reactive than the alumina-supported systems, and (2) surface-supported mononuclear catalysts, prepared by thermally controlled cluster fragmentation reactions, are more reactive catalysts than the cluster-supported complexes [82]. The reaction between $[Ru_3(CO)_{10}(\mu\text{-}CO)(\mu\text{-}H)]^-$ and 3,5-$Me_2$pyrazole gives $[Ru_3(CO)_7(\mu\text{-}CO)_3(\mu\text{-}3,5\text{-}Me_2\text{pyrazole})]^-$ in high yield. The chemistry of the pyrazole-substituted cluster with protic acids, alkynes, $R_3SiH$, and $R_3SnH$ has also been explored. The products from these reactions were characterized in solution by IR and NMR ($^1H$ and $^{13}C$) spectroscopy, and the molecular structure of $[Ru_3(CO)_6(\mu\text{-}CO)_2(\mu_3\text{-}PhC{\equiv}CPh)(\mu\text{-}3,5\text{-}Me_2\text{pyrazole})]^-$ was determined by X-ray diffraction analysis (Fig. 8) [83].

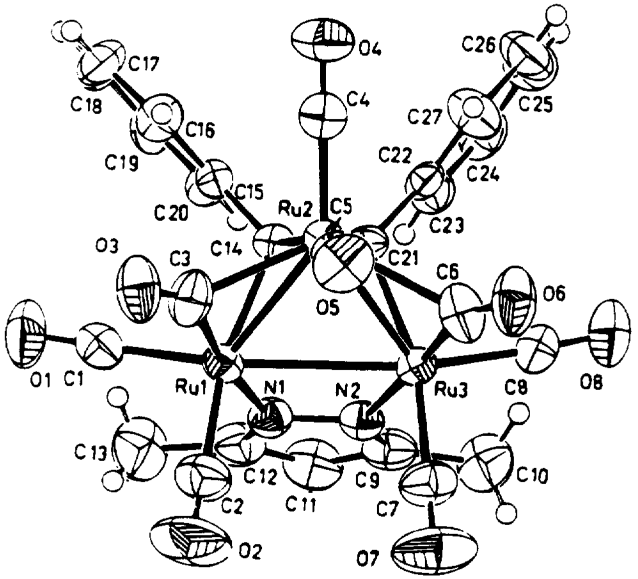

Fig. 8. X-ray structure of $[Ru_3(CO)_6(\mu\text{-}CO)_2(\mu_3\text{-}PhC{\equiv}CPh)(\mu\text{-}3,5\text{-}Me_2pyrazole)]^-$. Reprinted with permission from Organometallics. Copyright 1995 American Chemical Society.

The clusters $Os_3(CO)_{10}(NC_5H_4\text{-}N{=}N\text{-}Ph)$ and $Os_3(CO)_{10}(\mu\text{-}H)\{NC_5H_3\text{-}N\text{–}N(O)\text{-}Ph\}$ have been isolated from the reaction between 2-azopyridine and $Os_3(CO)_{10}(MeCN)_2$. The latter azo cluster contains an ortho-metalated pyridine ring and oxidized azo nitrogen atom. Besides solution characterization, the X-ray structures ascertain the identity of these azopyridine-substituted clusters [84]. The dynamics and coordination chemistry of a monometallic site in the $\mu_3$-imidoyl-substituted cluster $Os_3(CO)_9(\mu\text{-}H)\{\mu_3\text{-}\eta^2\text{-}\overline{C{=}N(C}H_2)_3\}$ with nitrogen donor ligands have been investigated. Several donor ligands are shown to attack the axial position at the unbridged osmium atom that is *syn* to the $\mu_3$-imidoyl ligand. The initially formed kinetic isomers rearrange, via a first-order process, to give *anti*/*syn* mixtures, whose ratio is dependent on the nature of the nitrogen donor ligand. Phosphine substitution chemistry and thermolysis reactivity are also reported. Included in this report are four X-ray structures [85]. HX addition to the $\mu_3$-imidoyl cluster $Os_3(CO)_9(\mu\text{-}H)(\mu_3\text{-}\eta^2\text{-}\overline{C{=}NCH_2CH_2C}H_2)$ affords the neutral acid adducts $Os_3(CO)_9(\mu\text{-}H)_2(\mu\text{-}\eta^2\text{-}\overline{C{=}NCH_2CH_2C}H_2)X$ (where X = Cl, Br, $CF_3SO_3$, $CF_3CO_2$). The X-ray structures of two of these products confirm the presence of an axially disposed X group, which is on the same face of the cluster as the μ-imidoyl ligand. Upon thermolysis, the X group migrates to the opposite face of the cluster. Variable-temperature $^1H$- and $^{13}C$-NMR measurements (1D and 2D methods) have been used to study the ligand dynamics about the cluster polyhedron. Mechanisms dealing with the ligand exchange properties are presented and discussed relative to the solid-state structures and 2D NMR data [86]. Quinolines react with $Os_3(CO)_{10}(MeCN)_2$ at room temperature to give

$Os_3(CO)_{10}(\mu\text{-}H)\{\mu\text{-}\eta^2\text{-}C_9H_4(R)(R')N\}$ (where $R=R'=H$; $R=4\text{-Me}$, $R'=H$; $R=H$, $R'=6\text{-Me}$). Thermal decarbonylation of these clusters yields the unsaturated clusters $Os_3(CO)_9(\mu\text{-}H)\{\mu_3\text{-}\eta^2\text{-}C_9H_4(R)(R')N\}$, whose reactivity with hydride and acids have been fully explored. Fig. 9 shows the X-ray structure of $Os_3(CO)_9(\mu\text{-}H)\{\mu_3\text{-}\eta^2\text{-}C_9H_4(4\text{-Me})(H)N\}$ [87].

The alkylidyne-capped cluster $Os_3(CO)_9(\mu\text{-}H)_3(\mu_3\text{-}CCl)$ reacts with DBU in the presence of 4,4′-bpy or 2,4′-bpy to give $Os_3(CO)_9(\mu\text{-}H)_2\{\mu_3\text{-}C(4,4'\text{-bpy})\}$ and $Os_3(CO)_9(\mu\text{-}H)_2\{\mu_3\text{-}C(2,4'\text{-bpy})\}$, respectively. Attachment of the pendant pyridyl ligands to the alkylidyne carbon was confirmed by X-ray crystallography [88]. Treatment of $Os_3(CO)_9(\mu\text{-}H)_3(\mu_3\text{-}CCl)$ with DBU and 4-vinylpyridine gives the functionalized cluster $Os_3(CO)_9(\mu\text{-}H)_2(\mu_3\text{-}CNC_5H_4CH{=}CH_2)$ in good yield. The pendant vinyl group was next functionalized by reaction with $Os_3(CO)_{10}(MeCN)_2$ to give $Os_3(CO)_9(\mu\text{-}H)_2(\mu_3\text{-}CNC_5H_4CH{=}CH)Os_3(CO)_{10}(\mu\text{-}H)$. In an analogous reaction, the vinyl group was converted to an acetyl group via a Wacker-type reaction using Wilkinson's catalyst. The isolated cluster $Os_3(CO)_9(\mu\text{-}H)_2\{\mu_3\text{-}CNC_5H_4\text{-}C(O)Me\}$ was structurally characterized by X-ray crystallography. All of the vinylpyridine-derived clusters exhibit MLCT transitions with large negative solvatochromism [89]. Thermally induced alkylidyne-alkyne coupling has been observed in the reaction between

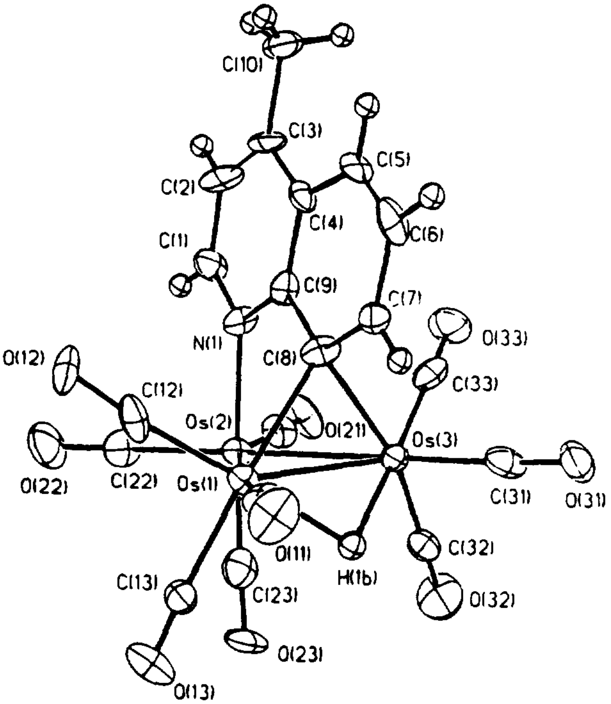

Fig. 9. X-ray structure of $Os_3(CO)_9(\mu\text{-}H)\{\mu_3\text{-}\eta^2\text{-}C_9H_4(4\text{-Me})(H)N\}$. Reprinted with permission from Organometallics. Copyright 1995 American Chemical Society.

$Os_3(CO)_9(\mu\text{-}H)_2(\mu_3\text{-}CNC_5H_4CH{=}CH_2)$ and phenylacetylene. The reaction yields the following two pairs of geometrical isomers: $Os_3(CO)_9(\mu\text{-}H)\{\mu_3\text{-}\eta^3\text{-}PhCCHC(CH{=}CHPh)\}$, $Os_3(CO)_9(\mu_3\text{-}\eta^1,\eta^2,\eta^2,\eta^1\text{-}PhCHCH{=}CHCH{=}CPh)$, and $Os_3(CO)_7\{\mu\text{-}\eta^2,\eta^3\text{-}CH_2{=}CHC(Ph)CHCPh\}\{\mu_3\text{-}\eta^2\text{-}C(O)C(Ph){=}CH\}$, $Os_3(CO)_7\{\mu\text{-}\eta^2,\eta^3\text{-}PhCH{=}CHC(Ph)CHCH\}\{\mu_3\text{-}\eta^2\text{-}C(O)C(Ph){=}CH\}$. When the same reaction is carried out at room temperature, the new cluster $Os_3(CO)_8(\mu\text{-}\eta^2\text{-}PhCCH_2)(\mu_3\text{-}\eta^3\text{-}CHCPhCH)$ may be isolated as the major product. These new clusters have been characterized in solution by IR and NMR spectroscopy, and the solid-state structures determined by X-ray crystallography. A mechanistic scheme showing how the ancillary 4-vinylpridine ligand is lost is presented [90]. Monophosphine and chiral diphosphine ligands have been studied for their reactivity at the alkylidyne carbon in $Os_3(CO)_9(\mu\text{-}H)_3(\mu_3\text{-}CCl)$. The cluster $Os_3(CO)_9(\mu\text{-}H)_2(\mu_3\text{-}CPBuPh_2)$ was isolated when $PBuPh_2$ was used, while the isomeric clusters (R)-$Os_3(CO)_9(\mu\text{-}H)_2\{\mu_3\text{-}CPPh_2CH(Me)CH_2PPh_2\}$ and (R)-$Os_3(CO)_9(\mu\text{-}H)_2\{\mu_3\text{-}CPPh_2CH_2CH(Me)PPh_2\}$ were obtained when the optically active ligand (R)-$Ph_2PCH(Me)CH_2PPh_2$ was employed. The former isomer undergoes decarbonylation, followed by capture of the pendant $PPh_2$ group, to give (R)-$Os_3(CO)_8(\mu\text{-}H)_2\{\mu_3\text{-}CPPh_2CH(Me)CH_2PPh_2\}$. The relative position of the phosphine's methyl group prevents the latter chiral cluster from adopting the required six-membered cluster-diphosphine ring in the product. The relationship between these zwitterionic clusters and Wittig reagents is discussed [91]. Site-selective protonation chemistry is reported for $Os_3(CO)_9(\mu\text{-}H)_2(\mu_3\text{-}CNC_5H_4C_5H_4N)$, which is prepared from $Os_3(CO)_9(\mu\text{-}H)_3(\mu_3\text{-}CCl)$ and 2,2′-bpy. The initial protonation occurs at the free nitrogen center to give the monocationic cluster $[Os_3(CO)_9(\mu\text{-}H)_2(\mu_3\text{-}CNC_5H_4C_5H_4NH)]^+$, with the metal core being the site of the second protonation. The water-soluble dicationic trihydride cluster has been structurally characterized. The same starting cluster was also examined in methylation reactions using Meerwein's reagent [92]. Replacement of the chloro group in $Os_3(CO)_9(\mu\text{-}H)_3(\mu_3\text{-}CCl)$ by thiane and 1,4-dithiane gives $Os_3(CO)_9(\mu\text{-}H)_2\{\mu_3\}\text{-}C\,S(CH_2)_4C\,H_2\}$ and $Os_3(CO)_9(\mu\text{-}H)_2\{\mu_3\text{-}C\,S(CH_2)_2SCH_2C\,H_2\}$, respectively. The latter cluster rearranges slowly to produce the ketenylidene-bridged cluster $Os_3(CO)_8(\mu\text{-}H)_2\{\,S(CH_2)_2SCH_2C\,H_2\}(\mu_3\text{-}CCO)$, which forms as a result of a S/CO exchange process. All three clusters were fully characterized in solution and by X-ray crystallography [93].

Unstable radical cations have been generated from $Ru_3(CO)_6(PPh_3)_3(\mu\text{-}H)_2(RCCR')$ (where R = R′ = Et, Ph; R = H, R′ = OEt) by electrochemical and chemical methods. The halide-induced disproportionation of the radical cation $Ru_3(CO)_6(PPh_3)_3(\mu\text{-}H)_2(EtCCEt)^+$ and the electrophilic addition of $Cl_2$, $I_2$, and TFA to the neutral clusters are discussed. Two X-ray structures are included in this report, and the details of the electrochemical and EPR studies on the 47-electron clusters are published [94]. The first ruthenium-lead clusters have been prepared. Treatment of $Pb(CH_2SiMe_3)_2$ with $Ru_3(CO)_{12}$ at 60°C affords $Ru_3(CO)_9(\mu\text{-}CO)_2\{\mu\text{-}Pb(CH_2SiMe_3)_2\}$ and $Ru_3(CO)_9(\mu\text{-}CO)\{\mu\text{-}Pb(CH_2SiMe_3)_2\}_2$. The X-ray structure of the latter cluster reveals the presence of a planar pentametallic core, where the two $PbR_2$ moieties bridge two sides of the $Ru_3$ triangle [95]. P–P-

Bonded cluster oligomers have been synthesized in order to probe intercluster electronic interactions. Treatment of the monofunctional clusters $Fe_3(CO)_9(\mu_3\text{-PMe})(\mu_3\text{-PH})$ and $Fe_3(CO)_9(\mu_3\text{-PMe})(\mu_3\text{-PCl})$ with $Et_3N$ at low temperature leads to P–P bond formation and the linked cluster $Me[PFe_3(CO)_9P]_2Me$. Using the tin derivative $Fe_3(CO)_9(\mu_3\text{-PSnMe}_3)_2$ and $Fe_3(CO)_9(\mu_3\text{-PMe})(\mu_3\text{-PCl})$ allows for the isolation of the tricluster product $Me[PFe_3(CO)_9P]_3Me$. The X-ray structure of the dicluster product and electronic absorption data for these clusters are presented [96]. The 1-naphthyl ligands $E(1\text{-}C_{10}H_7)_3$ (where E = P, As) were allowed to react with $M_3(CO)_{12}$ (where M = Ru, Os) to give the naphthyl complexes $M_3(CO)_8(\mu\text{-H})_2\{\mu_3\text{-}\eta^4\text{-}(C_{10}H_7)_2E(C_{10}H_5)\}$. These clusters arise by a double metalation of the unsubstituted aryl ring. Metalation of the substituted aryl ring furnishes the cluster $Os_3(CO)_9(\mu\text{-H})\{(C_{10}H_7)_2P(C_{10}H_5)\}$. The cluster $Ru_4(CO)_{10}(\mu\text{-CO})\{\mu_4\text{-As}(C_{10}H_7)\}(\mu_4\text{-}C_{10}H_6)$ (Fig. 10), which results from the cleavage of an As-naphthyl bond, possesses a $Ru_4$ plane and is formally electron deficient [97].

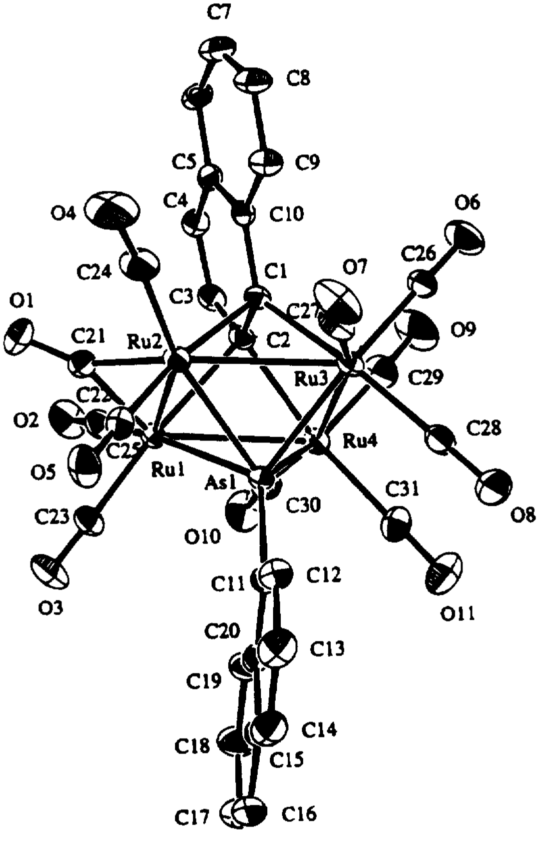

Fig. 10. X-ray structure of $Ru_4(CO)_{10}(\mu\text{-CO})\{\mu_4\text{-As}(C_{10}H_7)\}(\mu_4\text{-}C_{10}H_6)$. Reprinted with permission from Organometallics. Copyright 1995 American Chemical Society.

The application of in situ FT-IRRAS (Fourier transform-infrared reflection absorption spectroscopy) with a thin-layer electrochemical cell has been demonstrated with the cluster $Ru_3(CO)(\mu_3\text{-}O)(\mu\text{-}AcO)_6(py)_2$. The higher oxidation states of this cluster were able to be analyzed by the FT-IRRAS technique despite their instability [98]. Chemical oxidation ($Ag^+$, $O_2$, $Me_3NO$) of $Ru_3(CO)_6(\mu\text{-dppm})_3$ gives the oxo cluster $Ru_3(CO)_3(\mu\text{-}CO)(\mu_3\text{-}O)(\mu\text{-dppm})_3$. The oxo-bridged cluster exhibits reversible protonation at the oxo cap to furnish the hydroxo-bridged cluster $[Ru_3(CO)_3(\mu\text{-}CO)(\mu_3\text{-}OH)(\mu\text{-dppm})_3]^+$. The molecular structure of the latter cluster has been determined by X-ray crystallography, and the fluxionality found in these clusters is discussed with respect to the steric congestion present in the $Ru_3(\mu\text{-dppm})_3$ unit [99].

$SO_2$ substitution chemistry in $[Ru_3(CO)_{11}]^{2-}$ has been published. The major products isolated were $[Ru_3(CO)_9(SO_2)]^{2-}$ and $[Ru_3(CO)_7(SO_2)_3]^{2-}$. Both of these clusters have been characterized by IR and $^{13}C$-NMR spectroscopy. The $SO_2$ group in the former cluster is bound in a $\mu_3,\eta^2$ mode, with the latter cluster exhibiting both $\mu_2$- and $\mu_3,\eta^2$-bound $SO_2$ ligands. The molecular structure of the tris(sulfur dioxide) cluster was confirmed by X-ray crystallography. Data are also presented showing the course of $SO_2$ acetylation in $[Ru_3(CO)_9(SO_2)]^{2-}$ [100]. The clusters $Os_3(CO)_{10}(\mu\text{-}H)(C_{14}H_{11}OS)$ (two isomers) and $Os_3(CO)_9(\mu\text{-}H)(C_{14}H_{11}OS)$ were obtained from the reaction of $Os_3(CO_{10}(MeCN)_2$ with 2-(benzylthio)benzaldehyde. The bonding modes exhibited by the ancillary thio ligand are discussed [101]. Cleavage of the S–Ph bond in $SPh_2$ occurs in the thermolysis reaction with $Ru_3(CO)_{12}$. No evidence for ortho-metalation is observed in the formation of $Ru_3(CO)_8(\mu\text{-}SPh)(\mu\text{-}\eta^1\text{:}\eta^6\text{-}C_6H_5)$. Treatment of $Ru_3(CO)_{12}$ with SFcPh gives the analogous cluster $Ru_3(CO)_8(\mu\text{-}SFc)(\mu\text{-}\eta^1\text{:}\eta^6\text{-}C_6H_5)$, along with minor amounts of $Ru_3(CO)_7(\mu\text{-}SFc)_4$ and $Ru_4(CO)_8(\mu_4\text{-}S)(\mu\text{-}SFc)_6$ [102]. The use of $Ph_3P{=}Se$ as a convenient synthon in the construction of clusters is described. Both $Fe_3(CO)_{12}$ and $Ru_3(CO)_{12}$ react with $Ph_3P{=}Se$ to give a variety of $PPh_3$-substituted selenium-capped clusters. The X-ray structures of $Fe_3(CO)_7(\mu\text{-}CO)(PPh_3)_2(\mu_3\text{-}Se)$, $M_3(CO)_7(PPh_3)_2(\mu_3\text{-}Se)_2$, and $Ru_4(CO)_7(\mu\text{-}CO)_2(PPh_3)_2(\mu_4\text{-}Se)_2$ are presented [103]. The polysulfur and polyselenium species $[S_8]^{2+}$ and $[Se_8]^{2+}$ react with $Fe(CO)_5$ and $Fe_2(CO)_9$ to give a variety of chalcogen-substituted clusters. X-Ray diffraction analysis of $[Fe_3(CO)_{10}(Se_2)_2]^{2+}$ reveals the existence of a picnic-basket shaped cluster, where two iron centers are linked by two $Se_2$ groups, all of which are capped by an $Fe(CO)_4$ moiety. The $Se_2$ group bridges two $Fe_2Se_2$ units in the X-ray structure of $[Fe_4(CO)_{12}(Se_2)_3]^{2+}$ [104]. Triangulated dodecahedral based clusters containing an $Fe_4E_4$ skeleton (where E = P, As) have been prepared from the thermolysis of $\{CpFe(CO)_2\}_2$ with added $E_4$. This report presents the X-ray structures of $Cp_4Fe_4(E_2)_2$ and $Cp_4Fe_4(P_2X_2)_2$ (where X = S, Se). The $Cp_4Fe_4(P_2X_2)_2$ clusters were obtained from the former phosphine-based cluster upon treatment with $S_8$ and gray selenium [105]. The use of $\{CpFe(CO)_2\}_2(\mu\text{-}S)$ as a building block in the synthesis of $[\{CpFe(CO)_2\}_3S]^+$ is described. The oxidation and decarbonylation chemistry exhibited by this triiron cluster is also reported [106]. Polysulfides and polyselenides of different chain lengths have been allowed to react with $Fe(CO)_5$. Several X-ray structures are reported, and the cyclic voltammetric data for the chalcogen-bridged clusters are discussed relative to the nature of the redox state [107]. The solid-state structure of the telluride-capped cluster $[Fe_3(CO)_9(\mu_3\text{-}Te)]^{2-}$, which was prepared from $Fe(CO)_5$ and $[Te]^{2-}$ in high yield, has been solved by X-ray diffraction analysis. The reaction of electrophiles with the apical telluride center has been investigated with a diverse group of electrophiles. The molecular structures of $[Fe_3(CO)_9(\mu_3\text{-}Te)(\mu\text{-}AuPPh_3)]^-$, $[\{Fe(CO)_4\}_4Te]^{2-}$, and $[Fe_3(CO)_9(Te)_2I]^-$ are discussed [108]. The effect that the presence or absence of the non-bonding electron pair associated with the capping arsenic atom has on the structure and reactivity in several clusters has been investigated. The synthesis and X-ray structure of $[HAs\{Fe(CO)_4\}_3]^{2-}$ are reported, and the reactivity of this cluster in pyrolysis, photolysis, and protonation studies is described. Complexation of the arsenic atom's lone electron pair by bonding with another group results in complicated cluster fragmentation and reorganization patterns [109]. The triangular clusters $(Cp^*Ru)_3(\mu_3\text{-}S)(\mu_3\text{-}Cl)$ and $(Cp^*Ru)_3(\mu_3\text{-}S)(\mu_3\text{-}SPr^i)$ have been prepared from $(Cp^*Ru)_4(\mu_3\text{-}Cl)_4$ and the appropriate sulfide. Use of $(Me_3Si)_2S$ leads to the former sulfido cluster and $(Cp^*Ru)_3(\mu_3\text{-}S)_2(\mu_2\text{-}H)$. The reaction of $(Cp^*Ru)_3(\mu_3\text{-}S)(\mu_3\text{-}Cl)$ with CO leads to the new carbonyl clusters $(Cp^*Ru)_3(\mu_3\text{-}S)(\mu\text{-}CO)_2(\mu_2\text{-}Cl)$ and $[(Cp^*Ru)_3(\mu_3\text{-}S)(\mu\text{-}CO)_3]^+$, the molecular structures of which were determined by X-ray crystallography (Fig. 11). Methyl propiolate is trimerized by $(Cp^*Ru)_3(\mu_3\text{-}S)(\mu_3\text{-}Cl)$ to the 1,3,5-, 1,2,4-isomers of $C_6H_3(CO_2Me)_3$ [110].

The reactivity of 1,4-dithiacyclohexane with $Os_3(CO)_{12-x}(MeCN)_x$ (where $x=0$, 1, 2) has been reported. MeCN displacement in the mono- and bisacetonitrile-substituted clusters yields $Os_3(CO)_{11}(\overline{SCH_2CH_2SCH_2C}\,H_2)$ and $Os_3(CO)_{10}(\overline{SCH_2CH_2SCH_2C}\,H_2)$, respectively. The decacarbonyl cluster possesses a chelating sulfur ligand, as shown by X-ray analysis. Thermolysis of this same cluster affords

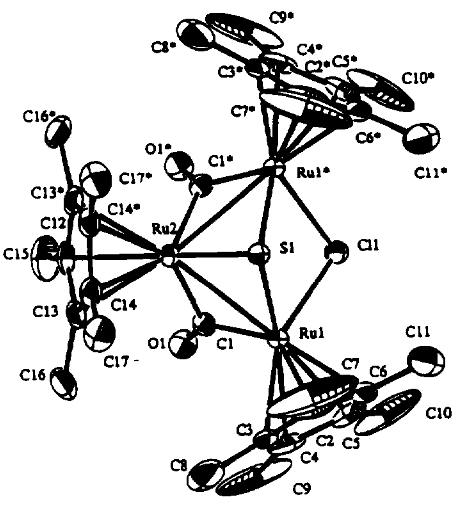

Fig. 11. X-ray structure of $[(Cp^*Ru)_3(\mu_3\text{-}S)(\mu\text{-}CO)_2(\mu\text{-}Cl)]^+$. Reprinted with permission from Organometallics. Copyright 1995 American Chemical Society.

$Os_3(CO)_9(\mu_3\text{-}\eta^2\text{-}CH{=}CH_2)(\mu\text{-}H)_2$, $Os_2(CO)_6(\mu\text{-}SCH_2CH_2S)$, $Os_3(CO)_{10}(\mu\text{-}SCH_2CH_2S)$, and $Os_3(CO)_8(\mu_3\text{-}\eta^2\text{-}CH{=}CH_2)(\overline{SCH_2CH_2SCH_2C}\,H_2)(\mu\text{-}H)_2$. NMR experiments reveal the presence of the coproduct ethylene [111]. Alkyne reactivity with the cyclobutyne-substituted cluster $Os_3(CO)_9\{\mu_3\text{-}\overline{C_2CH_2C}(Me)Bu^t\}(\mu_3\text{-}S)$ is reported. At low $RC{\equiv}CR$ levels, the clusters $Os_3(CO)_8\{\mu_3\text{-}SCC(Me)Bu^tCH_2CC(R)C(R)\}$ (where $R{=}Ph$, Et) may be isolated as the major products. The diphenylacetylene derivative contains an open triosmium core with a bridging thiol ligand formed by the formal cleavage of the cyclobutyne $C{\equiv}C$ bond and coupling of its carbon atoms with the diphenylacetylene molecule. Photolysis of the starting cyclobutyne cluster with added alkyne furnishes the *trans* and *cis* isomers of $[Os_3(CO)_8\{\mu_3\text{-}C_2CH_2C(Me)Bu^t\}(\mu_4\text{-}S)]_2$. The results of the chemistry in a large excess of added alkyne are presented, and mechanistic schemes outlining these cyclobutyne/alkyne activations are discussed [112]. The osmium compounds $Os_2(CO)_6(\mu\text{-}I)\{\mu\text{-}\overline{CC(Me)C}\,H_2CH_2\}$, $Os_3(CO)_9(\mu\text{-}I)\{\mu_3\text{-}CC(Me)CH_2CH_2\}$ (two different constitutional isomers), and $Os_3(CO)_{10}(\mu\text{-}I)\{\mu_3\text{-}\overline{CC(Me)CH_2C}\,H_2\}$ have been isolated from the reaction between $Os_3(CO)_{10}(MeCN)_2$ and 1-iodo-2-methylcyclobutene. The X-ray structures of the first three compounds are included. A mechanistic scheme showing the origin of the first three compounds from the intermediate cluster $Os_3(CO)_{10}(\mu\text{-}I)\{\mu_3\text{-}\overline{CC(Me)CH_2C}\,H_2\}$ is presented [113]. The coordination chemistry of polythiaethers to $Ru_3(CO)_{12}$ has been described. The clusters $Ru_3(CO)_7(\mu\text{-}CO)_2(1,1,1\text{-}\eta^3\text{-}1,5,9\text{-trithiacyclododecane})$ and $Ru_3(CO)_7(\mu\text{-}CO)_2(1,1,1\text{-}\eta^3\text{-}1,4,7\text{-trithiacyclononane})$ have been isolated and shown to possess $Fe_3(CO)_{12}$-like structures by X-ray crystallography. Both variable-temperature $^{13}C$-NMR spectroscopy and EXSY measurements have been employed in the study of the fluxional behavior of the ancillary CO groups. Data are presented for the existence of two bridge-terminal CO exchange processes. Refluxing the latter cluster in THF leads to the new compound $Ru_2(CO)_6(\mu\text{-}\eta^2\text{-}SCH_2CH_2S)$ and the known cluster $Ru_3(CO)_9(\mu\text{-}\eta^3\text{-}SCH_2CH_2SCH_2CH_2S)$, as a result of trithiacyclononane ligand degradation [114]. The reactivity of benzothiophene and 1-bromobenzothiophene with $Os_3(CO)_{10}(MeCN)_2$ has been explored. Both $Os_3(CO)_{10}(\mu\text{-}_6\,\overline{CC(Me)CH_2C}\,{}_6H_5)(\mu\text{-}H)$ and $Os_3(CO)_9(\mu_3\}\text{-}\,\overline{SCC}C_6\,H_5)(\mu\text{-}H)_2$ have been isolated and crystallographically characterized from the reaction employing benzothiophene. Use of 1-bromobenzothiophene affords the clusters $Os_3(CO)_{10}(\mu\text{-}\,\overline{CC(Me)CH_2C}\,{}_6H_5)(\mu\text{-}Br)$ (Fig. 12) and $Os_3(CO)_9(\mu_3\text{-}\,\overline{CC(Me)CH_2C}\,{}_6H_5)(\mu\text{-}Br)$, both of which were fully characterized and their molecular structures determined. The relationship between the various benzothiophene clusters was demonstrated by control experiments [115].

New phosphine-substituted derivatives of the $\mu\text{-}\eta^2$-methylidyne cluster $HFe_4(CO)_{12}(\mu\text{-}\eta^2\text{-}CH)$ have been synthesized. Use of $PCy_3$ leads to the ionic compound $[HFe_4(C)(CO)_{12}][HPCy_3]$. Variable-temperature $^{13}C$-NMR studies on $HFe_4(CO)_{11}(PPh_3)(\mu\text{-}\eta^2\text{-}CH)$ confirm the presence of intrametal site CO scrambling, while the $^1H$-NMR data ($T_1$ relaxation studies) reveal a slow dynamic process that interconverts hydridic and agostic hydrogen sites within the cluster. The X-ray structure of the $PPh_3$ derivative and extended Hückel and Fenske-Hall MO calcula-

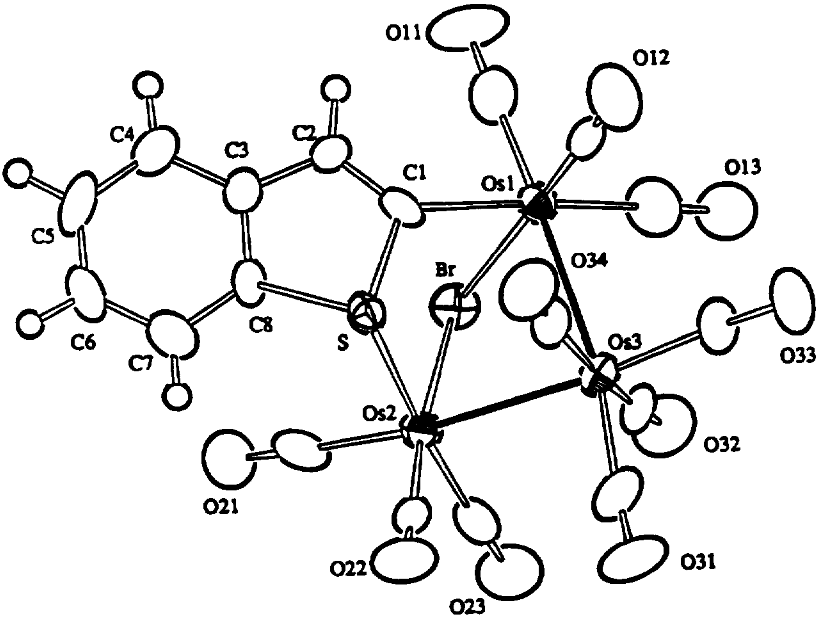

Fig. 12. X-ray structure of $Os_3(CO)_{10}(\mu\text{-}\overline{CC(Me)CH_2C}{}_6H5)(\mu\text{-}Br)$. Reprinted with permission from Organometallics. Copyright 1995 American Chemical Society.

tions on the model cluster $HFe_4(CO)_{11}(PH_3)(\mu\text{-}\eta^2\text{-}CH)$ are presented [116]. $Os_3(CO)_{12}$ reacts with 1,3-diethylindene to give $HOs_4(CO)_9(\mu_3\text{-}\eta^2\text{-}\eta^2\text{-}\eta^5\text{-}C_{13}H_{15})$. X-ray crystallography shows that this cluster possesses a distorted tetrahedral osmium core with one triangular face coordinated to the six-membered ring in a $\mu_3\text{-}\eta^2\text{-}\eta^2$ fashion and the five-membered ring coordinated to a single osmium center in an $\eta^5$ fashion [117]. New tetraruthenium butterfly clusters have been prepared and their crystal-packing forces explored. This latter aspect was studied with regards to the relationship that exists between the molecular and crystal structures. The X-ray structures of $Ru_4(CO)_{12}(\mu_4\text{-}\eta^2\text{:}\eta^2\text{-}C_6H_8)$ and $Ru_4(CO)_9(\mu_4\text{-}\eta^2\text{:}\eta^2\text{-}C_6H_8)(\eta^6\text{-}C_6H_6)$ (two isomers) are discussed [118]. The tetrahedral cluster $Ru_4(CO)_9(\eta^4\text{-}C_6H_8)(\mu_3\text{-}C_{16}H_{16})$ has been isolated from the reaction between $Ru_3(CO)_9(\mu_3\text{-}\eta^2\text{:}\eta^2\text{:}\eta^2\text{-}C_{16}H_{16})$ and cyclohexa-1,3-diene in the presence of added $Me_3NO$. Thermolysis of $Ru_4(CO)_{12}(\mu_4\text{-}C_6H_8)$ in octane with excess [2.2]paracyclophane and $Me_3NO$ leads to the new butterfly isomers $Ru_4(CO)_9(\mu_4\text{-}C_6H_8)(\eta^6\text{-}C_{16}H_{16})$ and $Ru_4(CO)_9(\mu\text{-}C_6H_8)(\mu_3\text{-}\eta^2\text{:}\eta^2\text{:}\eta^2\text{-}C_{16}H_{16})$. Heating the former $Ru_4$ isomer irreversibly furnishes the latter $Ru_4$ isomer. Two X-ray structures are presented [119].

The hydrogenation-isomerization of 1,3- and 1,4-cyclohexadiene using the clusters $H_4Ru_4(CO)_{12}$, $H_2Ru_4(CO)_{13}$, and $H_2FeRu_3(CO)_{13}$ has been investigated. Evidence is presented showing the involvement of cluster fragmentation species as the active catalysts in these reactions. The diene- and arene-substituted clusters and organometallic species observed in solution after the hydrogenation reactions are discussed

[120]. Various tetraruthenium clusters containing $\mu_3$-semiquinone ligands have been isolated from the reaction between $Ru_3(CO)_{12}$ and catechol and 3,5-di-*tert*-butyl-1,2-benzoquinone. The reactivity of $Ru_4(CO)_8(\mu_3\text{-}O_2C_6H_2R_2)_2$ (where $R=H$, $Bu^t$) toward THF, MeCN, and alkynes has been investigated. Cyclic voltammetric data and four X-ray structures are presented [121].

Treatment of $Os_3(CO)_{10}$(cyclooctene)$_2$ with $Os(CO)_5$ at −15°C gives the binary carbonyl $Os_4(CO)_{15}$. The synthesis of the related clusters $Os_4(CO)_{13}(PMe_3)\{P(OMe)_3\}$ and $Os_4(CO)_{14}(CNBu^t)$ is also described. All three of these clusters exhibit planar osmium skeletons, as determined by X-ray crystallography. $^{13}C$-NMR data are presented on the fluxional properties of the CO ligands, and the highly nonrigid behavior observed is discussed relative to a facile all-equatorial, merry-go-round process [122]. The CO substitution chemistry of the butterfly cluster $HRu_4(CO)_{12}(BH_2)$ with tertiary phosphines, diphosphines, and excess $P(OMe)_3$ has been examined. Twenty-two ligand-substituted clusters have been isolated and fully characterized in solution. The ligand stereochemistry in these clusters is discussed, and the molecular structures of three clusters are presented [123]. Thermolysis of $Ru_3(CO)_{12}$ with cyclopolyphosphane, $(PhP)_5$, at 135°C gives the new clusters $Ru_4(CO)_{10}(\mu_3\text{-}PPh)_2\{\mu_4\text{-}(PPh)_2\}$ and $Ru_4(CO)_8(\mu\text{-}PHPh)_2(\mu_4\text{-}PPh)\{\mu_4\text{-}(PPh)_2\}$. Use of the activated cluster $Ru_3(CO)_{10}(MeCN)_2$ in the reaction led to $Ru_3(CO)_{10}\{(PhP)_5\}$. The molecular structures of these products were crystallographically determined. Whereas the former $Ru_4$ cluster displays a skewed, chain structure, the latter $Ru_4$ cluster adopts a rectangular geometry. The X-ray structure of the $Ru_3$ cluster shows the cyclopolyphane ligand occupying the equatorial sites in the triruthenium plane, via the two P atoms in the 1,3 positions [124]. The principal components of the $^{31}P$ chemical shift tensor of several phosphinidene-capped ruthenium clusters have been characterized by using slow MAS $^{31}P$-NMR spectroscopy. The orientation of the phosphorus chemical shift tensor is discussed by using Ramsey's theory and extended Hückel MO calculations [125]. The atropoisomeric diphosphine ligands (S)-binap and (S)-mobiph react with $H_4Ru_4(CO)_{12}$ in toluene under hydrogen pressure to give $H_4Ru_4(CO)_{10}\{(S)\text{-binap}\}$ and $H_4Ru_4(CO)_{10}\{(S)\text{-mobiph}\}$. Both clusters exhibit a chelating diphosphine ligand, as shown by X-ray crystallography [126]. The reductive chemistry of $H_4Ru_4(CO)_{12}$ has been examined by using a variety of electrochemical methods. The transient radical anion, $[H_4Ru_4(CO)_{12}]^{\dot{-}}$, is shown to be a precursor to $[H_3Ru_4(CO)_{12}]^-$. ETC behavior in $H_4Ru_4(CO)_{12}$ is observed in the presence of added $PPh_3$, leading to mono- and bisubstituted $PPh_3$ derivatives. Spectroscopic data obtained by using an optically transparent thin-layer electrochemical cell are presented and used in the mechanistic discussions [127]. Phosphine- and arsine-substituted clusters derived from $H_4Ru_4(CO)_{12}$ have been synthesized by using $\{CpFe(CO)_2\}_2$ as a catalyst initiator. Good selectivity to tri- and tetrasubstituted clusters may be achieved through careful control of the ligand/cluster ratio. The stereochemical nonrigidity of selected clusters has been explored by multinuclear NMR studies. Correlations between the solid-state and solution structures are discussed, and the X-ray structure of $H_4Ru_4(CO)_{10}\{P(OEt)_3\}_2$ is presented (Fig. 13) [128].

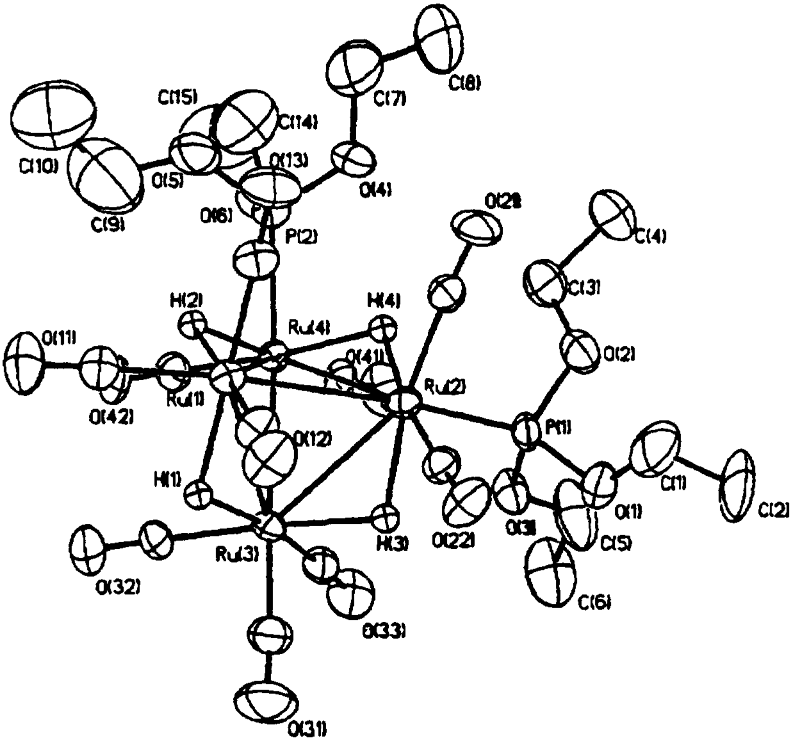

Fig. 13. X-ray structure of $H_4Ru_4(CO)_{10}\{P(OEt)_3\}_2$. Reprinted with permission from Organometallics. Copyright 1995 American Chemical Society.

Thietane and 1,5,9-trithiacyclodecane have been allowed to react with $H_4Os_4(CO)_{11}(MeCN)$ and $H_4Ru_4(CO)_{12}$. These reactions have led to the isolation of the new clusters $H_4M_4(CO)_{11}(\overline{SCH_2CH_2C}H_2)$ and $H_4M_4(CO)_{11}(\overline{SCH_2CH_2SCH_2CH_2SCH_2C}H_2)$, of which the X-ray structure of the latter osmium cluster has been solved. The catalytic efficiency of the thietane-substituted clusters in cyclooligomerization reactions to give 1,5,9-trithiacyclododecane and 1,5,9,13,17,21-hexathiacyclotetracosane has been studied, with catalysis being reported from an intact tetraosmium cluster complex. Both ruthenium clusters exhibited extensive fragmentation and lower selectivity in the catalysis reactions. A working cyclooligomerization mechanism using the osmium cluster catalyst is discussed [129]. Treatment of $Fe_2(CO)_6(\mu\text{-}SC{\equiv}CPh)(\mu\text{-}C{\equiv}CPh)$ with excess $Fe(CO)_5$ gives the tetrairon cluster $Fe_4(CO)_{12}(\mu_4\text{-}S)(\mu\text{-}C{\equiv}CPh)$. The molecular structure was established by X-ray diffraction analysis [130]. The selenide reagent $CH_2\{Ph_2P(Se)\}_2$ reacts with $Ru_3(CO)_{12}$ in toluene to produce $Ru_3(CO)_7(dppm)(\mu_3\text{-}Se)_2$, $Ru_4(CO)_9(dppm)(\mu_4\text{-}Se)_2$, and $Ru_4(CO)_{10}(\mu_3\text{-}Se)_4$; the latter cluster is the first 72-electron ruthenium-selenium cubane cluster to be structurally characterized [131]. The compound $[Cp^*_2Cp_2Ru_4S_4]^{2+}$, which was prepared from $Cp^*_2Ru_2S_2$ and $[CpRu(MeCN)_3]^+$, has been explored in terms of the stereodynamic behavior associated with the Ru–Ru bonds. The difference in the arrangement of the Ru–Ru bonds can be seen by $^1$H-NMR spectroscopy and cyclic voltammetry data [132]. The synthesis and X-ray structure of $[Fe_4(Te_2)_2(Te)_2(TeMe)_2(CO)_8]^{2-}$ have appeared. This cluster is obtained from the sealed-tube reaction in MeOH solvent containing $Fe_3(CO)_{12}$, $Na_2Te_2$, and $Me_4NBr$. $Ru_3(CO)_{12}$ reacts with $Na_2Te_2$ and $Ph_4PBr$ under similar conditions to give the corresponding ruthenium cluster [133]. A detailed study on the pairwise mobility of Ru–Ru bonds in $[(MeCpRu)_4S_3(SMe)]^+$ has been reported. Variable-temperature $^1$H-NMR data and electrochemical studies dealing with bond-making and bond-breaking sequences available to this cluster are presented [134].

Redox-mediated ligand-transfer reactions have been employed in the synthesis of cyclobutadiene-substituted clusters. Treatment of the carbido clusters $[Ru_5C(CO)_{14}]^{2-}$ and $[Ru_6C(CO)_{16}]^{2-}$ with $[Pd(\mu\text{-}C_4Ph_4)(acetone)_2]^{2+}$ gives the neutral clusters $Ru_5C(CO)_{13}(\mu\text{-}C_4Ph_4)$ and $Ru_6C(CO)_{15}(\mu\text{-}C_4Ph_4)$, respectively. These new clusters were characterized in solution and their solid-state structures determined. The $Ru_6$ cluster exhibits one elongated Ru–Ru bond, whose origin is discussed relative to the extended Hückel MO data [135]. The photochemistry of $Ru_5C(CO)_{12}(\eta^6\text{-}C_6H_6)$ embedded within a polymethylmethacrylate film has been investigated. Optical excitation promotes the migration of the aryl ring to the apical site, while heating reverses this process and restores the original basal isomer. Mechanistic pathways for this isomerization are presented [136]. $Ru_5C(CO)_{15}$ reacts with NaCp, followed by treatment with $HBF_4$, to yield the wingtip-bridged butterfly cluster $HRu_5C(CO)_{13}(\eta^5\text{-}Cp)$ in high yield. Solution data and the X-ray structure are presented. The Cp ring coordinates to the bridging ruthenium center, with the hydride ligand bridging the Ru–Ru hinge. The chemical and structural relationships of this cluster with $Ru_5C(CO)_{13}(\eta^6\text{-}C_6H_6)$ are discussed [137]. The use of triruthenaborane clusters as precursors to the anionic cluster $[H_2Ru_5(CO)_{14}(\mu_4\text{-}COH)][PPN]$ is described. The presence of the face-capping $\mu_4$-COH moiety has been confirmed by X-ray diffraction analysis. This particular cluster does not serve as a precursor to other $Ru_5C$-carbido species [138].

A phosphaalkyne-bridged iron cluster has been synthesized from the reaction between $Fe_2(CO)_6(\mu\text{-}Se)_2$ and $P\equiv CBu^t$. $\{Fe_3Se_2(CO)_8\}(\mu\text{-}PCBu^t)\{Fe_2Se(CO)_6\}$ has been isolated and its X-ray structure solved [139]. The sulfido-bridged clusters $[Fe_5S_4(CO)_{12}]^{2-}$ and $[Fe_5S_4(CO)_{12}]^-$ have been prepared and structurally characterized. The former cluster exhibits an $O_2$-specific oxidation to give the known cluster $[Fe_6S_6(CO)_{12}]^{2-}$. The mechanism associated with this transformation is unknown [140].

The synthesis and characterization of precursors capable of affording polymeric compounds containing the redox-active unit $Ru_6C$ are reported. Thermolysis of $Ru_3(CO)_{12}$ with dicyclic arene ligands having the form $C_6H_5(CH_2)_nC_6H_5$ yields $Ru_6C(CO)_{14}\{\eta^6\text{-}C_6H_5(CH_2)_nC_6H_5\}$. The X-ray structures of the derivatives $n=0$, 1, 2 have been established, and the electronic inductive effects observed in the $^1$H-NMR spectra discussed. The reaction between *trans*-stilbene (excess) and $Ru_6C(CO)_{17}$ furnishes *trans*-$Ru_6C(CO)_{14}\{\eta^6\text{-}C_6H_5(CH)_2Ph\}$ in good yield [141]. Oxidative decarbonylation of $Ru_6C(CO)_{17}$ using $Me_3NO$ in the presence of fulvene derivatives produces the fulvene-substituted clusters $Ru_6C(CO)_{14}$(fulvene). Reported in this study are the X-ray structures of $Ru_6C(CO)_{14}(\mu\text{-}\eta^2\text{:}\eta^2\text{-}C_5H_4CPh_2)$, $Ru_6C(CO)_{14}(\mu_3\text{-}\sigma\text{:}\eta^2\text{:}\eta^2\text{:}\eta^3\text{-}C_5H_4CPh_2)$, $Ru_6C(CO)_{14}(\mu\text{-}\eta^5\text{:}\eta^1\text{-}C_5H_4CH_2)$, $Ru_6C(CO)_{13}\{\mu\text{-}\eta^5\text{:}\eta^1\text{-}C_5H_4C(CH_2)_2\}$, and $Ru_6C(CO)_{12}(\eta^5\text{-}C_5H_4CMe_2H)(\eta^5\text{-}C_5H_4CMe_2OH)$ [142]. The reaction of syn gas with zeolite-encapsulated $Ru^{III}(NH_3)_6$ gives $[Ru_6(CO)_{18}]^{2-}$. The fragmentation and reconstruction reactivity of this cluster inside the NaX zeolite cavity is described. Structural information on the ruthenium compounds was ascertained by EXAFS spectroscopy [143]. The synthesis and characterization of $Ru_6C(CO)_{14}(\eta^6\text{-Ph-Ph})$, $Ru_6C(CO)_{14}(\eta^6\text{-Ph-O-Ph})$, $\{Co_4(CO)_9\}_2(\eta^6\text{:}\eta^6\text{-PhSiMe}_2\text{Ph})$, $Co_4(CO)_9(\eta^6\text{-Ph-O-Ph})$, and mixed $Cr(CO)_3/Co_4(CO)_9$-arene derivatives have been published. Detailed NMR ($^1H$, $^{13}C$, $^{17}O$, and $^{29}Si$) studies have been carried out, and the relationship between $\delta(^{13}C{\equiv}O)$ and $\delta(^{17}O{\equiv}C)$ discussed relative to $\pi$-backbonding [144]. Dihydrotoluene reacts with $Ru_6C(CO)_{14}(\eta^6\text{-}C_6H_4Me_2\text{-}1,3)$ in the presence of $Me_3NO$ to give $Ru_6C(CO)_{12}(\eta^6\text{-}C_6H_4Me_2\text{-}1,3)(\mu_2\text{-}C_6H_7Me)$, $Ru_6C(CO)_{11}(\eta^6\text{-}C_6H_4Me_2\text{-}1,3)(\mu_3\text{-}C_6H_5Me)$, and *cis*-$Ru_6C(CO)_{11}(\eta^6\text{-}C_6H_4Me_2\text{-}1,3)(C_6H_5Me)$. The reaction conducted with toluene yields the bis(arene) cluster $Ru_6C(CO)_{11}(\eta^6\text{-}C_6H_4Me_2\text{-}1,3)(\eta^6\text{-}C_6H_5Me)$. The crystal structures of the last two clusters are presented [145]. Thermolysis of hexamethylbenzene with $Ru_3(CO)_{12}$ in octane solution produces $Ru_6(\eta^2\text{-}\mu_4\text{-}CO)_2(CO)_{13}(\eta^6\text{-}C_6Me_6)$. The structure of this cluster is isostructural with the known cluster $Ru_6(\eta^2\text{-}\mu_4\text{-}CO)_2(CO)_{13}(\eta^6\text{-}C_6H_3Me_3)$. While the mesitylene-substituted cluster rearranges to the carbido cluster $Ru_6C(CO)_{14}(\eta^6\text{-}C_6H_3Me_3)$, the hexamethylbenzene cluster does not undergo a similar transformation [146]. Another new cluster has been isolated from the thermolysis reaction between $Ru_3(CO)_{12}$ and [2.2]paracyclophane. X-ray diffraction analysis revealed the identity of this cluster as $Ru_6C(CO)_{15}(\mu_3\text{-}\eta^1\text{:}\eta^2\text{:}\eta^2\text{-}C_{16}H_{16}\text{-}\mu\text{-}O)$. Heating this cluster leads to the carbido cluster $Ru_6C(CO)_{14}(\mu_3\text{-}\eta^1\text{:}\eta^2\text{:}\eta^2\text{-}C_{16}H_{16})$ and $CO_2$. The origin of the oxo ligand in the former cluster derives from the cleavage of a CO group. Mechanistic proposals involving the disproportionation of CO are discussed [147]. A report describing the attack of PhLi at coordinated arene rings in $Ru_6$ clusters has appeared. Addition of PhLi to $Ru_6C(CO)_{12}(\eta^6\text{-}C_6H_6)(\mu\text{-}\eta^2\text{:}\eta^2\text{-}C_6H_8)$, $Ru_6C(CO)_{11}(\eta^6\text{-}C_6H_6)(\mu_3\text{-}\eta^2\text{:}\eta^2\text{:}\eta^2\text{-}C_6H_6)$, and $Ru_6C(CO)_{14}(\eta^6\text{-}C_6H_6)$, followed by hydride abstraction using $[Ph_3C][BF_4]$, gives $Ru_6C(CO)_{12}(\eta^6\text{-}C_6H_5Ph)(\mu\text{-}\eta^2\text{:}\eta^2\text{-}C_6H_8)$, $Ru_6C(CO)_{11}(\eta^6\text{-}C_6H_5Ph)(\mu_3\text{-}\eta^2\text{:}\eta^2\text{:}\eta^2\text{-}C_6H_6)$, and $Ru_6C(CO)_{14}(\eta^6\text{-}C_6H_4Ph_2\text{-}1,4)$, respectively. Solution spectroscopic data and the X-ray structure of the last cluster confirm the nucleophilic attack on the polyene ring in these clusters [148]. Dehydrogenation of cyclohexane occurs in refluxing octane using $Ru_3(CO)_{12}$. Besides the normally isolated clusters containing $C_6H_8$ and $C_6H_6$ rings, the cluster $Ru_6(CO)_{13}(\mu_3\text{-}H)(\mu_4\text{-}\eta^2\text{-}CO)_2(\eta^5\text{-MeCp})$ has been isolated and structurally characterized. The X-ray structure reveals the C–C bond activation and ring contraction that are attendant in the formation of the $Ru_6$ cluster. A plausible mechanism involving cyclohexane dehydrogenation to give a cluster-stabilized cyclohexenyl ($C_6H_7$) fragment is discussed [149]. Allyl bromide reacts with $[Ru_6C(CO)_{15}(\mu\text{-}\eta^3\text{-}C_3H_5)]^-$ to furnish the pentanuclear cluster

$Ru_5C(CO)_{11}(\mu\text{-}Br)_2(\eta^3\text{-}C_3H_5)(\mu\text{-}\eta^3\text{-}C_3H_5)$, as determined by X-ray crystallography. The product cluster displays a pyramidal frame containing two symmetrically bridging bromide groups across the cleaved apical-to-basal edges. The reactivity of $[Ru_6C(CO)_{16}(Me)]^-$ and $[Ru_6C(CO)_{16}]^{2-}$ with alkylating agents is also reported [150]. Pyrolysis of $H_2Ru_3(CO)_9(NOMe)$ yields the two hexaruthenium clusters $Ru_6(CO)_{15}(\mu\text{-}CO)_2(\mu_4\text{-}NH)(\mu\text{-}OMe)\{\mu_3\text{-}\eta^2\text{-}N(H)C(O)OMe\}$ and $Ru_6(CO)_{16}(\mu\text{-}CO)_2(\mu_4\text{-}NH)(\mu\text{-}OMe)(\mu\text{-}NCO)$, the structures of which were crystallographically determined [151].

Triphenylphosphoniocyclopentadienide reacts with $Ru_6C(CO)_{17}$ to give the zwitterionic cluster $Ru_6C(CO)_{14}(\eta^5\text{-}C_5H_4PPh_3)$. The X-ray structure reveals intermolecular interactions typical of zwitterionic compounds [152]. $Ru_3(CO)_{11}(Ph_2PC{\equiv}C\text{-}C{\equiv}CR)$ (where R = Bu$^t$, Ph) is transformed into $Ru_6(CO)_{13}(\mu\text{-}CO)_2(\mu\text{-}PPh_2)(\mu_5\text{-}C)(\mu_3\text{-}C\text{-}C{\equiv}CR)$ in refluxing THF. The presence of the alkylidyne-carbide ligand in the product was verified by X-ray diffraction analysis [153].

Molecular hydrogen reacts with the 48-electron cluster $Ru_3(CO)_9(\mu\text{-}H)(\mu_3,\eta^2\text{-}ampy)$ to yield the 92-electron cluster $Ru_6(CO)_{14}(\mu\text{-}H)_6(\mu_3,\eta^2\text{-}ampy)_2$. Treatment of the $Ru_6$ cluster with CO regenerates the original $Ru_3$ cluster. Reaction of the $Ru_6$ cluster with $PR_3$ (where R = Ph, 4-tolyl) gives $Ru_6(CO)_{12}(PR_3)_2(\mu\text{-}H)_6(\mu_3,\eta^2\text{-}ampy)_2$. One X-ray structure is presented, confirming the existence of two connected $Ru_3$ fragments. The catalytic hydrogenation reactivity of the $Ru_6$ cluster has been examined, with kinetic data suggesting the involvement of the hexaruthenium cluster as the active catalyst [154]. The synthesis and X-ray structure of the vertex-linked cluster $Ru_6(CO)_{18}(\mu_3\text{-}ampy)_2$ are reported [155].

Thermally induced metal framework condensation of $Ru_3(CO)_9(\mu\text{-}H)(\mu_3,\eta^2\text{-}SCNHPhNPh)$ gives the crystallographically characterized cluster $Ru_6(CO)_{14}(\mu\text{-}CO)_2(\mu_4\text{-}S)(\mu_3,\eta^2\text{-}SCNHPhNPh)(\mu_3,\eta^2\text{-}NHPhCNHPh)$, along with $Ru_6(CO)_{16}(\mu_2\text{-}H)(\mu_5\text{-}S)(\mu_3,\eta^2\text{-}SCNHPhNPh)$. The latter cluster reacts with hydrogen to give $Ru_6(CO)_{14}(\mu_2\text{-}H)_6(\mu_3,\eta^2\text{-}SCNHPhNPh)$. The molecular structure of this hexahydrido cluster has been ascertained by X-ray diffraction analysis [156]. Transformations of selenium-iron carboxylates in Hieber's synthesis have been investigated. The cluster $[Fe_6Se_6(CO)_{12}]^{2-}$ has been isolated and thoroughly characterized in solution. The solid-state structure was established by X-ray diffraction analysis [157]. The reactions of several polythiaether macrocycle ligands with $Ru_6(\mu_6\text{-}C)(CO)_{17}$ are reported. Fig. 14 shows the X-ray structure of one of the four crystallographically determined clusters [158].

The heptaruthenium clusters $Ru_7C(CO)_{16}(C_9H_8)$ and $Ru_7C(CO)_{16}(C_{12}H_{12})$ have been synthesized from $Ru_3(CO)_{12}$ and isopropenyl- or 1,3-diisopropenylbenzene. The molecular structures reveal spiked octahedra, with the arene ligand coordinated via all four of the $\pi$ bonds to a metal face and by two $\sigma$ bonds to the spike center [159]. The synthesis and X-ray structure of $H_2Os_7(CO)_{21}P(OMe)_3$ have been published. The osmium atoms exhibit a trigonal bipyramid core that shares an equatorial vertex with the two remaining osmium atoms. Comparisons of the title cluster with $H_2Os_7(CO)_{22}$ are presented [160]. The disproportionation of $Fe_2(CO)_9$ in THF

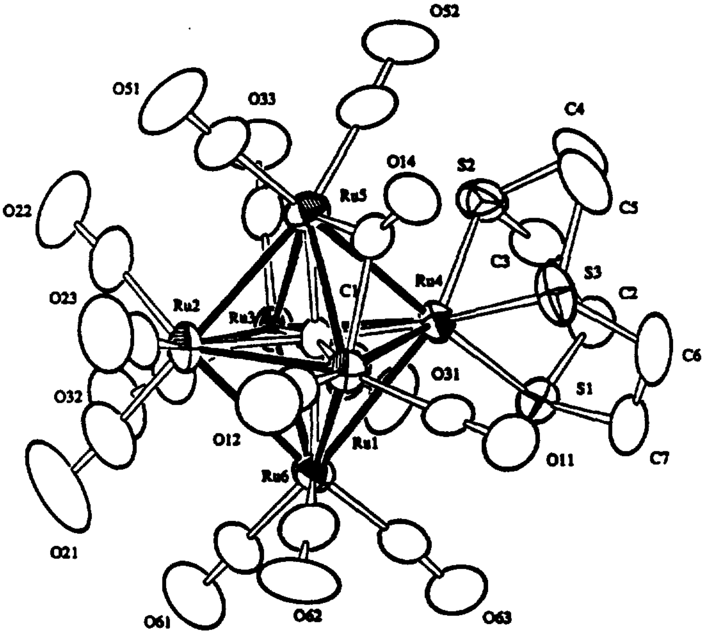

Fig. 14. X-ray structure of $Ru_6(CO)_{14}(\mu_6\text{-}C)(\eta^3\text{-}SCH_2CH_2SCH_2CH_2SCH_2CH_2)$. Reprinted with permission from Organometallics. Copyright 1995 American Chemical Society.

affords the crystallographically characterized cluster $Fe(THF)_4\{HFe_3(CO)_{11}\}_2$. The solvated iron center coordinates the two $Fe_3$ units via the bridging hydride ligands [161].

Thermolysis of $Ru_3(CO)_{12}$ in octane in the presence of benzene or [2.2]paracyclophane allows for the isolation of $H_4Ru_8(CO)_{18}(\eta^6\text{-arene})$. X-ray diffraction data on this cluster show that the metal core geometry is derived by removal of two capping ruthenium atoms from the corresponding tetracapped octahedral $M_{10}$ cluster. The benzene-substituted cluster fragments to $H_4Ru_4(CO)_{12}$ and $H_2Ru_4(CO)_{13}$ under CO gas [162]. The clusters $Ru_8(CO)_{19}(\mu_6\text{-}\eta^2\text{-}CO)(\mu\text{-}H)(\eta^6\text{-}C_{16}H_{16})$ and $Ru_8(CO)_{18}(\mu_6\text{-}\eta^2\text{-}CO)(\mu_4\text{-}\eta^2\text{-}CO)(\eta^6\text{-}C_{16}H_{16})$ have been isolated and structurally characterized. The elongation of the bridging $\mu_6\text{-}\eta^2\text{-}CO$ group in these clusters is discussed relative to carbide formation, given the quantitative conversion of the latter cluster into $Ru_6C(CO)_{14}(\mu_3\text{-}\eta^2\text{:}\eta^2\text{:}\eta^2\text{-}C_{16}H_{16})$ and $Ru_3(CO)_{12}$ [163,164]. Treatment of $Fe(CO)_5$ in KOH with methanolic $K_2TeO_3$ gives the dianionic cluster $[Fe_8(CO)_{24}Te_6]^{2-}$. This particular cluster is an intermediate in Hieber's synthesis of $Te_2Fe_3(CO)_9$ and $Te_2Fe_2(CO)_6$. The solid-state identity of this $Fe_8$ cluster was unequivocally determined by X-ray crystallography [165].

The preparation of $[HRu_{10}C(CO)_{24}]^-$ from the thermolysis of $Ru_3(CO)_{12}$ in the presence of $1,3,5\text{-}C_6H_3Me_3$ has been published. The corresponding dianion is obtained by deprotonation of the $HRu_{10}$ cluster using DBU. The isostructural nitrido cluster $[Ru_{10}N(CO)_{24}]^-$ is obtained from the reaction between $Ru_3(CO)_{12}$

and [PPN][N$_3$] or by $Ru_3(CO)_{12}$ addition to the nitride clusters $[Ru_5N(CO)_{14}]^-$ and $[Ru_6N(CO)_{16}]^-$. The X-ray structures of all three $Ru_{10}$ clusters are presented, and the CO-induced fragmentation chemistry of these clusters is fully discussed.[166] Stepwise addition of $PPh_3$ to $[Ru_{10}(CO)_{24}(\mu_6\text{-}C)(\mu\text{-}H)]^-$ gives $[Ru_{10}(CO)_{24-x}(PPh_3)_x(\mu_6\text{-}C)(\mu\text{-}H)]^-$ (where $x = 1$–$4$). The initial site of $PPh_3$ attack occurs at the apical ruthenium center that is connected to the μ-H ligand. Subsequent $PPh_3$ addition takes place at the remaining apical sites. The X-ray structure of the monosubstituted cluster (Fig. 15) confirms the site selectivity associated with first substitution step [167].

## 2.5. *Group 9 clusters*

The reaction between $MeCCo_3(CO)_9$ and $(Me_2P\text{-}\eta^6\text{-}C_6H_5)(\eta^6\text{-}C_6H_6)Cr$ and $(Me_2P\text{-}\eta^6\text{-}C_6H_5)_2Cr$ gives the substitution products $(Me_2P\text{-}\eta^6\text{-}C_6H_5)(\eta^6\text{-}C_6H_6)Cr\{MeCCo_3(CO)_8\}$, $\{(Me_2P\text{-}\eta^6\text{-}C_6H_5)_2Cr\}\{MeCCo_3(CO)_8\}_2$, and $\{(Me_2P\text{-}\eta^6\text{-}C_6H_5)_2Cr\}\{MeCCo_3(CO)_7\}$ via an ETC sequence. Cyclic voltammetric and EPR data that support the ETC mechanism are presented. The X-ray structures of the latter two clusters are included in this report [168]. The syntheses of $[Bi\{Co(CO)_4\}_4][K(18\text{-crown-}6)]$ and $[Bi\{Co(CO)_4\}_4][PPN]$ have been published, along with the X-ray structure of the PPN salt [169]. The alkylidyne-capped clusters

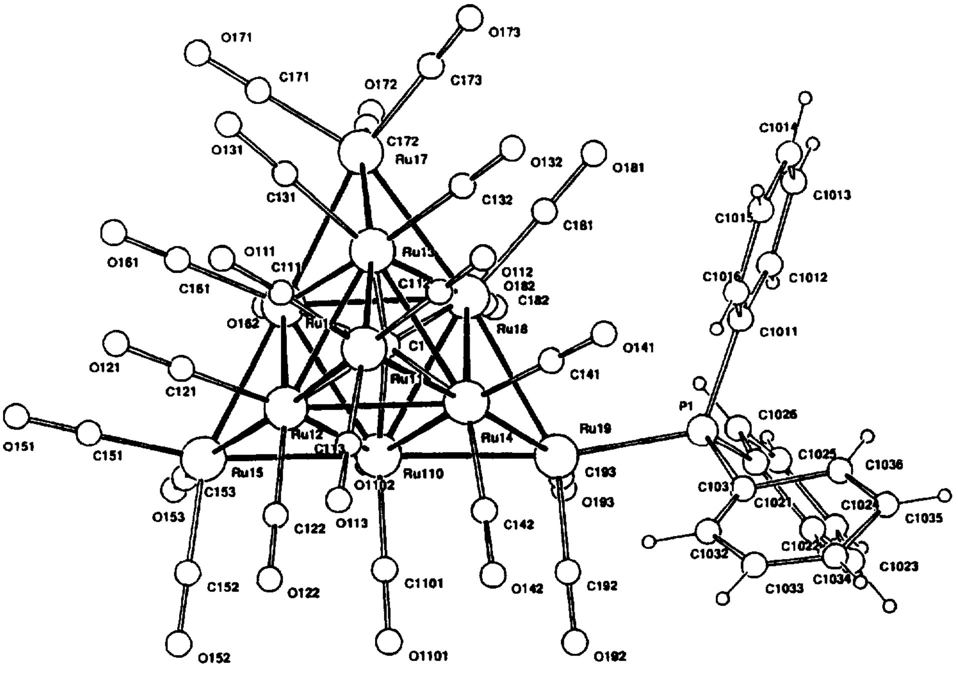

Fig. 15. X-ray structure of $[Ru_{10}(CO)_{23}(PPh_3)(\mu_6\text{-}C)(\mu\text{-}H)]^-$. Reprinted with permission from Organometallics. Copyright 1995 American Chemical Society.

$Co_3(CO)_9\{\mu_3\text{-}CC(O)OCH_2CH{=}CH_2\}$ and $Co_3(CO)_9\{\mu_3\text{-}CC(O)O(CH_2)_2OC(O)CH{=}CH_2\}$ have been prepared and polymerized to give polyacrylate resins containing intact $CCo_3(CO)_9$ moieties. The X-ray structure of the former monomer accompanies this report [170]. The tetrakis-trichloroacetate ester $C(CH_2O_2CCCl_3)_4$ reacts with $Co_2(CO)_8$ to give the tris-cluster compound $C\{CH_2O_2CCCo_3(CO)_9\}_3(CH_2O_2CCCl_3)$. A space filling model of the tetrakis derivative $C\{CH_2O_2CCCo_3(CO)_9\}_4$ exhibits extreme molecular crowding, providing a rationale for the absence of this product in the above reaction [171]. Treatment of $ClCCo_3(CO)_9$ with $Me_3NO$ in the presence of dppe and triphos gives the phosphine-tethered clusters $\{ClCCo_3(CO)_8\}_2(\mu\text{-dppe})$ and $\{ClCCo_3(CO)_8\}\{ClCCo_3(CO)_7\}(\mu\text{-triphos})$. The molecular structure of each cluster was established by X-ray crystallography [172]. Polyhedral expansion in $Co_3(CO)_6\{\mu_2\text{-}\eta^2{:}\eta^1\text{-}C(Ph)\overline{C{=}C(PPh_2)C(O)OC}(O)\}(\mu_2\text{-}PPh_2)$ has been observed upon treatment with $PMe_3$. The *hypho* cluster $Co_3(CO)_5(\mu_2\text{-}CO)(PMe_3)\{\mu_2\text{-}\eta^2{:}\eta^1\text{-}C(Ph)\overline{C{=}C(PPh_2)C(O)OC}(O)(\mu_2\text{-}PPh_2)$ results from the site-selective $PMe_3$ addition to the $PPh_2$(maleic anhydride)-substituted cobalt center. The cleaved Co–Co bond that accompanies this reaction was verified by X-ray diffraction analysis. The role played by the ancillary maleic anhydride ring in directing the site of $PMe_3$ attack is discussed, and a mechanism is presented that accounts for the polyhedral opening of the *arachno* cluster upon $PMe_3$ addition and formation of the solid-state structure of the intermediate *hypho* cluster. Facile CO loss occurs at room temperature to yield the new *arachno* cluster $Co_3(CO)_5(PMe_3)\{\mu_2\text{-}\eta^2{:}\eta^1\text{-}C(Ph)\overline{C{=}C(PPh_2)C(O)OC}(O)\}(\mu_2\text{-}PPh_2)$, whose structure was solved by X-ray crystallography [173]. $PMe_3$ addition to $Co_3(CO)_5(PMe_3)\{\mu_2\text{-}\eta^2{:}\eta^1\text{-}C(Ph)\overline{C{=}C(PPh_2)C(O)OC}(O)\}(\mu_2\text{-}PPh_2)$ occurs by a second-order process, as determined by UV-visible spectroscopic measurements. The reported second-order rate constants and the activation parameters support an associative reaction involving a rate-limiting addition of $PMe_3$ to the cluster. The role of a coordinatively flexible maleic anhydride ring in the substitution reaction is presented. The product cluster, $Co_3(CO)_4(PMe_3)_2\{\mu_2\text{-}\eta^2{:}\eta^1\text{-}C(Ph)\overline{C{=}C(PPh_2)C(O)OC}(O)\}(\mu_2\text{-}PPh_2)$, whose molecular structure is shown in Fig. 16, arises from the site-selective addition of $PMe_3$ to the maleic anhydride-substituted cobalt center. The cyclic voltammetric behavior and the extended Hückel data on the nature of the HOMO and LUMO are discussed [174].

The application of atom-atom packing potential-energy calculations and computer graphics in the study of intermolecular aggregation in crystalline samples of $(CpM)_3(\mu_3\text{-}\eta^2{:}\eta^2{:}\eta^2\text{-}C_6H_5R)$ (where M = Co, R = CH(Ph)Me, $CH_2CH_2Ph$, CHCHMe; M = Rh, R = H) has been discussed. Polyene ring reorientation in the solid state has been examined by calculating intra- and intermolecular potential energy barriers. With the exception of benzene, the facially coordinated arenes do not exhibit any reorientation in the solid state [175]. The relationship between the molecular and crystal structures of $Cp_3M_3(CO)_3$ (where M = Co, Rh, Ir; Cp = $C_5H_5$, $C_5H_4Me$, $C_5Me_5$) has been studied by using extended Hückel MO calculations, empirical atom-atom pairwise packing potential energy calculations, and computer graphics. The observed inter- and intramolecular interactions are discussed

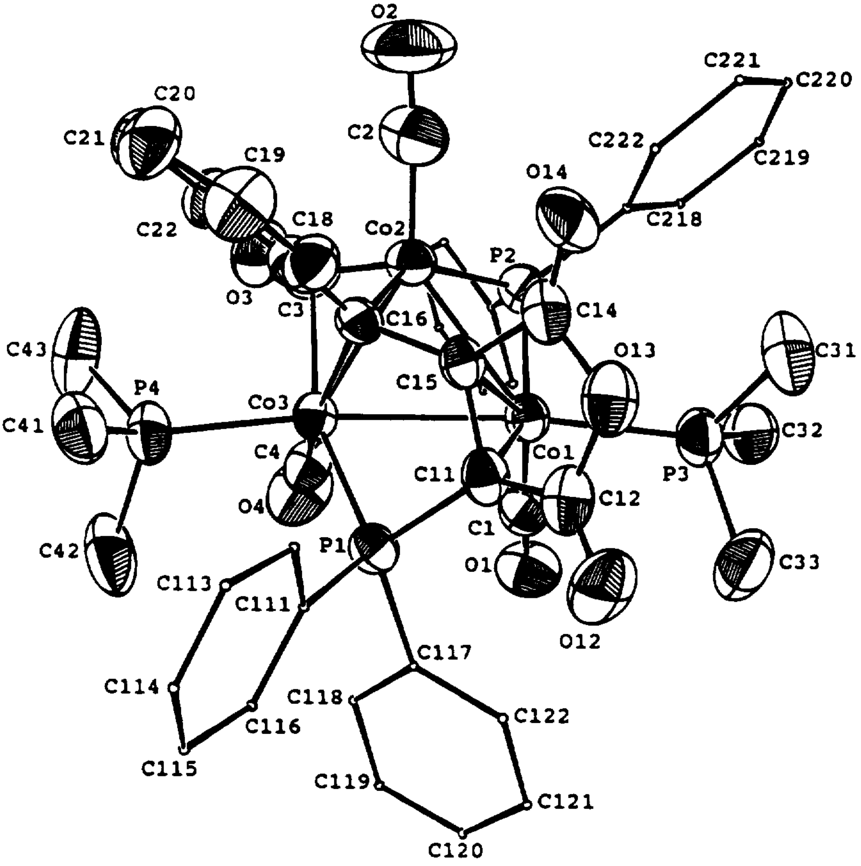

Fig. 16. X-ray structure of $Co_3(CO)_4(PMe_3)_2\{\mu_2\text{-}\eta^2\text{:}\eta^1\text{-}C(Ph)\overline{C{=}C(PPh_2)C(O)OC}(O)\}(\mu_2\text{-}PPh_2)$. Reprinted with permission from Organometallics. Copyright 1995 American Chemical Society.

and compared in crystal isomers and polymorphs. The data from $(Ind)_3Ir_3(\mu_2\text{-}CO)_3$ are also presented [176]. Treatment of Cp*Co(acac) in pyridine with potassium metal gives $(\eta^5\text{-}Cp^*)(\eta^4\text{-}C_5HMe_5)Co$ and $(Cp^*Co)_3(\mu\text{-}NC_5H_4)(\mu\text{-}H)$. The cyclometalation of pyridine was ascertained by solution measurements and preliminary X-ray data [177]. Double C–H bond activation is observed when $CpCo(ethylene)_2$ is treated with cycloalkenes. Clusters containing $\mu_3\text{-}\eta^1\text{:}\eta^1\text{:}\eta^2\text{-}(\eta\text{-}\eta^2\text{-}\|\text{-})\text{-}$ and $\mu_4\text{-}\eta^2\text{:}\eta^1\text{:}\eta^1\text{:}\eta^2$-coordinated alkynes have been isolated [178]. The reaction of the Jonas reagent, $CpCo(ethylene)_2$, with various alkenylnaphthalene compounds has been investigated. Spectroscopic data are presented for clusters having the composition $(CpCo)_3(\mu_3\text{-}\eta^2\text{:}\eta^2\text{:}\eta^2\text{-arene})$ [179]. Facile hydrogen transfer has been observed when $Cp^*_3Co_3(\mu_3\text{-}CMe)(\mu_3\text{-}H)$ is treated with $(Me_3Si)CHN_2$ and $\{EtOC(O)\}CHN_2$. The diazenide clusters $Cp^*_3Co_3(\mu_3\text{-}CMe)(\mu_3\text{-}\eta^1\text{-}NNCH_2SiMe_3)$ and $Cp^*_3Co_3(\mu_3\text{-}CMe)(\mu_3\text{-}\eta^1\text{-}NNCH_2CO_2Et)$ have been isolated and fully characterized in solution. The molecular structure of the former diazenide cluster was established by X-ray crystallography. A scheme showing the likely pathways to the observed products is presented and discussed [180]. The kinetics and mechanism for the formation of $Cp^*_3Co_3(\mu_3\text{-}CMe)_2$ from $Cp^*_3Co_3(\mu_2\text{-}H)_3(\mu_3\text{-}H)$ and acetylene have been reported. The kinetically formed intermediates $Cp^*_3Co_3(\mu_2\text{-}H)_3(\mu_3\text{-}CMe)$ and $Cp^*_3Co_3(\mu_3\text{-}H)(\mu_3\text{-}CMe)$ have been isolated, while the intermediate cluster $Cp^*_3Co_3(\mu\text{-}H)_2(\mu_3\text{-}\eta^2\text{-}HCCH)$ has been characterized by $^1H$-NMR spectroscopy. Isotopic labeling studies using $DC{\equiv}CD$ give $Cp^*_3Co_3(\mu_2\text{-}H)_2(\mu_2\text{-}D)(\mu_3\text{-}CCH_2D)$, which is consistent with the intervention of the ethylidene dihydride cluster $Cp^*_3Co_3(\mu_2\text{-}H)_2(\mu_2\text{-}CDCH_2D)$ in the reaction scheme [181]. The tricobalt cluster $Cp^*_3Co_3(\mu_2\text{-}H)_3(\mu_3\text{-}H)$ reduces $CO_2$ at elevated temperature to afford $\{Cp^*Co(\mu\text{-}CO)\}_2$ in 45% yield. The fate of the reduced $CO_2$ could not be assessed. Analogous reactions were conducted with $CS_2$ and phenyl isocyanate, leading to $Cp^*_3Co_3(\mu_3\text{-}CS)(\mu_3\text{-}S)$ and $Cp^*_2Co_2(\mu_2,\mu_2\text{-}\eta^2\text{-}PhNCONPh)$. Fig. 17 shows the X-ray structure of the former cluster. Several schemes and detailed discussions concerning the activation of these small molecules at the tricobalt cluster are presented [182].

The molecular structure and crystal organization of neutral and ionic derivatives of $M_4(CO)_{12}$ (where M = Co, Rh, Ir) have been investigated by extended Hückel and packing analysis calculations. Intermolecular hydrogen-bonding interactions between the carbonyl groups and the hydrogen atoms of the cation have also been studied [183]. The synthesis and NMR ($^1H$, $^{13}C$, $^{17}O$) study of diphenylmethane-substituted clusters are reported. The clusters studied include $Ph_2CH_2Co_4(CO)_9$, $Ph_2CH_2\{Co_4(CO)_9\}_2$, $Ph_2CH_2Cr(CO)_3Co_4(CO)_9$, and $Ph_2CH_2Ru_6C(CO)_{14}$. The inverse relationship that exists between the $^{13}C$- and $^{17}O$-NMR chemical shifts is explained by the effect of π-backbonding [184]. Pyrolysis of $Co_2(\mu\text{-}MeCCMe)(CO)_5(\mu\text{-}\eta^1{:}\eta^2\text{-}Ph_2PC{\equiv}CPh)Co_2(CO)_6$ gives the butterfly cluster $Co_4\{\mu_4\text{-}\eta^3\text{-}PhCCC(Me){=}C(Me)C(O)\}(\mu\text{-}PPh_2)(\mu\text{-}CO)_2(CO)_6$, whose molecular

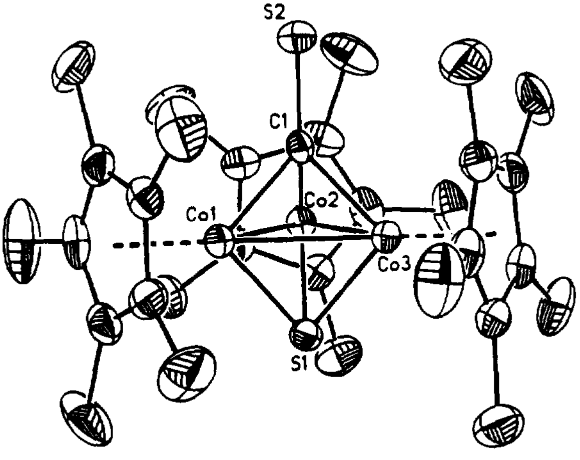

Fig. 17. X-ray structure of $Cp^*_3Co_3(\mu_3\text{-}CS)(\mu_3\text{-}S)$. Reprinted with permission from Inorganic Chemistry. Copyright 1995 American Chemical Society.

structure accompanies this report [185]. The X-ray structure of $Ir_4(CO)_8(Ph_2Ppy)_3$ has been published. Two of these P,N ligands function as monodentate ligands via phosphorus coordination, while the other P,N ligand bridges adjacent iridium centers via the nitrogen and phosphorus atoms [186]. $Ir_4(CO)_{12}$ reacts with $Ph_2Ppy$ to give $Ir_4(\mu\text{-}CO)_3(CO)_5(\mu\text{-}Ph_2Ppy)(Ph_2Ppy)_2$. Treatment of this cluster with CO gives $Ir_4(\mu\text{-}CO)_3(CO)_6(Ph_2Ppy)_3$. The CO addition reaction is fully reversible, as shown by $^1H$- and $^{31}P$-NMR spectroscopy [187].

$Co_2(CO)_8$ reacts with $BH_3 \cdot SMe_2$ to afford $Co_2(CO)_6B_2H_4$ and $Co_5(CO)_{13}(\mu\text{-}CO)B_2H$. The X-ray structure (Fig. 18) of the $Co_5$ cluster exhibits a *trans* $Co_4B_4$ octahedral core with a Co atom capping a $Co_2B$ triangular face. The electronic structure of this same cluster has been analyzed by extended Hückel MO calculations [188].

The bonding of interstitial carbide and nitride atoms in several clusters ($Rh_6$, $Co_6$, $Ni_9$) has been examined through the use of NMR spectroscopy. The observed shielding anisotropy suggests that the hybridization of the encapsulated atom is dependent on the metal geometry, being sp in an octahedron, $sp^2$ in a trigonal-prismatic core, and $sp^3$ in a square-antiprismatic metal skeleton [189]. The clusters $Co_3(CO)_9(\mu_3\text{-}Se)$, $Co_4(CO)_{10}(\mu_4\text{-}Se)_2$, $\{Co_3(CO)_7(\mu_3\text{-}Se)\}_2(\mu_4\text{-}Se_2)$, and $Co_6(CO)_6(\mu_3\text{-}Se)_8$ have been obtained from the reaction between $Co_2(CO)_8$ and red selenium in THF. The X-ray structures of the two $Co_6$ clusters are included in this report. Infrared and Raman spectral data are presented, with the main vibrational modes assigned and compared with those of the related sulfur compounds [190].

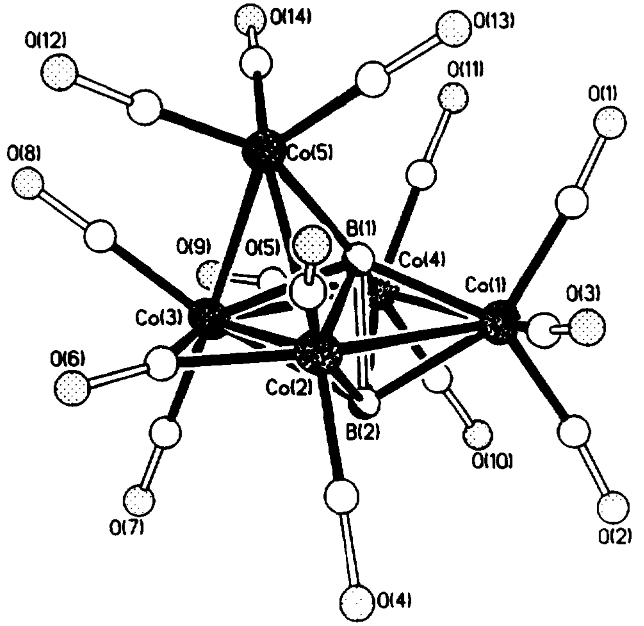

Fig. 18. X-ray structure of $Co_5(CO)_{13}(\mu\text{-}CO)B_2H$. Reprinted with permission from Inorganic Chemistry. Copyright 1995 American Chemical Society.

The X-ray structure of $Ir_6(CO)_{14}$(dppm) has been solved. The dppm ligand functions as a bridging diphosphine, replacing two equatorial CO groups in the *cis* positions [191]. Treatment of $Rh_4(CO)_{12}$ with 1,3-cyclohexadiene in the presence of $Me_3NO$ furnishes the hexarhodium cluster $Rh_6(CO)_{10}(\mu_3\text{-}CO)_4(\eta^4\text{-}C_6H_8)$, whose structure was established by X-ray crystallography and NMR spectroscopy. The observed solid-state structure is based on the structure of $Rh_6(CO)_{12}(\mu_3\text{-}CO)_4$ with the polyene ligand replacing two terminal CO groups [192]. Large crystallites of $Ir_6(CO)_{16}$ have been deposited on silica from solution. Heating the surface-supported $Ir_6(CO)_{16}$ at 100°C under argon leads to $Ir_4(CO)_{12}$ and iridium particles covered by CO. These iridium particles are converted to $Ir_4(CO)_{12}$ by treatment with $O_2$, followed by CO at elevated temperature. Aspects of this alternative synthesis of $Ir_4(CO)_{12}$ from $Ir_6(CO)_{16}$ are discussed [193]. One-electron oxidation of $[Ir_6(CO)_{15}]^{2-}$, followed by treatment with NO at low temperature, gives the nitrosyl-containing cluster $[Ir_6(CO)_{14}(NO)]^-$. The nitrosyl ligand adopts a linear conformation, as determined by X-ray diffraction analysis [194].

### 2.6. *Group 10 clusters*

The structural systematics in nickel carbonyl cluster anions have been reviewed [195]. $Ni(COD)_2$ cleaves the central C–C bond of 1,4-diphenyl-1,3-butadiyne in the presence of added dppm to afford the trinickel cluster $Ni_3(\mu\text{-dppm})_3(\mu_3\text{-}\eta^1\text{-}C{\equiv}CPh)_2$. The molecular structure of this phenylacetylide-capped cluster has been determined by X-ray crystallography [196]. Ni(cyclododeca-1,5,9-triene) reacts with 2,5,5-trimethylhex-3-yn-2-ol to give the air-sensitive cluster $Ni_3(\text{alkyne})_4$, whose X-ray structure reveals an opened $Ni_3$ triangle [197]. Plasma desorption and fast atom bombardment mass spectrometry have been employed in the characterization of several $Ni_3$ and $Ni_6$ clusters. Strong molecular ion peaks were found for most of the trinickel clusters by both techniques [198]. The nickel clusters $Ni_3(L)(cod)_3$ (where $L = Me_3SiC{\equiv}C\text{-}C{\equiv}CSiMe_3$, $PhC{\equiv}C\text{-}C{\equiv}CPh$) have been synthesized and their molecular structures determined [199]. Treatment of nickelocene with PhLi in the presence of terminal olefins yields clusters having the form $(CpNi)_3CR$. This method allows for the synthesis of a wide variety of RC-capped tris(cyclopentadienylnickel) clusters [200]. The dimeric compound $[Pt_2(dpmp)_2(RCN)_2]^{2+}$ reacts with $M_3(RNC)_6$ (where M = Pd, Pt) to give the linear clusters $[Pt_2M(dpmp)_2(RNC)_2]^{2+}$ [201]. The steric effects of the diphosphine ligands $R_2PCH_2PR_2$ (where R = various aryl groups) on the formation and reaction chemistry of $[Pt_3(\mu_3\text{-}CO)(\mu\text{-}R_2PCH_2PR_2)_3(O_2CCF_3)]^+$ and $[Pt_3(\mu_3\text{-}CO)(\mu\text{-}R_2PCH_2PR_2)_3]^{2+}$ have been examined. The ligand substitution chemistry and NMR ($^1H$ and $^{31}P$) data are discussed. Fig. 19 shows the X-ray structure of $[Pt_3(\mu_3\text{-}CO)\{\mu\text{-}(3,5\text{-}Cl_2C_6H_3)_2PCH_2P(3,5\text{-}Cl_2C_6H_3)_2\}_3(O_2CCF_3)]^+$ [202].

The palladium cluster $Pd_4(PBu^t_3)_4(\mu_3\text{-}CH)(\mu\text{-}Cl)_3$ has been prepared from $Pd_2(dba)_3$ and $PBu^t_3$ in $CHCl_3$. This 60-electron cluster possesses a tetrahedral core, in agreement with PSEP theory. The molecular structure was confirmed by X-ray diffraction analysis [203]. X-ray and EXAFS data are reported for $Pd_4(CO)_4(OAc)_4$. This cluster exhibits non-rigid behavior when stored at room temperature for an extended period of time [204]. The first carbonylplatinum clusters

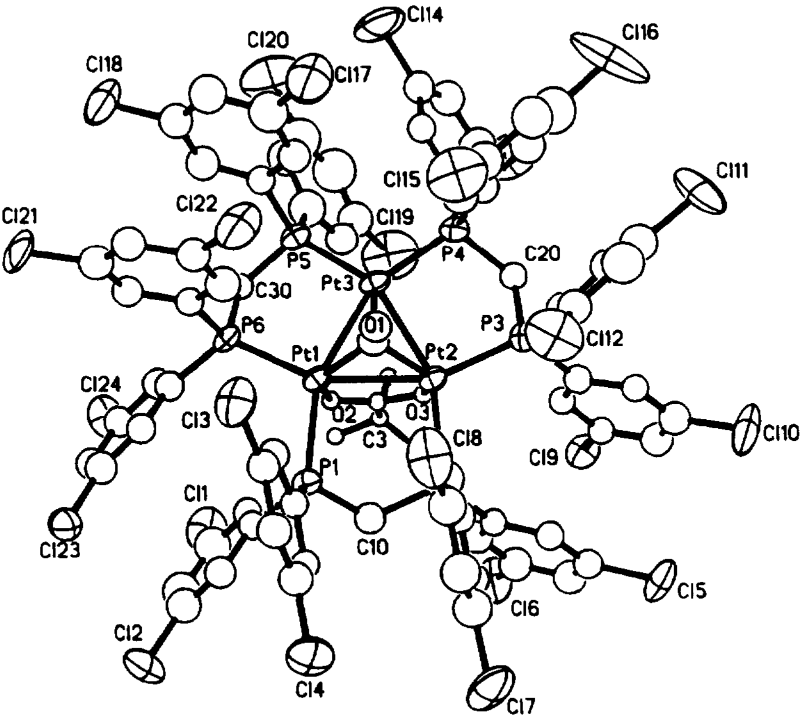

Fig. 19. X-ray structure of $[Pt_3(\mu_3\text{-}CO)\{\mu\text{-}(3,5\text{-}Cl_2C_6H_3)_2PCH_2P(3,5\text{-}Cl_2C_6H_3)_2\}_3(O_2CCF_3)]^+$. Reprinted with permission from Organometallics. Copyright 1995 American Chemical Society.

possessing tetrahedral platinum cores have been crystallographically characterized. The structural differences between $[HPt_4(CO)(\mu\text{-}CO)_3(PCy_3)_4]^+$ and $Pt_4(\mu\text{-}CO)_2(PCy_3)_4(ReO_4)_2$ are discussed [205].

The synthesis and molecular structures of $[Pt_8(CO)_{10}(ECl_2)_4]^{2-}$ (where E = Sn, Ge) are reported. These clusters are obtained from the reaction of $[Pt_{15}(CO)_{30}]^{2-}$ with $SnCl_2$ and $GeCl_4$. The $ECl_2$ ligands cap the four independent exposed butterfly surfaces [206].

The bonding in metal-centered hexacapped $M_9L_8(\mu_4\text{-}E)_6$ clusters has been explored by extended Hückel and self-consistent field-multiple scattering-X$\alpha$ calculations. The rationalization of why clusters with different metallic valence electrons have the same cubic molecular structure is presented [207].

### 2.7. Group 11 clusters

The hypercoordinate methanium cations $[(R_3Si)_2C\{Au(PPh_3)\}_3]^+$ (where $R_3 = Me_3$, $Me_2Ph$) have been isolated from the reaction of monoaurated bis(silyl)-methane compounds, $(R_3Si)_2CHAuPPh_3$, with $[(Ph_3PAu)_3O]^+$. Both the $R_3$ derivatives have been analyzed by X-ray crystallography, which confirms the pentacoordinate nature of the central carbon atom [208]. The synthesis and reactivity of $[\{Au(C_6F_5)_3(Ph_2PCHPPh_2)_2\}_2Au]^-$ is described. Treatment of this trinuclear gold complex with $Au(acac)(PPh_3)$ (4 equiv.) leads to $[\{Au(C_6F_5)_3Ph_2PC(AuPPh_3)_2PPh_2\}_2Au]^+$ [209].

The alkynes $HC{\equiv}CSiMe_3$, $HC{\equiv}CPh$, and $HC{\equiv}CC_6H_4Me$-4 react with the copper alkoxide compounds $Cu\{OCH(CF_3)_2\}(PPh_3)_3$, $Cu(OCHPh_2)(PPh_3)_3$, and $\{Cu(OPh)(PPh_3)_2\}_2$ to give alkynylcopper(I) complexes having the form $\{Cu(C{\equiv}CR)(PPh_3)\}_4$. The X-ray structure of the trimethylsilyl derivative shows a cubane-like core with $\mu_3$-$\eta^1$:$\eta^1$:$\eta^1$-acetylide ligands [210].

The X-ray structure of the copper-disordered hexakis(phenylethynyl)pentaargentate(I) cluster $[Ag_{4.46}Cu_{0.54}(C_8H_5)_6][PPN]$ has been solved [211]. The reaction between $Cu(MeCN)_4(O_3SCF_3)$ and $LiC{\equiv}CBu^t$ in the presence of added 2,2′-bpy affords $[Cu_5(C{\equiv}CBu^t)_2(2,2'\text{-bpy})_4]^{3+}$, whose solid-state structure contains a nearly planar array of five copper atoms tethered by two bridging acetylide ligands [212]. The synthesis and X-ray structure of $[(Ph_3PAu)_5N]^{2+}$ are reported. The molecular structure is based on a trigonal-bipyramidal $Au_5N$ core [213].

## 3. Heteronuclear clusters

### 3.1. *Trinuclear clusters*

Treatment of $(\eta^5\text{-}C_5H_4SiMe_3)_2Nb(CO)H$ with various coinage metal cations leads to $[\{(\eta^5\text{-}C_5H_4SiMe_3)_2Nb(CO)(\mu\text{-}H)\}_2M]^+$ (where M = Cu, Ag, Au). The Nb–H–M bonding in these compounds has been examined by extended Hückel analysis. The X-ray structure of $[\{(\eta^5\text{-}C_5H_4SiMe_3)_2Nb(CO)(\mu\text{-}H)\}_2Cu]^+$ accompanies this report [214].

Irradiation of equimolar mixtures of $\{CpW(CO)_3\}_2$ and $\{CpMo(CO)_3\}_2$ affords the cluster compounds $Cp_2(\mu\text{-}\eta^1,\eta^5\text{-}C_5H_4)Mo_2W(CO)_6$, $Cp_2(\mu\text{-}\eta^1,\eta^5\text{-}C_5H_4)MoW_2(CO)_6$, and $Cp_2(\mu\text{-}\eta^1,\eta^5\text{-}C_5H_4)W_3(CO)_6$. Each of these 46-electron clusters exhibits a V-shaped metal core, as determined by X-ray crystallography. 2D EXSY NMR measurements reveal the existence of a slow proton exchange between the cyclopentadienylidene and cyclopentadienyl rings. The fluxional properties of these clusters have also been studied by NMR spectroscopy, with rearrangement pathways being discussed [215]. The gold halides $ClAu(PR_3)$ (where R = Ph, Me) react with the anions $[Cp_2M_2(CO)_4(\mu\text{-}\sigma\text{:}C_2Ph)]^-$ (where M = Mo, W) to give the $\mu$-alkyne bonded compounds $Cp_2M_2(CO)_4(\mu\text{-}PhC_2AuPR_3)$. These compounds possess $M_2C_2$ cores, as determined by the X-ray structure of $Cp_2W_2(CO)_4(\mu\text{-}PhC_2AuPPh_3)$ [216]. The thermal stability of $Cp_2Cr_2(\mu\text{-}SCMe_3)_2(\mu_3\text{-}S)Re(CO)_2(NO)Cl_2$ in the presence of CO and $Co_2(CO)_8$ has been examined. The cluster $\{CpCr(\mu\text{-}SCMe_3)_2(\mu_3\text{-}S)Re(CO)(NO)\}_2$ is the predominant product formed under both sets of reaction conditions. This tetranuclear cluster transforms into the antiferromagnetic compound $Cp_2Cr_2(\mu\text{-}SCMe_3)_2(\mu_3\text{-}S)_2Re(CO)(NO)$ and the paramagnetic compound $CpCr(\mu\text{-}SCMe_3)Re(CO)(NO)(\mu_3\text{-}S)_2(\mu\text{-}SCMe_3)Re(CO)_2(NO)$ under CO.

Treatment of the antiferromagnetic cluster with $I_2$ affords $Cp_2Cr_2(\mu\text{-}SCMe_3)_2(\mu_3\text{-}S)_2Re(NO)I$, whose structure has been established (Fig. 20) [217].

The deprotonation and anion-functionalization chemistry of $Mn_2(CO)_8(\mu\text{-}H)(\mu\text{-}PCyH)$ has been investigated. Using DBU as base and the electrophiles $ClAuPR_3$ (where R = Cy, Ph, p-$C_6H_4OMe$, p-$C_6H_4F$) leads to the mono- and diaurated pairs of isomers: $Mn_2(CO)_8(\mu\text{-}AuPR_3)(\mu\text{-}PCyH)$ and $Mn_2(CO)_8(\mu\text{-}H)\{\mu_3\text{-}PCy(AuPR_3)\}$; $Mn_2(CO)_8(\mu\text{-}AuPR_3)\{\mu\text{-}PCy(AuPR_3)\}$ and $Mn_2(CO)_8(AuPR_3)_2(\mu_4\text{-}PCy)$. These compounds have been isolated and fully characterized in solution by IR, NMR ($^1H$ and $^{31}P$), and UV-vis spectroscopy. Two representative structures have been determined by X-ray crystallography. The kinetics for isomer interconversion are reported, and the nature of the transition state associated with these reactions is discussed [218]. Thiophenol reacts with the acetylide cluster $Cp^*WRe_2(CO)_9(CCPh)$ to yield the crystallographically characterized clusters $Cp^*WRe_2(CO)_8(\mu_3\text{-}SPh)(CH{=}CPh)$ and $Cp^*WRe_2(CO)_7(\mu\text{-}SPh)(CH{=}CPh)$. The octacarbonyl cluster possesses a V-shaped polyhedral core with a face-bridging thiolate ligand and a $\mu_3\text{-}\eta^2$ (‖) acetylide ligand, while the heptacarbonyl cluster contains a triangular frame with an edge-bridging thiolate and a $\mu_3\text{-}\eta^2$ (⊥) acetylide ligand. Different chemistry is observed in the reaction of the vinylacetylide clusters $Cp^*WRe_2(CO)_9\{CC\overline{C{=}CH(C}H_2)_4\}$ and $Cp^*WRe_2(CO)_9\{CCC(Me){=}CH_2\}$ with thiophenol [219].

$PPh_3$ adds to $[Fe_2Rh(CO)_{10}]^-$ to give $[Fe_2Rh(CO)_9(PPh_3)]^-$, which shows a triangular metal frame and a rhodium-bound $PPh_3$ group. The report also includes data from the reaction between $[Fe_2Rh_2(CO)_{12}]^{2-}$ and $ClAu(PPh_3)$ [220]. The clusters $CpFe_2Co(CO)_6(\mu_3\text{-}Se)_2$ and $CpFe_2Co(CO)_6(\mu_3\text{-}Se)(\mu_3\text{-}S)$ have been prepared

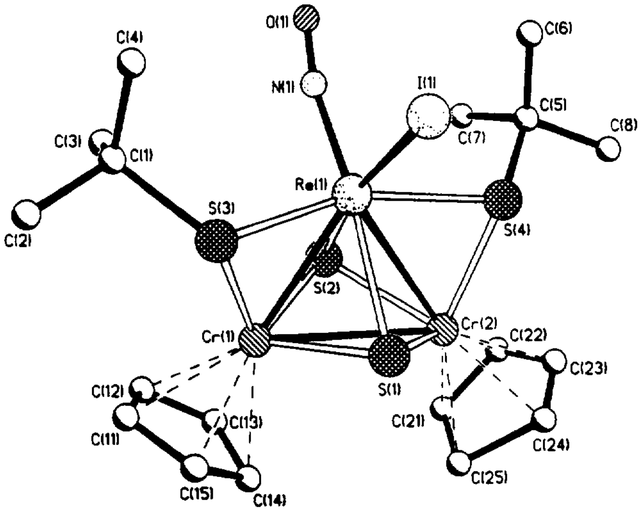

Fig. 20. X-ray structure of $Cp_2Cr_2(\mu\text{-}SCMe_3)_2(\mu_3\text{-}S)_2Re(NO)I$. Reprinted with permission from Organometallics. Copyright 1995 American Chemical Society.

from $Fe_2(CO)_6(\mu\text{-SSe})$ and $CpCo(CO)_2$. Both clusters were characterized in solution and by X-ray diffraction analysis. Both of these products are 50-electron clusters, possessing *nido* polyhedral structures [221]. Photolysis of a mixture of $Cp_2MH_2$ (where M = Mo, W) and $\{CpRu(CO)_2\}_2$ yields the trinuclear compounds $Cp(\mu,\sigma\text{-}\eta^5\text{-}C_5H_4)M(\mu\text{-}CO)_2RuCpRuCp(CO)H$. These clusters contain the original Ru–Ru bond, a new M–Ru bond, and one bridging $(\mu,\sigma\text{-}\eta^5\text{-}C_5H_4)$ ring between the M atom and the other Ru center. The spectroscopic and diffraction data are discussed [222]. The reaction between $Os_2(CO)_8(\mu\text{-}\eta^1,\eta^1\text{-}C_2H_4)$ and $CpRh(CO)(PR_3)$ (where R = Me, Ph) yields the known clusters $CpOs_2Rh(CO)_9$ and $Os_3(CO)_{11}(PR_3)$, in addition to the new cluster $CpOs_2Rh(CO)_8(PR_3)$. The fluxional behavior of the CO groups in the new cluster was examined by NMR spectroscopy. The CO exchange pathways and the steric effect of the $PMe_3$ ligand on the CO scrambling are discussed [223]. Rational synthetic routes to chalcogenide clusters are presented. Treatment of $Fe_3(CO)_9E_2$ (where E = Te, Se) with $[Co(CO)_4]^-$ gives the tetrahedral clusters $[EFe_2Co(CO)_9]^-$. $[Mn(CO)_5]^-$ reacts with $Te_2Fe_3(CO)_9$ to give the bridging butterfly cluster $[Te_2Fe_2Mn(CO)_{10}]^-$, while the use of $Se_2Fe_3(CO)_9$ affords the square-pyramidal cluster $[Se_2Fe_2Mn(CO)_9]^-$. The X-ray structures of $[SeFe_2Co(CO)_9]^-$, $[Te_2Fe_2Mn(CO)_{10}]^-$ (Fig. 21), and $[Se_2Fe_2Mn(CO)_9]^-$ are presented [224].

The rhenium carbyne complex $CpRe(CO)_2\{C(O)C_2HB_{10}H_{10}\}(\equiv CPh)$ reacts with $Co_2(CO)_8$ to furnish the bridging carbyne cluster $CpReCo_2(CO)_5(\mu\text{-}CO)_2(\mu_3\text{-}CPh)(C_2HB_{10}H_{10})$. X-ray analysis reveals that the carboranyl ligand has been transferred from the formacyl group to the cobalt center. The product exhibits a tetrahedral core, with a bridging CO group that spans each Co–Re vector [225]. The synthesis and X-ray structure of $(CpCo)_2Fe(CO)_2(PPh_3)(\mu_3\text{-}S)\{\mu_3\text{-}CNC(O)Ph\}$ have been reported. This new cluster

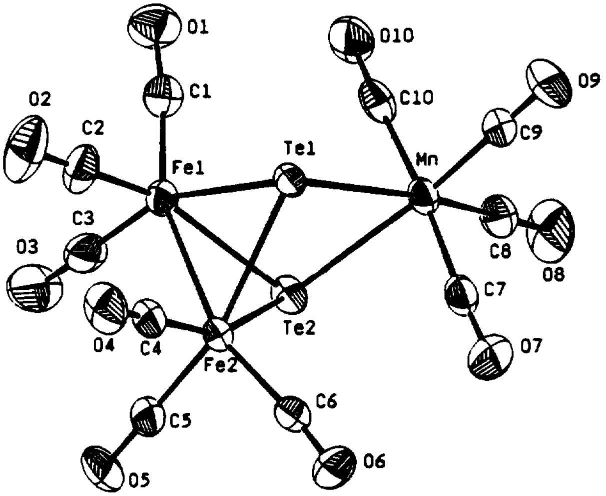

Fig. 21. X-ray structure of $[Te_2Fe_2Mn(CO)_{10}]^-$. Reprinted with permission from Inorganic Chemistry. Copyright 1995 American Chemical Society.

has been obtained from the reaction between $Fe(CO)_2(PPh_3)_2\{\eta^2\text{-SCNC(O)Ph}\}$ and $CpCo(PPh_3)_2$ [226]. Six new heterometallic tetrahedrane clusters have been prepared from $RCCo_3(CO)_9$ using metal-exchange procedures. The new clusters have the formula $RCCo_2M(CO)_8MeCp$ and $RCCoM_2(CO)_7(MeCp)_2$ (where R = Ph, $EtO_2C$; M = Mo, W) [227]. Treatment of $PhCCo_3(CO)_9$ with $[RCpW(CO)_3]^-$ (where R = HCO, MeCO, $EtO_2C$) yields the corresponding tetrahedral clusters $PhCCo_2W(CO)_8(RCp)$. The new clusters were characterized by IR and $^1H$-NMR spectroscopy, and by X-ray diffraction analysis in the case of the acyl derivative [228]. The use of $PhCCo_2Mo(CO)_8\{RC(O)Cp\}$ (where R = H, Me, EtO) in the synthesis of chiral tetrahedral clusters is reported. Electron-withdrawing groups on the cyclopentadienyl ring in $[RC(O)CpMo(CO)_3]^-$ retard the rate of metal exchange with $PhCCo_3(CO)_9$ [229].

The reaction of $Cp(CO)_2MnPt(\mu\text{-C=CHPh})(PPh_3)(L)$ (where L = $PPh_3$, CO) with $Fe_2(CO)_9$ in benzene at room temperature affords the $\mu_3$-vinylidene cluster $CpMnFePt(\mu_3\text{-C=CHPh})(CO)_6(PPh_3)$ in quantitative yield. The phosphite-substituted compounds $Cp(CO)_2MnPt(\mu\text{-C=CHPh})L_2$ {where L = $P(OEt)_3$, $P(OPr^i)_3$} react with $Fe_2(CO)_9$ to give $CpMnFePt(\mu_3\text{-C=CHPh})(CO)_5L_2$ and $CpMnFePt(\mu_3\text{-C=CHPh})(CO)_6L$. Use of the dppm-substituted compound $Cp(CO)_2MnPt(\mu\text{-C=CHPh})(dppm)$ gives the analogous trimetal cluster as a minor product and the tetrametal cluster $(dppm)PtFe_3(\mu_4\text{-C=CHPh})(CO)_9$ as the major product [230]. Isolobal displacement reactions have been studied in $\mu_3$-sulfido capped clusters, and plausible reaction pathways discussed [231]. Treatment of $FeCo_2(CO)_9(\mu_3\text{-S})$ with $[(RCp)M(CO)_3]^-$ {where R = $CO_2Me$, $CO_2Et$; M = Mo; R = $CO_2Me$, $CO_2Et$, C(O)Me; M = W} leads to tetrahedral clusters having a MFeCoS core. The reduction of the pendant cyclopentadienyl R group by Grignard reagents and $NaBH_4$ has been studied, and the use of the product alcohols in cluster-linking reactions presented. Two X-ray structures are included in this report [232].

### 3.2. Tetranuclear clusters

The cubane-like compound $Cp^*Ti(\mu_3\text{-O})_3\{Rh(COD)\}_3$ has been synthesized from $Cp^*TiMe_3$ and $\{Rh(\mu_2\text{-OH})(COD)\}_2$. The catalytic activity of this compound in Fischer-Tropsch reactions was explored, with CO conversion being on the order of 30% [233].

The sulfido-bridged clusters $MeCp_3Mo_3CoS_4(CO)$, $MeCp_3Mo_3FeS_4(SH)$, and $MeCp_2Mo_2Co_2S_2(PPh_3)(CO)$ have been prepared and their molecular structures determined. These clusters possess a tetrahedral metal core, giving a cubane-like geometry. Cluster generalizations are made concerning the number of valence electrons, the nature of the HOMO, and the adopted structural motif [234].

$[Mn_3(CO)_{12}(\mu\text{-H})]^{2-}$ reacts with $ClAu(PR_3)$ (where R = Ph, Me) and $(AuCl)_2(\mu\text{-dppe})$ to give $[Mn_3(CO)_{12}(\mu_3\text{-H})(\mu\text{-AuPR}_3)]^-$ and $[\{Mn_3(CO)_{12}(\mu_3\text{-H})Au\}_2(\mu\text{-dppe})]^{2-}$, respectively. Use of $(AuCl)_3$(triphos) leads to three aurated-Mn clusters depending on the molar ratio of the reagents employed. The cluster $[Fe_3(CO)_{11}]^{2-}$ has also been used in these auration reactions [235]. Cluster expansion in $Fe_3(CO)_9(\mu_3\text{-}\eta^2\text{-N}\equiv\text{CPh})$ with various reagents leads to new mixed-metal clusters having the composition $Fe_3(CO)_9ML(\mu_4\text{-}\eta^2\text{-}N{\equiv}CPh)$ {where $ML = Fe(CO)_3$, CpRh, $Ru(CO)_3$}. The unsymmetrical capping mode exhibited by the benzonitrile ligand was confirmed by X-ray crystallography. These product clusters possess a butterfly polyhedral core [236]. Unexpected gold-containing boride clusters have been prepared from $Cp^*Ru_3Rh(CO)_9(BH_2)$ and selected gold reagents. Included in this report are the X-ray structures of $Cp^*Ru_3Rh(CO)_9(H)B(AuPPh_3)_2(AuCl)$ and $Cp^*Ru_3Rh(CO)_9(H)B\{Au_2(dppf)\}(AuCl)$. The linked cluster compound $\{Cp^*Ru_3Rh(CO)_9(H)B(AuCl)\}_2\{\mu\text{-}Au(dppa)Au\}_2$ has also been synthesized and characterized in solution [237]. $[H_2Ru_3Rh(CO)_{12}]^-$ reacts with $[AuPPh_3]^+$ to give the hexanuclear cluster $AuHRu_3Rh_2(CO)_{13}(PPh_3)_2$. X-ray diffraction analysis reveals that the geometry of this cluster consists of a bicapped tetrahedral core with the Ru atoms defining a trigonal plane and the Rh atoms adjacent to each other. The $AuPPh_3$ moiety caps a $Rh_2Ru$ face [238]. The reaction between $Ru_3(CO)_{12}$ and the carbene compound $Cp_2Ta(=CH_2)(Me)$ has been examined with respect to CO deoxygenation chemistry. The cluster $Cp_2Ta(Me)(\mu\text{-}O)Ru_3(CO)_9(C_4H_4)$ has been isolated and shown to possess a 4-cumulene ligand that bridges the three ruthenium centers. A likely mechanism illustrating the carbon–carbon bond-forming reaction is discussed [239]. Treatment of $Ru_3(CO)_{10}(\mu\text{-}COMe)(\mu\text{-}H)$ with $Pt(PR_3)(nbd)$ (where R = Cy, $Pr^i$) affords the clusters $Ru_3Pt(CO)_{10}(PR_3)(\mu_3\text{-}COMe)(\mu\text{-}H)$. The solid-state structure of $Ru_3Pt(CO)_{10}(PCy_3)(\mu_3\text{-}COMe)(\mu\text{-}H)$ was solved by X-ray crystallography (Fig. 22) and EXAFS spectroscopy. Two fluxional processes involving CO scrambling have been observed by NMR spectroscopy. The lowest energy process involves the equilibration of all the Ru-bound CO groups, while the higher energy process involves the complete CO scrambling about the cluster polyhedron [240].

Mixed-metal butterfly acetamidediato clusters have synthesized. Treatment of $[Ru_3(CO)_9(\mu_3\text{-}O)]^{2-}$ with $[M(CO)_3(MeCN)_3]^+$ (where M = Mn, Re) leads to $[MRu_3(CO)_{12}\{\eta^2\text{-}\mu_3\text{-}NC(\mu\text{-}O)Me\}]^-$. The X-ray structure of the $MnRu_3$ cluster exhibits a hinged butterfly array of metals with a bridging acetamidediato ligand that tethers the Mn and two Ru atoms by the $\mu_3$-N moiety. Reactivity comparisons are made between $[Ru_3(CO)_9(\mu_3\text{-}O)]^{2-}$ and $[Fe_3(CO)_9(\mu_3\text{-}O)]^{2-}$ [241]. The synthesis, structure, and bonding in the butterfly clusters $[Fe_3M(CO)_{12}(\mu_4\text{-}E)]^-$ (where M = Mn, Re; E = O, S) are reported. These clusters are prepared from $[Fe_3(CO)_9(\mu_3\text{-}E)]^{2-}$ and the electrophilic reagents $[Mn(CO)_3(MeCN)_3]^+$ and $Re(CO)_5(OSO_2CF_3)$. The X-ray structures of $[Fe_3Mn(CO)_{12}(\mu_4\text{-}O)]^-$ (Fig. 23) and $[Fe_3Mn(CO)_{12}(\mu_4\text{-}S)]^-$ are presented and their structural features discussed. The results of Fenske-Hall MO calculations on these oxo- and sulfido-bridged clusters are contrasted with the MO data obtained from for the clusters $[Fe_4(CO)_{12}(\mu_4\text{-}C)]^{2-}$ and $[Fe_4(CO)_{12}(\mu_4\text{-}N)]^-$. The variable-temperature behavior of the CO groups in these clusters has also been studied by $^{13}C$-NMR spectroscopy [242].

The ketenyl cluster $Cp^*WOs_3(CO)_9(C_2)(OC_2Ph)$ has been isolated from the known acetylide cluster $Cp^*WOs_3(CO)_9(C_2)(C_2Ph)$ after treatment with $O_2$. The ketenyl cluster loses CO upon heating to give the alkylidyne cluster

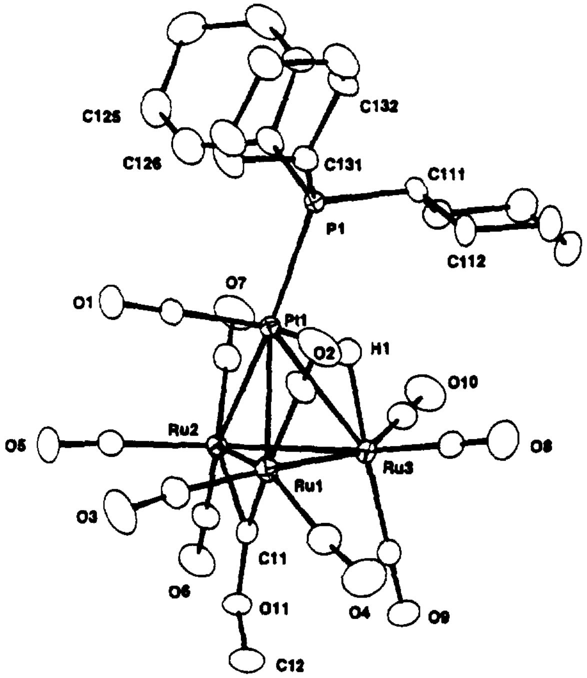

Fig. 22. X-ray structure of $Ru_3Pt(CO)_{10}(PCy_3)(\mu_3\text{-}COMe)(\mu\text{-}H)$. Reprinted with permission from Organometallics. Copyright 1995 American Chemical Society.

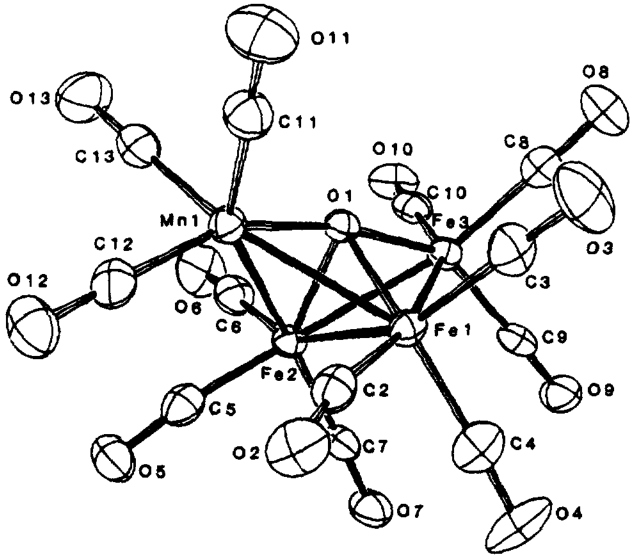

Fig. 23. X-ray structure of $[Fe_3Mn(CO)_{12}(\mu_4\text{-}O)]^-$. Reprinted with permission from Inorganic Chemistry. Copyright 1995 American Chemical Society.

$Cp^*WOs_3(CO)_9(C_2)(CPh)$. Both of these new clusters were structurally characterized by X-ray crystallography. This research provides a logical pathway for the oxidation of a cluster-bound acetylide ligand into a carbyne fragment [243]. Reversible C-C bond scission and C–H bond activation are reported for the butterfly clusters $Cp^*WOs_3(CO)_{11}(CCR)$ (where R = Ph, Bu, $CH_2OMe$) upon treatment with $Me_3NO$. The nature of the products observed is dependent on the R substituent, with the two main products being the carbido-alkylidyne cluster $Cp^*WOs_3(CO)_{10}(\mu_4\text{-}C)(\mu\text{-}CPh)$ and the carbido-vinylidene clusters $Cp^*WOs_3(CO)_9(\mu_4\text{-}C)(\mu\text{-}H)(CCHR')$ (where R′ = Pr, OMe). A scheme showing the mechanistic pathways responsible for the production of the observed products is presented and discussed. Two representative X-ray structures are also included in this report [244]. Skeletal rearrangement and acetylide ligand migration in $Cp^*WOs_3(CO)_{11}(C{\equiv}CCH_2Me)$ have been observed. The $WOs_3$ cluster has been synthesized from the reaction between $Cp^*W(CO)_2(C{\equiv}CCH_2Me)$ and $Os_3(CO)_{10}(MeCN)_2$ in refluxing toluene. The two isomers of $Cp^*WOs_3(CO)_{11}(C{\equiv}CCH_2Me)$ isolated both contain a butterfly skeletal core and a $\mu_4\text{-}\eta^2$-acetylide ligand. Relocation of $Cp^*W(CO)_2$ moiety from a hinge site to a wingtip site interconverts these isomers. This migration has been studied kinetically, the results of which are discussed relative to the proposed isomerization mechanism. The molecular structure of $Cp^*WOs_3(CO)_{11}(C{\equiv}CCH_2Me)$ {$Cp^*W(CO)_2$ wigtip isomer, Fig. 24} has been crystallographically established [245].

The reaction of tetrahydrothiophene with $HRuCo_3(CO)_{12}$, $HRuRh_3(CO)_{12}$, $H_4Ru_4(CO)_{12}$, and $Ru_3(CO)_{12}$ gives $HRuCo_3(CO)_{11}(SC_4H_8)$, $\{HRuRh_3(CO)_9\}_2(SC_4H_8)_3$, $H_2Ru_4(CO)_{12}(SC_4H_8)$, and $Ru_4(CO)_{13}(SC_4H_8)$, respectively. The X-ray structures of these products are reported [246].

The mixed-metal clusters $[Pt_3\{M(CO)_3\}(\mu\text{-dppm})_3]^+$ (where M = Mn, Re) have

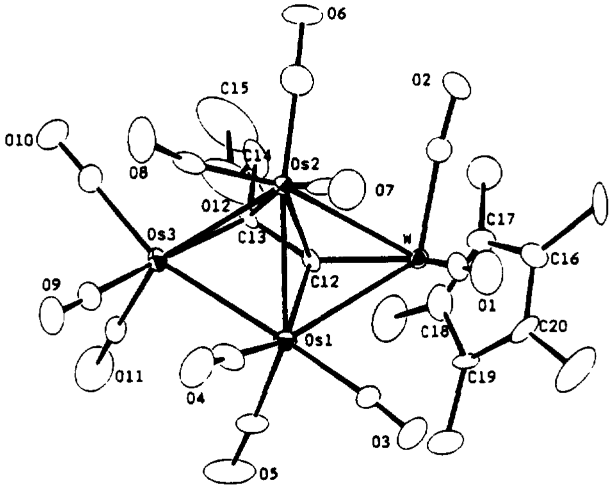

Fig. 24. X-ray structure of $Cp^*WOs_3(CO)_{11}(C{\equiv}CCH_2Me)$. Reprinted with permission from Organometallics. Copyright 1995 American Chemical Society.

been prepared from $[Pt_3(\mu_3\text{-}CO)(\mu\text{-dppm})_3]^{2+}$ and $[M(CO)_5]^-$. Each new cluster was characterized in solution and by X-ray diffraction analysis in the case of the $Pt_3Re$ cluster. A tetrahedral core, with short metal–metal bond lengths, is observed [247]. Halide addition occurs at the $Pt_3$ face in the clusters $[Pt_3(\mu_3\text{-}ReL_3)(\mu\text{-dppm})_3]^+$ (where L = CO, O). The resulting $Pt_3(\mu_3\text{-}X)(\mu_3\text{-}ReL_3)(\mu\text{-dppm})_3$ clusters (where X = Cl, Br, I) reversibly lose their halide ligand in a trend that is related to the overall stability of the cluster ($I^- > Br^- > Cl^-$). The X-ray structure of the iodo derivative and the addition of $[SnF_3]^-$ and $[SnCl_3]^-$ to the parent cationic clusters are discussed [248]. Site-selective ligand addition in the 54-electron cluster $[Pt_3\{Re(CO)_3\}(\mu\text{-dppm})_3]^+$ is reported to occur at the rhenium center, giving $[Pt_3\{Re(CO)_3L\}(\mu\text{-dppm})_3]^+$ (where L = phosphite, CO, isonitriles, thiols, terminal alkynes). The solid-state structure of the $P(OPh)_3$ derivative (Fig. 25) confirms the site of ligand addition. The reversible ligand addition and fluxional behavior of these adducts have been examined by NMR studies. The bonding in these 56-electron products has been investigated by extended Hückel calculations, and the strength of the Pt–Re bonds relative to the starting cluster discussed. The ligand addition selectivity is also discussed relative to reactivity patterns exhibited by heterogeneous Pt/Re catalysts [249].

The synthesis and X-ray structure of the stable bimetallic complex

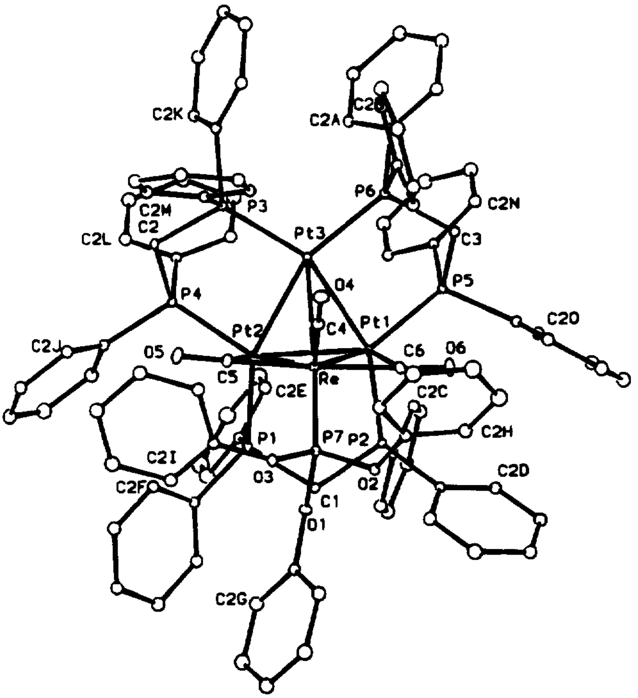

Fig. 25. X-ray structure of $[Pt_3\{Re(CO)_3P(OPh)_3\}(\mu\text{-dppm})_3]^+$. Reprinted with permission from Organometallics. Copyright 1995 American Chemical Society.

$\{(\eta^5\text{-}C_5H_4SiMe_3)_2Ti(C{\equiv}CSiMe_3)(C{\equiv}CCu)\}_2$ have been published [250]. Oxidation of the 60 VSE cubane cluster $(\eta^5\text{-}C_5Me_4Et)_2Mo_2Co_2S_4(CO)_2$ by $X_2$ (where X = Cl, Br, I) furnishes the corresponding 58 VSE cluster $(\eta^5\text{-}C_5Me_4Et)_2Mo_2Co_2S_4(X)_2$. The structural changes that accompany the oxidation have been assessed by X-ray crystallography and magnetic susceptibility measurements. The use of these electron-deficient clusters as models for desulfurization reactions is described [251]. The synthesis and X-ray structure of the first mixed-metal borole cluster have been published. The electron-deficient cluster $\{(\eta^5\text{-}C_4H_4BPh)Re(CO)_3\}_2Pd_2$ was obtained from $[(\eta^5\text{-}C_4H_4BPh)Re(CO)_3]^-$ and a variety of palladium reagents. The cyclic voltammetric data are reported for this new cluster, and these data are compared to related 58-electron planar, triangulated clusters. The HOMO-LUMO gap in the $Re_2Pd_2$ cluster has been calculated by the use of extended Hückel MO calculations [252]. The valence isomerization and rearrangement reactivity in the compounds $Mn_2(AuPR_3)_2(\mu_4\text{-}PCy)(CO)_8$ and $Mn_2(\mu\text{-}AuPR_3)\{\mu_3\text{-}PCy(AuPR_3)\}(CO)_8$ (where R = Ph, $p\text{-}C_6H_4F$, $p\text{-}C_6H_4OMe$, Cy, Et, $CH_2CH_2CN$) have been studied [253]. The reaction between $\{\eta^5\text{-}C_5H_4C(O)OMe\}_2Mo_2(CO)_4$ and $Fe_2(CO)_6(\mu\text{-}S)_2$ affords the new cluster $\{\eta^5\text{-}C_5H_4C(O)OMe\}_2Mo_2Fe_2(CO)_6(\mu_3\text{-}CO)_2(\mu_3\text{-}S)_2$. This cluster has been characterized in solution and by X-ray diffraction analysis [254]. The bonding in tetrametallic-carbide clusters has been examined by extended Hückel MO calculations. Isomerization schemes and the fluxionality pathways available to $Cp_2Fe_2Ru_2(CO)_9(C_2)$, $Cp^*_2Fe_2Ru_2(CO)_{10}(C_2)$, and $Ru_4(CO)_{12}(\mu\text{-}PPh_2)_2(C_2)$ are discussed [255]. The synthesis and spectroscopic characterization of the tetranuclear vinylidene clusters $Co_2M(CO)_9\{\mu_3\text{-}C{=}C(H)CpFe(CO)_2\}$ (where M = Fe, Ru; Cp = $C_5H_5$, $C_5Me_5$) are reported. These clusters readily lose CO to give the tetranuclear acetylide clusters $(\mu_4\text{-}C_2H)(CpFe)MCo_2(CO)_{10}$, whose solid-state structures possess a spiked triangular array of metals. Three X-ray structures are included in this report, along with a plausible mechanism showing the involvement of alkyne-cluster intermediates in these transformations [256]. CO substitution by dppm in $\{(CO)_4CoAu\}_2(dppm)$ gives $Co_2Au_2(CO)_6(\mu\text{-}dppm)_2$, whose structure was established by X-ray crystallography [257].

### 3.3. Pentanuclear clusters

The crystal structure of $Cp^*Ru_4Rh(CO)_{13}(H)(BH_2)$ has been determined, and the pentametal frame is best described as a "spiked-butterfly", with the rhodium atom located at the spike position. The bonding is this cluster has been explored by Fenske-Hall MO calculations, with ambiguities in the electron-counting scheme for this cluster discussed [258]. Treatment of $[H_2Ru_3Rh(CO)_{12}]^-$ with $PPh_3$ gives the neutral cluster $H_2Ru_3Rh_2(CO)_{13}(PPh_3)$. The X-ray structure of the $Ru_3Rh_2$ cluster exhibits a trigonal bipyramidal core, with the rhodium atoms occupying the apical positions. The $PPh_3$ ligand is coordinated to one of the rhodium centers [259]. Functionalization of the ketenylidene-bridged cluster $[Fe_3(CO)_9(\mu_3\text{-}CCO)]^{2-}$ using $ClAu(PPh_3)$ gives $(AuPPh_3)_2Fe_3(CO)_9(\mu_3\text{-}CCO)$. Use of allyl bromide gives $[Fe_3(CO)_9(\mu_3\text{-}CO)(\mu_3\text{-}CC_3H_5)]^-$. The auration of other cluster complexes is also discussed [260]. $H_2Os_3(CO)_{10}$ reacts with $(bpy)Pd(CO_2Me)_2$ to give $\{(bpy)Pd\}_2Os_3(CO)_{10}$ in good yield. The solid-state structure is based on an edge-bridged square metal core [261]. Ethanethiol addition to $HRuRh_3(CO)_{12}$ furnishes the cluster $Rh_2Ru_3(CO)_{10}(\mu\text{-}SEt)_8$, as a minor reaction product. The molecular structure was determined by X-ray diffraction analysis [262]. The bow-tie cluster $Co_2Ru_3(\mu_5\text{-}\eta^2,\eta^2\text{-}PhC_2C_2Ph)(CO)_{14}$ has been prepared in quantitative yield from the reaction between $Co_2(CO)_8$ and $Ru_3(CO)_9(\mu\text{-}CO)(\mu_3\text{-}\eta^2\text{-}PhC_2C_2Ph)$. The diyne ligand straddles the $Co_2Ru_3$ bow-tie frame, interacting with all five metal centers, as shown by X-ray crystallography [263]. An IR study on several pentametal clusters possessing trigonal bipyramidal polyhedra has been published. The bridging CO groups are shown to be more sensitive indicators of molecular geometry than the terminal CO groups [264]. The synthesis and molecular structure of the paramagnetic cluster $Co[(Cp^*Co)_2\{\mu_2\text{-}S_2(\text{ferrocene})\}_2]$ have been published [265]. Condensation of $Ru_3(CO)_{12}$ with $[CpW(CO)_3]^-$ and $[Cp^*M(CO)_3]^-$ (where M = Mo, W) affords the pentametal clusters $CpWRu_4(CO)_{14}(\mu_3\text{-}H)$, $Cp^*MoRu_4(CO)_{14}(\mu_3\text{-}H)$, and $Cp^*MoRu_4(CO)_{14}(\mu_3\text{-}H)$, after protonation with excess $CF_3CO_2H$. The molecular structure of the Cp derivative exhibits a trigonal-bipyramidal $Ru_4W$ core, with the W center occupying an equatorial site. The two Cp* clusters exhibit an edge-bridged tetrahedral geometry, where the tentacle Cp*M fragment bridges a Ru–Ru edge (Fig. 26). The facile fragmentation of these clusters under syn gas is presented [266].

### 3.4. Hexanuclear clusters

The following new clusters $Os_5Pd(CO)_{16}(\mu\text{-}H)_6$, $Os_5Pd(CO)_{16}(\mu\text{-}H)_4H(\mu\text{-}Cl)$, $Os_5Pd(CO)_{16}(\mu\text{-}H)_4(\mu\text{-}Cl)_2$, $\{Os_3Pd(CO)_9(\mu\text{-}H)_2(\mu\text{-}Cl)\}_2$, and $Os_4Pd(CO)_{11}$

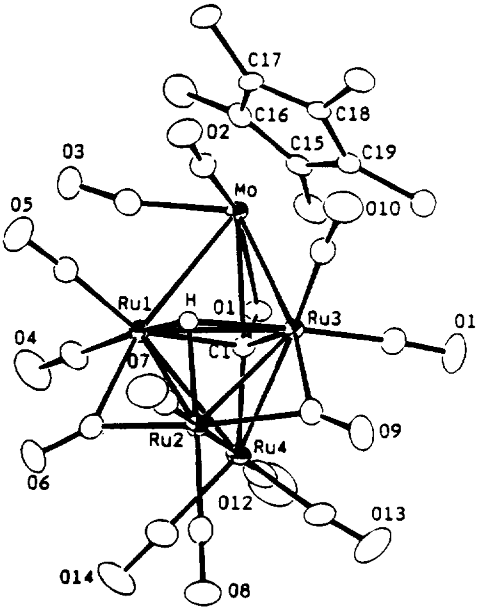

Fig. 26. X-ray structure of $Cp^*MoRu_4(CO)_{14}(\mu_3\text{-}H)$. Reprinted with permission from Organometallics. Copyright 1995 American Chemical Society.

$(\mu\text{-H})_3(\mu\text{-Cl})_3(py)$ have been isolated from the reaction between $H_2Os_3(CO)_{10}$ and *trans*-$Pd(py)_2Cl_2$. The X-ray structures of all five clusters have been determined [267]. The steric properties of the ligand $P(C_6H_4Me\text{-}2)_3$ in various clusters have been examined. The particular ligand has been allowed to react with the product formed from the reaction between $[H_2Ru_4(CO)_{12}]^{2-}$ and $[Ag(MeCN)_4]^+$ to give the mixed-metal cluster $Ag_2Ru_4(CO)_{12}(\mu_3\text{-H})_2\{P(C_6H_4Me\text{-}2)_3\}_2$. The solid-state structure displays a capped trigonal bipyramidal polyhedron. The ability of two of the three $C_6H_4Me\text{-}2$ rings in each of the two $P(C_6H_4Me\text{-}2)_3$ ligands to adopt orientations that minimize the calculated cone angle of 194° is discussed [268]. $Hg_2I_2$ reacts with the cluster $Pt_4(\mu\text{-CO})_5(PMe_2Ph)_4$ to yield the bicapped cluster $\{Pt_4(\mu\text{-CO})_4(PMe_2Ph)_4\}(\mu_3\text{-HgI})_2$. IR and NMR spectroscopic data and the X-ray structure are presented [269]. The reactivity of $Pt_2M_4(C{\equiv}CR)_8$ (where M = Ag, Cu; R = Ph, $Bu^t$) with neutral and anionic ligands has been investigated [270]. The mixed-metal clusters $M_2Ru_4(CO)_{12}(\mu_3\text{-H})_2(\mu\text{-dppf})$ (where M = Cu, Ag) have been prepared from $[Ru_4(CO)_{12}(\mu\text{-H})_2]^{2-}$, $[M(MeCN)_4]^+$, and dppf. The corresponding gold derivative has been isolated from the reaction between $[Ru_4(CO)_{12}(\mu\text{-H})_2]^{2-}$ and $Au_2(\mu\text{-dppf})Cl_2$. Skeletal isomerization of the metal framework has been verified by variable-temperature $^1H$- and $^{31}P$-NMR studies. The X-ray structures of these new clusters are discussed [271]. The first reported transformation involving the conversion of alkynes into two methylidyne groups has been published. The alkyne scission takes place in the reaction between $Cp_2Mo_2(CO)_4(\mu\text{-}R'C_2R)$ (where R′ = R = Me; R′ = H, R = H, Me, Ph) and $Ru_3(CO)_{12}$ in refluxing toluene or heptane. The isolated clusters $Cp_2Mo_2Ru_4(CO)_{12}(\mu_3\text{-CR}')(\mu_3\text{-CR})$ have been fully characterized in solution and X-ray crystallography in the case of the butyne-derived cluster [272]. The reaction between the butterfly cluster $[HRu_4(CO)_{12}(BH)]^-$ and $Rh_2(CO)_4Cl_2$ furnishes the octahedral boride cluster $[Rh_2Ru_4(CO)_{16}(B)]^-$. $^{11}B$-NMR data suggest the presence of both *cis*- and *trans*-isomers, with the latter isomer predominating in solution. This anionic cluster undergoes auration when treated with $ClAu(PCy_3)$. The corresponding iridium cluster, $[Ir_2Ru_4(CO)_{16}(B)]^-$, has been synthesized and its crystal structure determined. Functionalization of this $Ir_2Ru_4$ cluster with $ClAu(PCy_3)$ is discussed [273]. The synthesis and reactivity investigation of new $PtAg_2$ and $Pt_2Ag_4$ clusters containing bridging alkynyl ligands are reported. The molecular structure of $Pt_2Ag_4(C_6F_5)_4(\mu_3\text{-}\eta^2\text{-}C{\equiv}CPh)_4(PPh_3)_2$ accompanies this report [274]. The reaction of $[Fe_2(CO)_6(\mu\text{-RE})(\mu\text{-CO})]$ (where RE = various thiol and seleno groups) with $S_2Cl_2$ affords a variety of single-, double- and triple-cluster complexes [275]. The synthesis and X-ray structural determination of $[Pt_5(CO)_5(PCy_3)_4Re(\mu\text{-O})_3(\mu\text{-OH})(ReO_4)]^+$ (Fig. 27) are reported, and the data are discussed relative to $Pt/Re\text{-}Al_2O_3$ catalysts. Extended Hückel MO calculations on the model cluster $[Pt_5(CO)_5(PH_3)_4ReO_4]^+$ have been carried out, and the evidence for Pt/Re multiple bonding presented [276].

### 3.5. *Higher nuclearity clusters*

The photolysis of $R_3PAuN_3$ leads to the reductive elimination of azide and generation of $R_3PAu^{(0)}$ moieties, which combine to yield Au clusters. Irradiation of

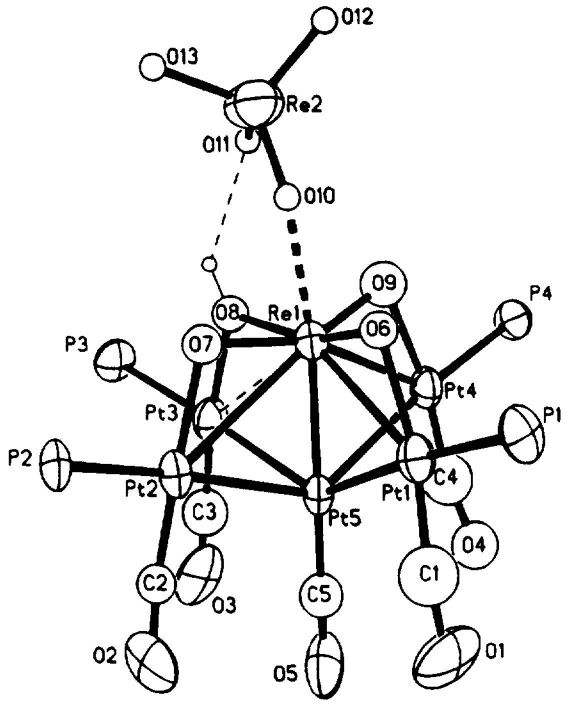

Fig. 27. X-ray structure of $[Pt_5(CO)_5(PCy_3)_4Re\,(\mu\text{-}O)_3(\mu\text{-}OH)(ReO_4)]^+$. Reprinted with permission from Journal of American Chemical Society. Copyright 1995 American Chemical Society.

$R_3PAuN_3$ in the presence of $M(dppe)(N_3)_2$ (where M = Pd, Pt) gives heteronuclear Pd/Au and Pt/Au clusters, in addition to a $PdAu_{12}$ cluster that possesses a complete $Au_{12}$ icosahedron containing an encapsulated Pd atom [277]. Thermolysis of the mixed-metal dicarbide clusters $\{\mu_3\text{-}C\equiv CFeCp(CO)_2\}Ru_3(CO)_9(\mu\text{-}H)$ and $[\{\mu_3\text{-}C\equiv CFeCp(CO)_2\}Ru_3(CO)_9]^-$ leads to coupling of the $(C_2)FeRu_3$ cores and formation of the heptanuclear clusters $Cp_2Fe_2Ru_5(\mu_5\text{-}C_2)_2(CO)_{17}$ and $CpFeRu_6(\mu_5\text{-}C_2)(\mu_5\text{-}C_2H)(CO)_{16}$, and the octanuclear cluster $Cp_2Fe_2Ru_6(\mu_6\text{-}C_2)_2(CO)_{17}$. Mechanisms are presented that deal with the direct radical and thermal coupling of these precursor clusters as a route to the observed products [278].

The synthesis and X-ray structure of $Ru_6C(CO)_{15}(\mu\text{-}dppf)$ have been published. Variable-temperature $^{31}P$-NMR data reveal a high degree of stereochemically non-rigid behavior. Cyclic voltammetric data confirm the existence of a significant degree of electronic communication between the redox-active sites. The HOMO is presumed to be largely ferrocene-based but with considerable $Ru_6$-cage character, while the LUMO is primarily cage-based with added ferrocene character. The paramagnetic behavior of this cluster was ascertained by magnetic susceptibility studies [279]. $[Ir_6(CO)_{15}]^{2-}$ reacts with $[AuPPh_3]^+$ to yield $Ir_6(CO)_{15}(AuPPh_3)_2$, whose molecular structure consists of an octahedral arrangement of iridium atoms and a face capping

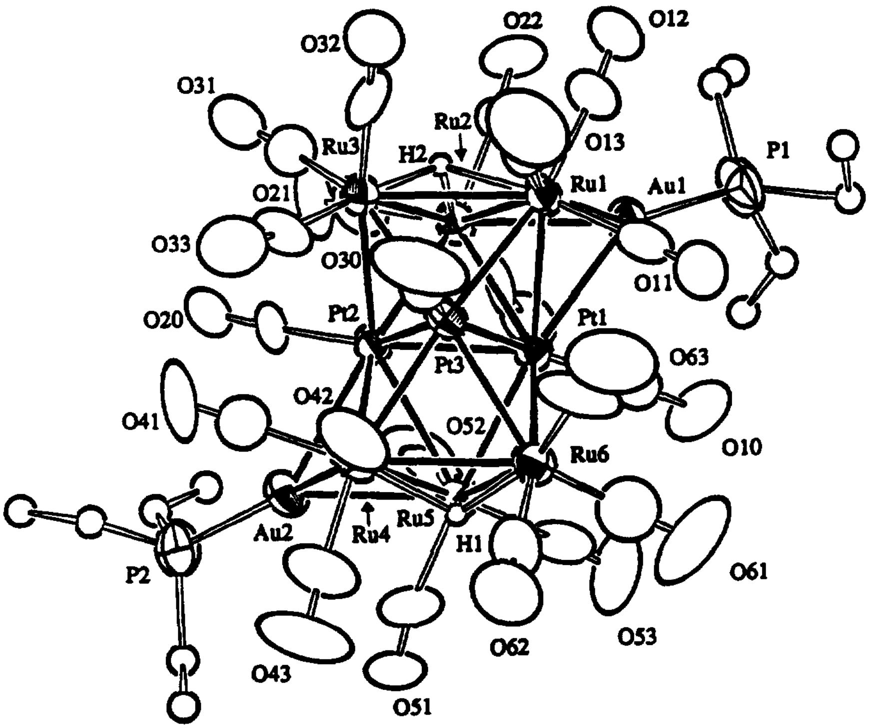

Fig. 28. X-ray structure of $Pt_3Ru_6\{Au(PEt_3)\}_2(CO)_{21}(\mu\text{-}H)_2$. Reprinted with permission from Organometallics. Copyright 1995 American Chemical Society.

$AuPPh_3$ moiety. The remaining $AuPPh_3$ group spans one Ir–Au edge. The synthesis and X-ray structure of $[Ir_6(CO)_{14}(HgCl)_2]^{2-}$ are also presented [280]. Deprotonation of $Pt_3Ru_6(CO)_{21}(\mu_3\text{-}H)(\mu\text{-}H)_3$ using $[Bu_4N][OH]$, followed by treatment with $[Au(PEt_3)]^+$, affords the layer-segregated clusters $Pt_3Ru_6\{Au(PEt_3)\}(CO)_{21}(\mu\text{-}H)_3$ and $Pt_3Ru_6\{Au(PEt_3)\}_2(CO)_{21}(\mu\text{-}H)_2$ (Fig. 28). Both clusters were characterized in solution by IR and $^1H$-NMR spectroscopy, and their solid-state structures were established by X-ray crystallography [281].

## 4. Abbreviations

| | |
|---|---|
| acac | acetylacetonate |
| ampy | 2-amino-6-methylpyridinate |
| binap | 2,2′-bis(diphenylphosphino)-1,1′-binapthyl |
| bma | 2,3-bis(diphenylphosphino)maleic anhydride |
| bpcd | 4,5-bis(diphenylphosphino)-4-cyclopenten-1,3-dione |
| bpm | 2,2′-bipyrimidine |
| bpy | 2,2′-bipyridine |
| COD | 1,5-cyclooctadiene |

| | |
|---|---|
| p | cyclopentadienyl |
| p* | pentamethylcyclopentadienyl |
| y | cyclohexyl |
| ba | dibenzylideneacetone |
| BU | 1,8-diazabicyclo[5.4.0]undec-7-ene |
| mpm | bis(dimethylphosphino)methane |
| pmp | $(Ph_2PCH_2)_2PPh$ |
| pb | 2,3-dipyrid-2-ylbenzoquinoxaline |
| pp | 2,3-dipyrid-2-ylpyrazine |
| ppa | 1,2-bis(diphenylphosphino)acetylene |
| ppe | 1,2-bis(diphenylphosphino)ethane |
| ppf | 1,1′-bis(diphenylphosphino)ferrocene |
| ppm | bis(diphenylphosphino)methane |
| ppp | 1,3-bis(diphenylphosphino)propane |
| c | ferrocenyl |
| AS | magic angle spinning |
| es | mesityl |
| eCp | methylcyclopentadienyl |
| obiph | 2,2′-bis(diphenylphosphino)-6,6′-dimethoxy-1,1′-biphenyl |
| PN | bis(triphenylphosphine)iminium |
| y | pyridine |
| FA | trifluoroacetic acid |
| HT | tetrahydrothiophene |
| ol | tolyl |

## eferences

[1] J.W. Bacon, Diss. Abstr. B, 55 (1995) 2718, DA9423841.
[2] J.-H. Chung, Diss. Abstr. B, 55 (1995) 4367, DA9505177.
[3] Z. Li, Diss. Abstr. B, 55 (1995) 4843, DA9508136.
[4] G. Hsu, Diss. Abstr. B, 55 (1995) 5338, DA9512401.
[5] J.E. Cortopassi, Diss. Abstr. B, 56 (1995) 231, DA9517263.
[6] Z. Xu, Diss. Abstr. B, 55 (1995) 3272, DA9500652.
[7] D.A. Dobbs, Diss. Abstr. B, 55 (1995) 2721, DA9430459.
[8] S.H. Druker, Diss. Abstr. B, 56 (1995) 2008, DA9527613.
[9] H. Yao, Diss. Abstr. B, 56 (1995) 2107, DA9525641.
10] G.B. Karet, Diss. Abstr. B, 55 (1995) 3301, DA9433866.
11] S. Xu, Diss. Abstr. B, 55 (1995) 4847, DA9510734.
12] C.-S. Jun, Diss. Abstr. B, 56 (1995) 233, DA9516624.
13] D.E. Gindelberger, Diss. Abstr. B, 56 (1995) 2622, DA9529318.
14] R.E. Bachman, Diss. Abstr. B, 55 (1995) 5335, DA9514150.
15] K. Yang, Diss. Abstr. B, 56 (1995) 238, DA9517660.
16] R.A. Widenhoefer, Diss. Abstr. B, 55 (1995) 4846, DA9501580.
17] M.E. Smith, Diss. Abstr. B, 55 (1995) 2687, DA9430693.
18] R. Andrés, M. Galakhov, A. Martín, M. Mena and C. Santamaría, J. Chem. Soc., Chem. Co (1995) 551–552.

[19] T.A. Budzichowski, M.H. Chisholm, K. Folting, M.G. Fromhold and W.E. Streib, Inorg. Chim. Acta, 235 (1995) 339–347.
[20] L.Y. Goh, W. Chen, R.C.S. Wong and K. Karaghiosoff, Organometallics, 14 (1995) 3886–3896.
[21] M. Akita, K. Noda, Y. Takahashi and Y. Moro-oka, Organometallics, 14 (1995) 5209–5220.
[22] T. Kilthau, B. Nuber and M.L. Ziegler, Chem. Ber., 128 (1995) 197–199.
[23] J.W. van Hal, K.H. Whitmire, B. Zouchoune, J.-F. Halet and J.-Y. Saillard, Inorg. Chem., 34 (1995) 5455–5460.
[24] E. Solari, F. Musso, E. Gallo, C. Floriani, N. Re, A. Chiesi-Villa and C. Rizzoli, Organometallics, 14 (1995) 2265–2276.
[25] G. Kong, G.N. Harakas and B.R. Whittlesey, J. Am. Chem. Soc., 117 (1995) 3502–3509.
[26] K.T. Holman and M.J. Zaworotko, J. Chem. Crystallogr., 25 (1995) 93–95.
[27] H. Abourahma, S.B. Copp, M.-A. MacDonald, R.E. Meléndez, S.D. Batchilder and M.J. Zaworotko, J. Chem. Crystallogr., 25 (1995) 731–736.
[28] S.B. Copp, K.T. Holman, J.O.S. Sangster, S. Subramanian and M.J. Zaworotko, J. Chem. Soc., Dalton Trans., (1995) 2233–2243.
[29] B. Schiemenz, G. Huttner, L. Zsolnai, P. Kircher and T. Diercks, Chem. Ber., 128 (1995) 187–191.
[30] T. Beringhelli, L. Carlucci, G. D'Alfonso, G. Ciani and D.M. Proserpio, J. Organomet. Chem., 504 (1995) 15–26.
[31] T. Beringhelli, G. D'Alfonso and M. Zarini, J. Chem. Soc., Dalton Trans., (1995) 2407–2415.
[32] J. Lewis and P.R. Raithby, J. Organomet. Chem., 500 (1995) 227–237.
[33] N.E. Leadbeater, J. Chem. Soc., Dalton Trans., (1995) 2923–2934.
[34] N.J. Tro, J.C. King and C.B. Harris, Inorg. Chim. Acta, 229 (1995) 469–471.
[35] H.D. Gafney and S.-P. Xu, Inorg. Chim. Acta, 240 (1995) 645–651.
[36] A. Sironi, Inorg. Chem., 34 (1995) 1342–1349.
[37] D. Braga, F. Grepioni, E. Tedesco, M.J. Calhorda and P.E.M. Lopes, Inorg. Chim. Acta, (1995) 3297–3306.
[38] F. Ragaini, J.-S. Song, D.L. Ramage, G.L. Geoffroy, G.A.P. Yap and A.L. Rheingold, Organometallics, 14 (1995) 387–400.
[39] S. Aime, W. Dastrù, R. Gobetto, J. Krause and L. Milone, Organometallics, 14 (1995) 4435–4438.
[40] N. Lugan, G. Lavigne, J.M. Soulié, S. Fabre, P. Kalck, J.Y. Saillard and J.F. Halet, Organometallics, 14 (1995) 1712–1731.
[41] L.A.P. Kane-Maguire, M. Manthey and B. Robinson, J. Chem. Soc., Dalton Trans., (1995) 905–908.
[42] R.H.E. Hudson and A.J. Poë, Organometallics, 14 (1995) 3238–3248.
[43] A. Neubrand, A.J. Poë and R. van Eldik, Organometallics, 14 (1995) 3249–3258.
[44] S. Aime, P.J. Barrie, D.F. Brougham, R. Gobetto and G.E. Hawkes, Inorg. Chem., 34 (1995) 3557–3559.
[45] M.G. Karpov, S.P. Tunik, V.R. Denisov, G.L. Starova, A.B. Nikol'skii, F.M. Dolgushin, A.I. Yanovsky and Y.T. Struchkov, J. Organomet. Chem., 485 (1995) 219–225.
[46] W.G.-Y. Ho and W.-T. Wong, Polyhedron, 14 (1995) 2849–2855.
[47] D.W. Knoeppel, J.-H. Chung and S.G. Shore, Acta Crystallogr. C, 51 (1995) 42–45.
[48] S. Aime, W. Dastrù, R. Gobetto, J. Krause and E. Sappa, Organometallics, 14 (1995) 3224–3228.
[49] H. Adams, A.G. Carr, B.E. Mann and R. Melling, Polyhedron, 14 (1995) 2771–2785.
[50] L. Heuer and D. Schomburg, J. Organomet. Chem., 495 (1995) 53–59.
[51] U. Bodensieck, H. Vahrenkamp, G. Rheinwald and H. Stoeckli-Evans, J. Organomet. Chem., 488 (1995) 85–90.
[52] N.M.J. Brodie and A.J. Poë, Can. J. Chem., 73 (1995) 1187–1195.
[53] S.E. Kabir, A. Miah, L. Nesa, K. Uddin, K.I. Hardcastle, E. Rosenberg and A.J. Deeming, J. Organomet. Chem., 492 (1995) 41–51.
[54] M.I. Bruce, J.R. Hinchliffe, B.W. Skelton and A.H. White, J. Organomet. Chem., 495(1995) 141–148.
[55] H. Shen, S.G. Bott and M.G. Richmond, Organometallics, 14 (1995) 4625–4634.
[56] J.W.M. van Outersterp, M.T.G. Oostenbrink, H.A. Nieuwenhuis, D.J. Stufkens and F. Hartl, Inorg. Chem., 34 (1995) 6312–6318.

[57] H.-G. Ang, S.-G. Ang, W.-L. Kwik and Q. Zhang, J. Organomet. Chem., 485 (1995) C10-C13.

[58] S. Aime, W. Dastrù, R. Gobetto, J. Krause and L. Violano, Inorg. Chim. Acta, 235 (1995) 357–366.

[59] A.J. Arce, Y. De Sanctis, R. Machado, M.V. Capparelli, J. Manzur and A.J. Deeming, Organometallics, 14 (1995) 3592–3595.

[60] H. Shen, T.J. Williams, S.G. Bott and M.G. Richmond, J. Organomet. Chem., 505 (1995) 1–9.

[61] G. Gervasio and E. Sappa, J. Organomet. Chem., 498 (1995) 73–80.

[62] M.V. Capparelli, Y. De Sanctis and A.J. Arce, Acta Crystallogr. C, 51 (1995) 1819–1822.

[63] A.A. Koridze, N.M. Astakhova, F.M. Dolgushin, A.I. Yanovsky, Y.T. Struchkov and P.V. Petrovskii, Organometallics, 14 (1995) 2167–2169.

[64] A.J. Edwards, N.E. Leadbeater, J. Lewis and P.R. Raithby, J. Chem. Soc., Dalton Trans., (1995) 3785–3787.

[65] L.V. Rybin, S.V. Osintseva, M.I. Rybinskaya, F.M. Dolgushin, A.I. Yanovsky and Y.T. Struchkov, J. Organomet. Chem., 485 (1995) 253–255.

[66] A.J. Blake, P.J. Dyson, B.F.G. Johnson and C.M. Martin, J. Organomet. Chem., 492 (1995) C17-C19.

[67] D. Braga, F. Grepioni, M.J. Calhorda and L.F. Veiros, Organometallics, 14 (1995) 1992–2001.

[68] A.J. Blake, P.J. Dyson, S.L. Ingham, B.F.G. Johnson and C.M. Martin, Organometallics, 14 (1995) 862–868.

[69] J.A. Ramsden, D.J. Milner, P.D. Hempstead, N.A. Bailey and C. White, J. Chem. Soc., Dalton Trans., (1995) 2101–2106.

[70] S.L. Ingham, B.F.G. Johnson and J.G.M. Nairn, J. Chem. Soc., Chem. Commun., (1995) 189–190.

[71] J.T. Park, J.-J. Cho and H. Song, J. Chem. Soc., Chem. Commun., (1995) 15–16.

[72] A.J. Edwards, J.U. Köhler, J. Lewis and P.R. Raithby, J. Chem. Soc., Dalton Trans., (1995) 3251–3252.

[73] D. Braga, J.J. Byrne, F. Grepioni, E. Parisini, P.J. Dyson, P.E. Gaede, B.F.G. Johnson and D. Reed, Organometallics, 14 (1995) 4892–4898.

[74] D. Wang, H. Shen, M.G. Richmond and M. Schwartz, Inorg. Chim. Acta, 236 (1995) 1–6.

[75] D. Wang, H. Shen, M.G. Richmond and M. Schwartz, Organometallics, 14 (1995) 3636–3640.

[76] P. Suter and H. Vahrenkamp, Chem. Ber., 128 (1995) 793–797.

[77] B.F.G. Johnson, D.S. Shephard, A.J. Edwards, D. Braga, E. Parisini and P.R. Raithby, J. Chem. Soc., Dalton Trans., (1995) 3307–3312.

[78] M.P. Cifuentes, T.P. Jeynes, M. Gray, M.G. Humphrey, B.W. Skelton and A.H. White, J. Organomet. Chem., 494 (1995) 267–272.

[79] R. Agarwala, K.A. Azam, R. Dilshad, S.E. Kabir, R. Miah, M. Shahiduzzaman, K.I. Hardcastle, E. Rosenberg, M.B. Hursthouse and K.M.A. Malik, J. Organomet. Chem., 492 (1995) 135–144.

[80] M. Mintert and W.S. Sheldrick, J. Chem. Soc., Dalton Trans., (1995) 2663–2669.

[81] J.A. Cabeza, I. del Río, A. Llamazares, V. Riera, S. García-Granda and J.F. Van der Maelen, Inorg. Chem., 34 (1995) 1620–1623.

[82] J.A. Cabeza, J.M. Fernández-Colinas, A. Choplin and A. Theolier, Inorg. Chim. Acta, 237 (1995) 103–109.

[83] J.A. Cabeza, R.J. Franco, V. Riera, S. García-Granda and J.F. Van der Maelen, Organometallics, 14 (1995) 3342–3348.

[84] Y.-K. Au, K.-K. Cheung and W.-T. Wong, Inorg. Chim. Acta, 238 (1995) 193–195.

[85] S.E. Kabir, E. Rosenberg, M. Day, K. Hardcastle, E. Wolf and T. McPhillips, Organometallics, 14 (1995) 721–733.

[86] R. Gobetto, K.I. Hardcastle, S.E. Kabir, L. Milone, N. Nishimura, M. Botta, E. Rosenberg and M. Yin, Organometallics, 14 (1995) 3068–3080.

[87] S.E. Kabir, D.S. Kolwaite, E. Rosenberg, K. Hardcastle, W. Cressell and J. Grindstaff, Organometallics, 14 (1995) 3611–3613.

[88] W.-Y. Wong, W.-T. Wong and S.-Z. Hu, Inorg. Chim. Acta, 234 (1995) 5–8.

[89] W.-Y. Wong, S. Chan and W.-T. Wong, J. Organomet. Chem., 493 (1995) 229–237.

[90] W.-Y. Wong, S. Chan and W.-T. Wong, J. Chem. Soc., Dalton Trans., (1995) 1497–1509.

[91] W.-Y. Wong and W.-T. Wong, J. Chem. Soc., Dalton Trans., (1995) 2831–2836.

[92] W.-Y. Wong and W.-T. Wong, J. Chem. Soc., Dalton Trans., (1995) 3995–3999.

[93] W.-Y. Wong and W.-T. Wong, J. Chem. Soc., Dalton Trans., (1995) 2735–2740.
[94] W. Paw, C.H. Lake, M.R. Churchill and J.B. Keister, Organometallics, 14 (1995) 3768–3782.
[95] N.C. Burton, C.J. Cardin, D.J. Cardin, B. Twamley and Y. Zubavichus, Organometallics, 14 (1995) 5708–5710.
[96] M.R. Jordan, P.S. White, C.K. Schauer and M.A. Mosley, III, J. Am. Chem. Soc., 117 (1995) 5403–5404.
[97] W.R. Cullen, S.J. Rettig and T.C. Zheng, Organometallics, 14 (1995) 1466–1470.
[98] S. Ye, H. Akutagawa, K. Uosaki and Y. Sasaki, Inorg. Chem., 34 (1995) 4527–4528.
[99] H.A. Mirza, J.J. Vittal and R.J. Puddephatt, Inorg. Chem., 34 (1995) 4239–4243.
[100] G.B. Karet, C.L. Stern, J.A. Cody, S.J. Lange, M.A. Pell, C. Slebodnick and D.F. Shriver, J. Organomet. Chem., 495 (1995) 33–39.
[101] S.-M. Lee, K.-K. Cheung and W.-T. Wong, J. Organomet. Chem., 494 (1995) 273–278.
[102] W.R. Cullen, S.J. Rettig and T.C. Zheng, Polyhedron, 14 (1995) 2653–2661.
[103] P. Baistrocchii, D. Cauzzi, M. Lanfranchi, G. Predieri, A. Tiripicchio and M.T. Camellini, Inorg. Chim. Acta, 235 (1995) 173–183.
[104] G.W. Drake, G.L. Schimek and J.W. Kolis, Inorg. Chim. Acta, 240 (1995) 63–69.
[105] O.J. Scherer, G. Kemény and G. Wolmershäuser, Chem. Ber., 128 (1995) 1145–1148.
[106] I.-P. Lorenz and K. Thurow, J. Organomet. Chem., 496 (1995) 191–196.
[107] R.L. Holliday, L.C. Roof, B. Hargus, D.M. Smith, P.T. Wood, W.T. Pennington and J.W. Kolis, Inorg. Chem., 34 (1995) 4392–4401.
[108] L.C. Roof, D.M. Smith, G.W. Drake, W.T. Pennington and J.W. Kolis, Inorg. Chem., 34 (1995) 337–345.
[109] R.E. Bachman, S.K. Miller and K.H. Whitmire, Organometallics, 14 (1995) 796–803.
[110] K. Hashizume, Y. Mizobe and M. Hidai, Organometallics, 14 (1995) 5367–5376.
[111] R.D. Adams, L. Chen and J.H. Yamamoto, Inorg. Chim. Acta, 229 (1995) 47–54.
[112] R.D. Adams, X. Qu and W. Wu, Organometallics, 14 (1995) 1377–1384.
[113] R.D. Adams and X. Qu, Organometallics, 14 (1995) 4167–4172.
[114] R.D. Adams and J.H. Yamamoto, Organometallics, 14 (1995) 3704–3711.
[115] R.D. Adams and X. Qu, Organometallics, 14 (1995) 2238–2245.
[116] H. Wadepohl, D. Braga and F. Grepioni, Organometallics, 14 (1995) 24–33.
[117] J. Lewis, P.R. Raithby and G.N. Ward, J. Chem. Soc., Chem. Commun., (1995) 755–756.
[118] D. Braga, F. Grepioni, J.J. Byrne, C.M. Martin, B.F.G. Johnson and A.J. Blake, J. Chem. Soc., Dalton Trans., (1995) 1555–1562.
[119] A.J. Blake, P.J. Dyson, S.L. Ingham, B.F.G. Johnson and C.M. Martin, J. Chem. Soc., Dalton Trans., (1995) 1063–1068.
[120] M. Castiglioni, R. Giordano and E. Sappa, J. Organomet. Chem., 491 (1995) 111–120.
[121] W. Paw, J.B. Keister, C.H. Lake and M.R. Churchill, Organometallics, 14 (1995) 767–779.
[122] F.W.B. Einstein, V.J. Johnston, A.K. Ma and R.K. Pomeroy, Can. J. Chem., 73 (1995) 1223–1235.
[123] S.M. Draper, C.E. Housecroft, J.S. Humphrey and A.L. Rheingold, J. Chem. Soc., Dalton Trans., (1995) 3789–3799.
[124] H.-G. Ang, L.-L. Koh and Q. Zhang, J. Chem. Soc., Dalton Trans., (1995) 2757–2762.
[125] K. Eichele, R.E. Wasylishen, J.F. Corrigan, N.J. Taylor and A.J. Carty, J. Am. Chem. Soc., 117 (1995) 6961–6969.
[126] D. Braga, U. Matteoli, P. Sabatino and A. Scrivanti, J. Chem. Soc., Dalton Trans., (1995) 419–423.
[127] D. Osella, C. Nervi, M. Ravera, J. Fiedler and V.V. Strelets, Organometallics, 14 (1995) 2501–2505.
[128] S. Aime, M. Botta, R. Gobetto, L. Milone, D. Osella, R. Gellert and E. Rosenberg, Organometallics, 14 (1995) 3693–3703.
[129] R.D. Adams and S.B. Falloon, Organometallics, 14 (1995) 4594–4600
[130] C. Rosenberger, N. Steunou, S. Jeannin and Y. Jeannin, J. Organomet. Chem., 494 (1995) 17–35.
[131] D. Cauzzi, C. Graiff, M. Lanfranchi, G. Predieri and A. Tiripicchio, J. Chem. Soc., Dalton Trans., (1995) 2321–2322.
[132] Q. Feng, T.B. Rauchfuss and S.R. Wilson, J. Am. Chem. Soc., 117 (1995) 4702–4703.
[133] B.K. Das and M.G. Kanatzidis, Inorg. Chem., 34 (1995) 1011–1012.
[134] E.J. Houser, A. Venturelli, T.B. Rauchfuss and S.R. Wilson, Inorg. Chem., 34 (1995) 6402–6408.

[135] P.J. Dyson, S.L. Ingham, B.F.G. Johnson, J.E. McGrady, D.M.P. Mingos and A.J. Blake, J. Chem. Soc., Dalton Trans., (1995) 2749–2755.
[136] D.B. Brown, P.J. Dyson, B.F.G. Johnson and D. Parker, J. Organomet. Chem., 491 (1995) 189–193.
[137] A.J. Blake, P.J. Dyson, B.F.G. Johnson, D. Braga, J.J. Byrne and F. Grepioni, Polyhedron, 14 (1995) 2697–2703.
[138] J.R. Galsworthy, C.E. Housecroft, R.L. Ostrander and A.L. Rheingold, J. Organomet. Chem., 492 (1995) 211–216.
[139] P. Mathur, M.M. Hossain, P.B. Hitchcock and J.F. Nixon, Organometallics, 14 (1995) 3101–3103.
[140] D.E. Barber, M. Sabat, E. Sinn and B.A. Averill, Organometallics, 14 (1995) 3229–3237.
[141] A.J. Blake, B.F.G. Johnson, D. Reed and D.S. Shephard, J. Chem. Soc., Dalton Trans., (1995) 843–849.
[142] A.J. Blake, P.J. Dyson, B.F.G. Johnson, S. Parsons, D. Reed and D.S. Shephard, Organometallics, 14 (1995) 4199–4208.
[143] A.-M. Liu, T. Shido and M. Ichikawa, J. Chem. Soc., Chem. Commun., (1995) 507–508.
[144] E. Kolehmainen, K. Laihia, J. Korvola, V.S. Kaganovich, M.I. Rybinskaya and Z.A. Kerzina, J. Organomet. Chem., 487 (1995) 215–221.
[145] P.J. Dyson, B.F.G. Johnson, D. Braga, F. Grepioni, C.M. Martin and E. Parisini, Inorg. Chim. Acta, 235 (1995) 413–420.
[146] A.J. Blake, P.J. Dyson, S.L. Ingham, B.F.G. Johnson and C.M. Martin, Inorg. Chim. Acta, 240 (1995) 29–32.
[147] P.J. Dyson, B.F.G. Johnson, C.M. Martin, D. Reed, D. Braga and F. Grepioni, J. Chem. Soc., Dalton Trans., (1995) 4113–4119.
[148] T. Borchert, J. Lewis, H. Pritzkow, P.R. Raithby and H. Wadepohl, J. Chem. Soc., Dalton Trans., (1995) 1061–1062.
[149] S.L. Ingham, B.F.G. Johnson, C.M. Martin and D. Parker, J. Chem. Soc., Chem. Commun., (1995) 159–160.
[150] T. Chihara and H. Yamazaki, J. Chem. Soc., Dalton Trans., (1995) 1369–1377.
[151] K.K.H. Lee and W.T. Wong, J. Organomet. Chem., 503 (1995) C43-C45.
[152] A.J. Blake, B.F.G. Johnson, S. Parsons and D.S. Shephard, J. Chem. Soc., Dalton Trans., (1995) 495–496.
[153] P. Blenkiron, N.J. Taylor and A.J. Carty, J. Chem. Soc., Chem. Commun., (1995) 327–328.
[154] J.A. Cabeza, I. del Río, J.M. Fernández-Colinas, A. Llamazares and V. Riera, J. Organomet. Chem., 494 (1995) 169–177.
[155] J.A. Cabeza, I. del Río, V. Riera and F. Grepioni, Organometallics, 14 (1995) 3124–3126.
[156] L. Hoferkamp, G. Rheinwald, H. Stoeckli-Evans and G. Süss-Fink, Inorg. Chem., 34 (1995) 5786-5790.
[157] M. Shieh, M.-H. Shieh, Y.-C. Tsai and C.-H. Ueng, Inorg. Chem., 34 (1995) 5088-5090.
[158] R.D. Adams, S.B. Falloon, K.T. McBride and J.H. Yamamoto, Organometallics, 14 (1995) 1739–1747.
[159] A.J. Blake, P.J. Dyson, P.E. Gaede, B.F.G. Johnson, D. Braga and E. Parisini, J. Chem. Soc., Dalton Trans., (1995) 3431–3432.
[160] G.L. Powell and T.F. Tekut, Inorg. Chim. Acta, 229 (1995) 483–486.
[161] D.J.R. Brook, V. Lynch and T.H. Koch, Inorg. Chem., 34 (1995) 5691–5693.
[162] D. Braga, F. Grepioni, P.J. Dyson, B.F.G. Johnson and C.M. Martin, J. Chem. Soc., Dalton Trans., (1995) 909–916.
[163] C.M. Martin, A.J. Blake, P.J. Dyson, S.L. Ingham and B.F.G. Johnson, J. Chem. Soc., Chem. Commun., (1995) 555–556.
[164] C.M. Martin, P.J. Dyson, S.L. Ingham, B.F.G. Johnson and A.J. Blake, J. Chem. Soc., Dalton Trans., (1995) 2741–2748.
[165] M. Shieh, P.-F. Chen, Y.-C. Tsai, M.-H. Shieh, S.-M. Peng and G.-H. Lee, Inorg. Chem., 34 (1995) 2251–2254.
[166] P.J. Bailey, G. Conole, B.F.G. Johnson, J. Lewis, M. McPartlin, A. Moule, H.R. Powell and D.A. Wilkinson, J. Chem. Soc., Dalton Trans., (1995) 741–751.

[167] M.P. Cifuentes, M.G. Humphrey, B.W. Skelton and A.H. White, Organometallics, 14 (1995) 1536–1538.
[168] C. Elschenbroich, T. Isenburg, A. Behrendt, G. Frenzen and K. Harms, J. Organomet. Chem., 501 (1995) 129–144.
[169] C.J. Carmalt, L.J. Farrugia, N.C. Norman and S. Sunley, Inorg. Chim. Acta, 234(1995) 189–193.
[170] B.F.G. Johnson, A.J. Blake, A.J. Brown, S. Parsons and P. Taylor, J. Chem. Soc., Chem. Commun., (1995) 2117–2118.
[171] L.C.F. Chao, A. Decken, J.F. Britten and M.J. McGlinchey, Can. J. Chem., 73 (1995) 1196–1205.
[172] S. Onaka and M. Otsuka, Chem. Lett., (1995) 269–270.
[173] K. Yang, S.G. Bott and M.G. Richmond, Organometallics, 14 (1995) 919–924.
[174] K. Yang, S.G. Bott and M.G. Richmond, Organometallics, 14 (1995) 2718–2724.
[175] D. Braga, F. Grepioni, E. Parisini, H. Wadepohl and S. Gebert, J. Chem. Soc., Dalton Trans., (1995) 1089–1093.
[176] D. Braga, F. Grepioni, H. Wadepohl, S. Gebert, M.J. Calhorda and L.F. Veiros, Organometallics, 14 (1995) 5350–5361.
[177] J.J. Schneider, Chem. Ber., 128 (1995) 321–322.
[178] H. Wadepohl, T. Borchert and H. Prizkow, J. Chem. Soc., Chem. Commun., (1995) 1447–1448.
[179] H. Wadepohl, T. Borchert, K. Büchner, M. Herrmann, F.-J. Paffen and H. Pritzkow, Organometallics, 14 (1995) 3817–3826.
[180] C.P. Casey, R.A. Widenhoefer and R.K. Hayashi, Inorg. Chem., 34 (1995) 2258–2262.
[181] C.P. Casey, S.L. Hallenbeck and R.A. Widenhoefer, J. Am. Chem. Soc., 117 (1995) 4607–4622.
[182] C.P. Casey, R.A. Widenhoefer and R.K. Hayashi, Inorg. Chem., 34 (1995) 1138–1144.
[183] D. Braga, F. Grepioni, J.J. Byrne and M.J. Calhorda, J. Chem. Soc., Dalton Trans., (1995) 3287–3296.
[184] E. Kolehmainen, K. Laihia, J. Korvola, V.S. Kaganovich, M.I. Rybinskaya and Z.A. Kerzina, J. Organomet. Chem., 485 (1995) 109–114.
[185] J.C. Jeffery, R.M.S. Pereira, M.D. Vargas and M.J. Went, J. Chem. Soc., Dalton Trans., (1995) 1805–1811.
[186] E. Galdecka, Z. Galdecki, K. Wajda-Hermanowicz and F.P. Pruchnik, J. Chem. Crystallogr., 25 (1995) 717–723.
[187] K. Wajda-Hermanowicz, F. Pruchnik, M. Zuber, G. Rusek, E. Galdecka and Z. Galdecki, Inorg. Chim. Acta, 232 (1995) 207–209.
[188] C.-S. Jun, J.-F. Halet, A.L. Rheingold and T.P. Fehlner, Inorg. Chem., 34 (1995) 2101–2107.
[189] B.T. Heaton, J.A. Iggo, G. Longoni and S. Mulley, J. Chem. Soc., Dalton Trans., (1995) 1985–1989.
[190] G. Gervasio, S.F.A. Kettle, F. Musso, R. Rossetti and P.L. Stanghellini, Inorg. Chem., 34 (1995) 298–305.
[191] M. Mazzanti, R. Roulet and K.J. Schenk, Acta Crystallogr. C, 51 (1995) 217–219.
[192] P.J. Dyson, S.L. Ingham, B.F.G. Johnson and A.J. Blake, J. Organomet. Chem., 498 (1995) 237–240.
[193] D. Roberto, E. Cariati, R. Psaro and R. Ugo, J. Organomet. Chem., 488 (1995) 109–114.
[194] R.D. Pergola, L. Garlaschelli, M. Manassero and N. Masciocchi, J. Organomet. Chem., 488 (1995) 199–204.
[195] A.F. Masters and J.T. Meyer, Polyhedron, 14 (1995) 339–365.
[196] M. Maekawa, M. Munakata, T. Kuroda-Sowa and K. Hachiya, Inorg. Chim. Acta, 233 (1995) 1–4.
[197] D. Walther, T. Klettke and H. Görls, Angew. Chem., Int. Ed. Engl., 34 (1995) 1860–1861.
[198] D.A. Morgenstern, C.C. Bonham, A.P. Rothwell, K.V. Wood and C.P. Kubiak, Polyhedron, 14 (1995) 1129–1137.
[199] M. Maekawa, M. Munakata, T. Kuroda-Sowa and K. Hachiya, Polyhedron, 14 (1995) 2879–2885.
[200] S. Pasynkiewicz, W. Buchowicz and A. Pietrzykowski, J. Organomet. Chem., 489 (1995) C48-C49.
[201] Y. Yamamoto, T. Tanase, H. Ukaji, M. Hasegawa, T. Igoshi and K. Yoshimura, J. Organomet. Chem., 498 (1995) C23-C26.
[202] L. Hao, I.R. Jobe, J.J. Vittal and R.J. Puddephatt, Organometallics, 14 (1995) 2781–2789.
[203] A.D. Burrows, D.M.P. Mingos, S. Menzer, R. Vilar and D.J. Williams, J. Chem. Soc., Dalton Trans., (1995) 2107–2108.

[204] I.I. Moiseev, J. Organomet. Chem., 488 (1995) 183–190.

[205] L. Hao, J.J. Vittal, R.J. Puddephatt, L. Manojlović-Muir and K.W. Muir, J. Chem. Soc., Chem. Commun., (1995) 2381–2382.

[206] E. Brivio, A. Ceriotti, L. Garlaschelli, M. Manassero and M. Sansoni, J. Chem. Soc., Chem. Commun., (1995) 2055–2056.

[207] E. Furet, A. Le Beuze, J.-F. Halet and J.-Y. Saillard, J. Am. Chem. Soc., 117 (1995) 4936–4944.

[208] S. Bommers, H. Beruda, N. Dufour, M. Paul, A. Schier and H. Schmidbaur, Chem. Ber., 128 (1995) 137–142.

[209] E.J. Fernández, M.C. Gimeno, P.G. Jones, A. Laguna, M. Laguna and J.M. López-de-Luzuriaga, Organometallics, 14 (1995) 2918–2922.

[210] K. Osakada, T. Takizawa and T. Yamamoto, Organometallics, 14 (1995) 3531–3528.

[211] K.A. Al-Farhan, O.M. Abu-Salah, M. Mukhalalati and M. Jaafar, Acta Crystallogr. C, 51 (1995) 1089–1092.

[212] D.L. Reger, J.E. Collins, M.F. Huff, A.L. Rheingold and G.P.A. Yap, Organometallics, 14 (1995) 5475–5477.

[213] K. Angermaier and H. Schmidbaur, Inorg. Chem., 34 (1995) 3120–3122.

[214] A. Antiñolo, F. Carrillo, B. Chaudret, M. Fajardo, S. García-Yuste, F.J. Lahoz, M. Lanfranchi, J.A. López, A. Otero and M.A. Pellinghelli, Organometallics, 14 (1995) 1297–1301.

[215] M.A. Alvarez, M.E. García, V. Riera, M.A. Ruiz, C. Bois and Y. Jeannin, J. Am. Chem. Soc., 117 (1995) 1324–1335.

[216] M. Ferrer, O. Rossell, M. Seco, M.A. Pellinghelli and A. Tiripicchio, Organometallics, 14 (1995) 57–62.

[217] I.L. Eremenko, S. Nefedov, H. Berke, B.I. Kolobkov and V.M. Novotortsev, Organometallics, 14 (1995) 1132–1138.

[218] H.-J. Haupt, M. Schwefer, H. Egold and U. Flörke, Inorg. Chem., 34 (1995) 5461–5467.

[219] J.J. Peng, S.-M. Peng, G.-H. Lee and Y. Chi, Organometallics, 14 (1995) 626–633.

[220] R.D. Pergola, L. Fracchia, L. Garlaschelli, M. Manassero and M. Sansoni, J. Chem. Soc., Dalton Trans., (1995) 2763–2768.

[221] P. Mathur, P. Sekar, C.V.V. Satyanarayana and M.F. Mahon, Organometallics, 14 (1995) 2115–2118.

[222] T. Nakajima, T. Mise, I. Shimizu and Y. Wakatsuki, Organometallics, 14 (1995) 5598–5604.

[223] J. Cooke and J. Takats, Organometallics, 14 (1995) 698–702.

[224] M. Shieh, T.-F. Tang, S.-M. Peng and G.-H. Lee, Inorg. Chem., 34 (1995) 2797–2803.

[225] B. Zhu, Y. Yu, J. Chen, Q. Wu and Q. Liu, Organometallics, 14 (1995) 3963–3969.

[226] A.R. Manning, L. O'Dwyer, P.A. McArdle and D. Cunningham, J. Organomet. Chem., 503 (1995) C46-C47.

[227] W. Heping, Z. Zhuanyun, Y. Yuanqi, J. Daosen and H. Xiaoying, Polyhedron, 14 (1995) 1543–1546.

[228] H.-P. Wu, Y.-Q. Yin and X.-Y. Huang, Polyhedron, 14 (1995) 2993–2997.

[229] H.-P. Wu, Y.-Q. Yin, X.-Y. Huang and K.-B. Yu, J. Organomet. Chem., 498 (1995) 119–125.

[230] A.B. Antonova, A.A. Johansson, N.A. Deykhina, A.G. Ginzburg, E.D. Korniyets, S.V. Kovalenko, N.I. Pavlenko, P.V. Petrovskii, A.I. Rubaylo and I.A. Sukhina, Inorg. Chim. Acta, 230 (1995) 97–104.

[231] L.-C. Song, J.-Y. Shen, Q.-M. Hu and X.-D. Qin, Polyhedron, 14 (1995) 2079–2085.

[232] L.-C. Song, J.-Y. Shen, Q.-M. Hu and X.-Y. Huang, Organometallics, 14 (1995) 98–106.

[233] R. Fandos, J.L.G. Fierro, M.M. Kubicki, A. Otero, P. Terreros and M.A. Vivar-Cerrato, Organometallics, 14 (1995) 2162–2163.

[234] M.D. Curtis, U. Riaz, O.J. Curnow, J.W. Kampf, A.L. Rheingold and B.S. Haggerty, Organometallics, 14 (1995) 5337–5343.

[235] O. Rossell, M. Seco and G. Segalés, J. Organomet. Chem., 503 (1995) 225–233.

[236] H. Bantel, P. Suter and H. Vahrenkamp, Organometallics, 14 (1995) 4424–4426.

[237] J.R. Galsworthy, C.E. Housecroft and A.L. Rheingold, J. Chem. Soc., Dalton Trans., (1995) 2639–2647.

[238] H.J. Kakkonen, L. Tunkkari, M. Ahlgrén, J. Pursiainen and T.A. Pakkanen, J. Organomet. Chem., 496 (1995) 93–97.

[239] G. Proulx, F.J. Hollander and R.G. Bergman, J. Can. Chem., 73 (1995) 1111–1115.
[240] D. Ellis, L.J. Farrugia, P. Wiegeleben, J.G. Crossley, A.G. Orpen and P.N. Waller, Organometallics, 14 (1995) 481–488.
[241] E.J. Voss, M. Sabat and D.F. Shriver, Inorg. Chim. Acta, 240 (1995) 49–61.
[242] C.K. Schauer, S. Harris, M. Sabat, E.J. Voss and D.F. Shriver, Inorg. Chem., 34 (1995) 5017–5028.
[243] T.-K. Huang, Y. Chi, S.-M. Peng, G.-H. Lee, S.-L. Wang and F.-L. Liao, Organometallics, 14 (1995) 2164–2166.
[244] Y. Chi, P.-C. Su, S.-M. Peng and G.-H. Lee, Organometallics, 14 (1995) 5483–5485.
[245] P.-C. Su, S.-J. Chiang, L.-L. Chang, Y. Chi, S.-M. Peng and G.-H. Lee, Organometallics, 14 (1995) 4844–4849.
[246] T. Teppana, S. Jääskeläinen, M. Ahlgrén, J. Pursiainen and T.A. Pakkanen, J. Organomet. Chem., 486 (1995) 217–228.
[247] J. Xiao, E. Kristof, J.J. Vittal and R.J. Puddephatt, J. Organomet. Chem., 490 (1995) 1–6.
[248] J. Xiao, L. Hao, R.J. Puddephatt, L. Manojlović-Muir, K.W. Muir and A.A. Torabi, Organometallics, 14 (1995) 2194–2201.
[249] J. Xiao, L. Hao, R.J. Puddephatt, L. Manojlović-Muir, K.W. Muir and A.A. Torabi, Organometallics, 14 (1995) 4183–4193.
[250] M.D. Janssen, M. Herres, L. Zsolnai, D.M. Grove, A.L. Spek, H. Lang and G. van Koten, Organometallics, 14 (1995) 1098–1100.
[251] M.A. Mansour, M.D. Curtis and J.W. Kampf, Organometallics, 14 (1995) 5460–5462.
[252] P. Braunstein, U. Englert, G.E. Herberich and M. Neuschütz, Angew. Chem., Int. Ed. Engl., 34 (1995) 1010–1012.
[253] H.-J. Haupt, M. Schwefer and U. Flörke, Inorg. Chem., 34 (1995) 292–297.
[254] L.-C. Song, J.-Q. Wang and Q.-M. Hu, Polyhedron, 14 (1995) 1101–1103.
[255] G. Frapper and J.-F. Halet, Organometallics, 14 (1995) 5044–5053.
[256] M. Akita, H. Hirakawa, K. Sakaki and Y. Moro-oka, Organometallics, 14 (1995) 2775–2780.
[257] A. Pons, O. Rossell, M. Seco and A. Perales, Organometallics, 14 (1995) 555–557.
[258] J.R. Galsworthy, C.E. Housecroft, A.J. Edwards and P.R. Raithby, J. Chem. Soc., Dalton Trans., (1995) 2935–2939.
[259] H.J. Kakkonen, M. Ahlgrén, J. Pursiainen and T.A. Pakkanen, J. Organomet. Chem., 491 (1995) 195–201.
[260] C. Thöne and H. Vahrenkamp, J. Organomet. Chem., 485 (1995) 185–189.
[261] S. Chan and W.-T. Wong, J. Organomet. Chem., 489 (1995) C78-C80.
[262] S. Jääskeläinen, J. Pursiainen and T.A. Pakkanen, J. Organomet. Chem., 487 (1995) 197–200.
[263] M.I. Bruce, N.N. Zaitseva, B.W. Skelton and A.H. White, Polyhedron, 14 (1995) 2647–2652.
[264] S.F.A. Kettle, E. Diana, P.L. Stanghellini, R.D. Pergola and A. Fumagalli, Inorg. Chim. Acta, 235 (1995) 407–411.
[265] M. Herberhold, G.-X. Jin and A.L. Rheingold, Angew. Chem., Int. Ed. Engl., 34 (1995) 656–657.
[266] C.-J. Su, Y. Chi, S.-M. Peng and G.-H. Lee, Organometallics, 14 (1995) 4286–4293.
[267] S. Chan and W.-T. Wong, J. Chem. Soc., Dalton Trans., (1995) 3987–3994.
[268] P.J. McCarthy, I.D. Salter and T. Adatia, J. Organomet. Chem., 485 (1995) 191–199.
[269] K.-H. Dahmen, D. Imhof, L.M. Venanzi, T. Gerfin and V. Gramlich, J. Organomet. Chem., 486 (1995) 37–43.
[270] J. Forniés, E. Lalinde, A. Martín and M.T. Moreno, J. Organomet. Chem., 490 (1995) 179–188.
[271] I.D. Salter, S.A. Williams and T. Adatia, Polyhedron, 14 (1995) 2803–2817.
[272] H. Adams, L.J. Gill and M.J. Morris, J. Chem. Soc., Chem. Commun., (1995) 899–900.
[273] J.R. Galsworthy, A.D. Hattersley, C.E. Housecroft, A.L. Rheingold and A. Waller, J. Chem. Soc., Dalton Trans., (1995) 549–557.
[274] I. Ara, J. Forniés, E. Lalinde, M.T. Moreno and M. Tomás, J. Chem. Soc., Dalton Trans., (1995) 2397–2405.
[275] L.-C. Song, C.-G. Yan, Q.-M. Hu, R.-J. Wang and T.C.W. Mak, Organometallics, 14 (1995) 5513–5519.
[276] L. Hao, J.J. Vittal, J. Xiao and R.J. Puddephatt, J. Am. Chem. Soc., 117 (1995) 8035–8036.
[277] J. Strähle, J. Organomet. Chem., 488 (1995) 15–24.

[278] M. Akita, H. Hirakawa, M. Tanaka and Y. Moro-oka, J. Organomet. Chem., 485 (1995) C14-C17.
[279] A.J. Blake, A. Harrison, B.F.G. Johnson, E.J.L. McInnes, S. Parsons, D.S. Shephard and L.J. Yellowlees, Organometallics, 14 (1995) 3160–3162.
[280] A. Ceriotti, R.D. Pergola, L. Garlaschelli, M. Manassero and N. Masciocchi, Organometallics, 14 (1995) 186–193.
[281] R.D. Adams, T.S. Barnard and J.E. Cortopassi, Organometallics, 14 (1995) 2232–2237.